



University of Zagreb

Faculty of Veterinary Medicine

Marina Prišlin Šimac

**MOLECULAR CHARACTERISTICS AND
SECRETOME COMPOSITION OF
CANINE MESENCHYMAL STEM CELLS
DURING CULTURE AND CANINE
HERPESVIRUS INFECTION *IN VITRO***

DOCTORAL DISSERTATION

Zagreb, 2025



Sveučilište u Zagrebu

Veterinarski fakultet

Marina Prišlin Šimac

**MOLEKULARNA OBILJEŽJA I SASTAV
SEKRETOMA MEZENHIMSKIH
MATIČNIH STANICA PASA TIJEKOM
IN VITRO UZGOJA I INFEKCIJE
PSEĆIM HERPESVIRUSOM**

DOKTORSKI RAD

Zagreb, 2025.



University of Zagreb

Faculty of Veterinary Medicine

Marina Prišlin Šimac

**MOLECULAR CHARACTERISTICS AND
SECRETOME COMPOSITION OF
CANINE MESENCHYMAL STEM CELLS
DURING CULTURE AND CANINE
HERPESVIRUS INFECTION *IN VITRO***

DOCTORAL DISSERTATION

Supervisors:

Prof Nenad Turk, PhD, MSc, DVM

Dragan Brnić, PhD, DVM

Zagreb, 2025



Sveučilište u Zagrebu

Veterinarski fakultet

Marina Prišlin Šimac

**MOLEKULARNA OBILJEŽJA I SASTAV
SEKRETOMA MEZENHIMSKIH
MATIČNIH STANICA PASA TIJEKOM
IN VITRO UZGOJA I INFEKCIJE
PSEĆIM HERPESVIRUSOM**

DOKTORSKI RAD

Mentori:

Prof. dr. sc. Nenad Turk

Dr. sc. Dragan Brnić

Zagreb, 2025.

VETERINARSKI FAKULTET

IZJAVA

Ja, Marina Prišlin Šimac, potvrđujem da je moj doktorski rad izvorni rezultat mogega rada te da se u njegovoj izradi nisam koristila drugim izvorima do onih navedenih u radu.

(potpis studenta)

Zagreb, 2025.

This dissertation was prepared in the Department of Virology of the Croatian Veterinary Institute, Croatia, within the project UIP-2019-04-2178 'Revealing the Mesenchymal Stem Cells Transcriptome and Secretome' (SECRET) of the Croatian Science Foundation. The research was conducted under the supervision of principal investigator Dragan Brnić, PhD, and Professor Nenad Turk, PhD.

INFORMATION ON SUPERVISORS

*Professor Nenad Turk works at the Department of Microbiology and Infectious Diseases with Clinic, Veterinary Faculty, University of Zagreb. He finished PhD at the Veterinary Faculty, University of Zagreb, in the field of molecular epizootiology of pathogenic bacteria. The topic of his dissertation was the molecular characterisation of different strains of pathogenic bacteria *Leptospira* spp. Scientific activity is focused on the investigation of infectious diseases in animals, particularly zoonoses as well as the investigation of the role of stem cells in therapy. His role as a mentor was in the development of the idea of the proposed investigation as well as an adviser in all aspects necessary for the preparation of this dissertation. Up to now, according to Scopus, he published 71 scientific papers with 901 citations and an h-index of 16.*

Dragan Brnić, Senior Research Associate, has been part of the Croatian Veterinary Institute since 2007 and has focused on virology research since 2010. He completed his PhD at the Faculty of Veterinary Medicine, University of Zagreb, with a thesis entitled “Detection and Phylogenetic Analysis of Astroviruses Isolated from Potential Animal Reservoirs in Croatia”. As a principal investigator of the research project “Revealing the Mesenchymal Stem Cells Transcriptome and Secretome,” under which the present study was conducted, Dr. Brnić has taken on a mentorship role. He has authored 54 scientific publications and has presented his research at more than 60 scientific conferences worldwide. According to Scopus, his work has been cited over 510 times and he has an h-index of 13.

Na prvom mjestu, neizmjereno zahvaljujem svojim mentorima: Nenadu Turku za nesebičnu pomoć i strpljenje te Draganu Brniću za podršku, uloženi trud, razgovore i savjete koji su mi bili izrazita motivacija tijekom izrade ovog doktorskog rada. Zahvaljujem Nini Krešić na prenesenom znanju i ljubavi prema matičnim stanicama, kao i Manueli Zadravec na svakoj riječi podrške i pomoći.

Veliku zahvalnost dugujem svim suradnicima za podršku u izradi doktorskog rada, kao i svim psima i njihovim vlasnicima, bez kojih ovaj rad ne bi bio moguć. Od srca hvala mojim divnim kolegicama Ivi, Valentini i Giovanni na svakodnevnoj podršci i mudrim savjetima, kao i svim djelatnicima Odjela za virologiju na toplim i iskrenim riječima ohrabrenja.

Posebno zahvaljujem svim svojim genijalnim prijateljima, svojim primarnim motivatorima Ariju i Smokiju, kao i svojim roditeljima i bratu na bezuvjetnoj podršci i motivaciji. Najveću zahvalnost dugujem svom Franu na beskonačnom strpljenju, razumijevanju i ljubavi.

ABSTRACT

Canine adipose-derived mesenchymal stem cells (cAD-MSCs) have significant promise in regenerative medicine due to their abundance, multipotency, and therapeutic properties, such as promoting tissue repair, angiogenesis, and reducing inflammation. However, *in vitro* expansion required for clinical applications may alter their immunophenotype, gene expression, and secretome, while also posing risks of viral contamination, particularly from canine alphaherpesvirus 1 (CHV). These effects on cAD-MSC functionality remain insufficiently understood. Thus, this dissertation investigates how *in vitro* ageing and CHV infection affect the properties of cAD-MSCs, including gene expression and secretome profile. Abdominal adipose tissue from 20 healthy dogs was harvested to isolate cAD-MSCs, which were validated by differentiation assays and immunophenotyping. The expression of surface markers (CD90, CD44, CD73, CD29, CD271, CD105, CD45 and CD14) was analysed at the protein and RNA level by flow cytometry and RT-qPCR array, respectively. Changes in gene expression and secretome profile during culture in passages 3 and 6 were analysed by RT-qPCR array and LC-MS/MS, and the effects of CHV infection on cAD-MSCs were evaluated by implementing the same methods. The findings demonstrate significant alterations in immunophenotype, gene expression, and secretome composition associated with *in vitro* ageing of cAD-MSCs. Specifically, *in vitro* ageing led to a decrease in CD73 protein expression and downregulation of the genes *IL10* and *PTPRC*. Moreover, secretome analysis revealed a loss of proteins associated with tissue regeneration pathways and an increase in proteins linked to coagulation pathways. Following CHV infection, changes were observed in both gene expression and secretome composition as well. These changes suggest that CHV infection contributes to a decline in the regenerative potential of cAD-MSCs by altering stem cell structure, impairing proliferation and migration, and promoting genes and proteins involved in differentiation towards an adipogenic phenotype. Therefore, prioritising early passage cells and performing regular viral screenings are essential to increase the therapeutic potential and safety of cAD-MSCs.

Keywords: mesenchymal stem cells; three lineage differentiation; immunophenotype; gene expression; secretome; canine herpesvirus; Varicellovirus canidalpha 1; veterinary regenerative medicine; real-time reverse transcription polymerase chain reaction array; liquid chromatography with tandem mass spectrometry

PROŠIRENI SAŽETAK

UVOD: Tijekom posljednjih nekoliko desetljeća, matične stanice postale su ključna tema biomedicinskih istraživanja zbog svojih regenerativnih svojstava. Jedna od najpoznatijih primjena u regenerativnoj medicini je transplantacija hematopoetskih matičnih stanica, koja je postala standard u liječenju raznih bolesti kod ljudi i životinja. Ipak, mnoge degenerativne i maligne bolesti i dalje nemaju adekvatne terapijske opcije. Danas je poznato kako različita tkiva, od embrionalnog do odraslog, sadrže matične stanice, što omogućuje njihovo izdvajanje i istraživanje s ciljem uvođenja inovativnih terapija i produljenja životnog vijeka. No sami proces izdvajanja matičnih stanica često zahtijeva invazivne postupke, uključujući kirurške zahvate, što postavlja etičke izazove. Međutim, otkriveno je da mezenhimsko tkivo u odraslih jedinki, poput masnog tkiva, sadrži visok udio matičnih stanica koje su relativno lako dostupne. Mezenhimske matične stanice dobivene iz masnog tkiva pasa (cAD-MSCs) pokazuju obećavajuće sposobnosti za regeneraciju tkiva, posebno djelovanjem njihovog sekretoma. Brojna su istraživanja utvrdila kako su obećavajući kandidat za različite terapijske primjene, čime se otvaraju nove mogućnosti u veterinarskoj medicini. Dosadašnja istraživanja pokazala su najveći uspjeh u liječenju osteoartritisa, ali i potencijal za terapiju neuroloških, dermatoloških, oftalmoloških, gastroenteroloških i hematoloških bolesti, čime se proširuju mogućnosti njihove primjene. Kako bi se osigurala terapijske doze cAD-MSC-a i njihova primjena u različitim bolestima, nužno je izdvajanje i umnažanje *in vitro*. Međutim, dugoročni *in vitro* uzgoj može dovesti do staničnog starenja, što negativno utječe na terapijske učinke, uključujući smanjenje proliferativnog kapaciteta, promjene u izražaju gena te umanjene imunomodulacijskog potencijala. Dodatni izazov predstavlja mogućnost mikrobiološke kontaminacije tijekom *in vitro* postupaka, pri čemu pohranjene serije cAD-MSC-a mogu biti kontaminirane bakterijama, gljivicama ili virusima. Iako se bakterijske i gljivične kontaminacije mogu kontrolirati antibioticima i antimikoticima, virusna kontaminacija i dalje predstavlja značajan izazov. Poznato je da su matične stanice ljudi prijemljive na infekcije RNA i DNA virusima, što može dovesti do stanične smrti, transformacije ili trajne infekcije, čime se smanjuje njihova funkcionalnost. Također, nedavno je utvrđeno da postoji značajna mogućnost kontaminacije serijskih pripravaka cAD-MSCs različitim patogenima, uključujući viruse poput psećeg herpesvirusa (CHV), što potencijalno može ugroziti njihovu regenerativnu sposobnost. Prema dostupnim podacima, posljedice virusne kontaminacije na cAD-MSCs nisu poznate, što

upućuje na potrebu za daljnjim istraživanjima u cilju osiguranja sigurnosti i učinkovitosti ovih terapija.

HIPOTEZA I CILJEVI: Ovo istraživanje temelji se na hipotezi da molekularna obilježja i sastav sekretoma cAD-MSC ostaju očuvani tijekom uzgoja i infekcije CHV-om u staničnoj kulturi. Da bi se ova hipoteza potvrdila ili opovrgnula, postavljeni su ciljevi. Opći cilj istraživanja je istražiti promjene molekularnih obilježja i sastava sekretoma cAD-MSC-a tijekom njihovog uzgoja i infekcije CHV-om u *in vitro* uvjetima. Specifični ciljevi uključuju istraživanje imunofenotipskih i funkcionalnih svojstava cAD-MSC-a u *in vitro* kulturi, analizu promjena u izražaju gena i sastavu sekretoma cAD-MSC-a u dvije vremenske točke uzgoja, utvrđivanje prijemljivosti cAD-MSC-a za infekciju CHV-om te analizu promjena u izražaju gena i sastavu sekretoma cAD-MSC-a nakon infekcije CHV-om u *in vitro* uvjetima.

MATERIJAL I METODE: Ovaj doktorski rad obuhvaća ukupno 20 uzoraka abdominalnog masnog tkiva pasa. Donori masnog tkiva bili su klinički zdravi psi koji su prošli elektivne operativne zahvate na Veterinarskom fakultetu Sveučilišta u Zagrebu i u Veterinarskoj klinici Buba u Zagrebu. Uzorci abdominalnog masnog tkiva prikupljeni su kao postoperativni biološki otpad, pohranjeni u sterilnim epruvetama i transportirani pri 4°C unutar dva sata nakon prikupljanja. Postupak izdvajanja cAD-MSC-a obuhvaćao je mehaničku i enzimsku razgradnju uzorka masnog tkiva, centrifugiranje i resuspenziju u hranjivom mediju uz dodatak antibiotika pri 37°C. Tijekom postupka izdvajanja, supernatant stanica testiran je na sterilnost, uključujući prisutnost aerobnih i anaerobnih bakterija, gljivica i mikoplazmi. Određivanje identiteta matičnih stanica je odrađeno prema kriterijima Međunarodnog društva za staničnu terapiju. Znanstveni članak I obuhvaća istraživanje imunofenotipskih svojstva nediferenciranih cAD-MSC-a u osam donora u svim pasažama do prosječnog proliferacijskog aresta, dok se u člancima II i III imunofenotipizacija protočnom citometrijom radila samo u 3. pasaži (P3) za potvrdu identiteta matičnih stanica. Metoda je uključivala jednostruko označavanje stanica površinskim biljezima CD90, CD44, CD105, CD73, CD29, CD271, CD45, CD14 te CD34 te očitavanje rezultata metodom protočne citometrije uporabom uređaja FACSVerser. Stanična vijabilnost procijenjena je bojenjem propidij jodidom, dok su rezultati analizirani FACSuite softverom i predstavljeni kao srednji intenzitet fluorescencije i postotak pozitivnosti. Podaci od navedenim površinskim markerima, istraženi su i na razini gena, uporabom mikromrežne analize lančanom reakcijom polimerazom uz prethodnu reverznu transkripciju (RT-qPCR array). Diferencijacijski potencijal cAD-MSC-a, u sva tri članka, određen je u P3 prema trilinijskom principu, diferencijacijom stanica u adipogenu, osteogenu i hondrogeno liniju uz

uporabu specijaliziranih medija. Nakon diferencijacije, kapljice masti, alkalna fosfataza i agrekan dokazani su specijaliziranim metodama bojenja. Rezultati su potvrđeni invertnim mikroskopom Axio Observer D1, a slike su snimljene Zeiss Axiovert kamerom.

U člancima I i II, analiza izražajnosti gena cAD-MSA-a tijekom *in vitro* uzgoja provedena je u 8, odnosno 12 donora cAD-MSAs RT-qPCR array metodom u P3 i P6. Nakon izdvajanja ukupne RNA korištenjem RNeasy Mini kita, cjelovitost RNA procijenjena je QIAxcel RNA QC kitom. Prethodno analizi izražajnosti gena, uklonjena je genomska DNA te je provedena sinteza cDNA uporabom RT2 First Strand kita. Izražajnost gena analizirana je RT2 Profiler™ PCR Array mikromrežnim komercijalnim kitom za pseće matične stanice uporabom Rotor-Gene Q uređaja. Podaci su statistički obrađeni RT2 Profiler PCR Array Data Analysis softverom primjenom t-testa, pri čemu su značajnim smatrani rezultati s vrijednostima $p < 0,05$. Sirovi podaci članka II pohranjeni su u javnom repozitoriju NCBI-a Gene Expression Omnibus (GEO) pod pristupnim brojem GSE255585. Promjene u sastavu sekretoma cAD-MSA-a tijekom *in vitro* uzgoja zabilježene su također u dvjema vremenskim točkama, P3 i P6, kod šest nasumično odabranih donora u II. članku. Stanice su uzgajane u čistom niskoglukožnom Dulbecco's Modified Eagle mediju bez dodatka goveđeg fetalnog seruma tijekom 48 sati, nakon čega su uzorci sekretoma sakupljeni, centrifugirani, filtrirani te pohranjeni do trenutka proteomske analize. Proteomska analiza provedena je uporabom tekućinske kromatografije s tandemskom masenom spektrometrijom (LC-MS/MS). Proteini sekretoma reducirani su i izdvojeni iz medija, a potom enzimatski razgrađeni. Peptidi su razdvojeni primjenom tekućinskog kromatografa nanoLC EASY-nLC 1200. Maseni spektri peptida zabilježeni su hibridnim Quadrapol-Orbitrap masenim spektrometrom Q Exactive Plus, čime su dobiveni precizni podaci o sastavu proteoma. Dobiveni podaci statistički su obrađeni softverskim alatom Scaffold Quant Q+S 5.3.0, s referentnom bazom sekvenci proteina za vrstu *Canis lupus familiaris*. Statistička značajnost promjena u proteinskom sastavu potvrđena je t-testom, pri čemu su značajnim smatrani rezultati s vrijednostima $p < 0,05$. Sirovi podaci masene spektrometrije deponirani su u bazi podataka ProteomeXchange konzorcija putem PRIDE repozitorija pod pristupnim brojem PXD049324. Bioinformatička analiza pronađenih proteina provedena je primjenom Gene Ontology (GO) Panther 18.0 softvera, kako bi se analizirale stanične sastavnice, molekularne funkcije i biološki procesi te proteinski putevi na koje je utjecalo *in vitro* starenje.

Nadalje, u III. članku istraživana je utjecaj virusne infekcije na svojstva cAD-MSA-a. Primarno, postupak infekcije stanica proveden je nastavno testiranju svih istraživanih stanica

na prisutnost CHV-a kvantitativnom lančanom reakcijom polimeraze u stvarnom vremenu (qPCR). Virus koji je korišten za infekcije je autohtoni divlji tip CHV-a, soj 29107, izdvojen iz organa šteneta metodom homogenizacije te verificiran metodom sekvenciranja nove generacije (NGS). Cjeloviti genom autohtonog CHV soja 29107 pohranjen je u NCBI GenBank-u pod pristupnim brojem PP349830. Za potrebe istraživanja infekcije cAD-MSC-a s CHV-om, šest donora nasumično je odabrano za provođenje pet serijskih pasaža virusa, a za potvrdu uspješnosti infekcije provedena je mikroskopska pretraga citopatogenog učinka te detekcija prisutnosti genoma CHV-a qPCR-om. Izražajnost gena inficiranih stanica analizirana je mikromrežnom metodom kako je prethodno opisano za Članak I i II, a rezultati su pohranjeni u NCBI GEO bazu s pristupnim brojem GSE267402. Također, proteomska analiza sastava sekretoma inficiranih stanica provedena je sukladno prethodno opisanom postupku primjenom LC-MS/MS tehnologije, a sirovi rezultati su pohranjeni pod pristupnim brojem PXD052289.

REZULTATI I RASPRAVA: Budući da za pseće matične stanice ne postoje međunarodno prihvaćeni standardi, u ovom doktorskom radu primijenjeni su kriteriji za ljudske matične stanice koje je postavila Međunarodna udruga za staničnu terapiju (ISCT). Vodeći se ovim kriterijima potvrdili smo izražajnost svojstva prijanjanja na plastiku, sposobnost proliferacije *in vitro* te imunofenotipska obilježja i mogućnost multipotencije kod pasa. Prvi dio dokorskog rada, predstavljen u članku I, usredotočen je na imunofenotipska i funkcionalna obilježja cAD-MSC-a. Imunofenotipska obilježja odnose se na prisutnost specifičnih površinskih biljega koji su važni za identifikaciju i potencijalnu primjenu cAD-MSC-ova u terapiji. Rezultati nam ukazuju da se izražajnost biljega mijenja tijekom starenja u *in vitro* uvjetima te dolazi do značajnog smanjenja izražajnosti CD73 biljega u kasnijim pasažama, što bi moglo imati važan utjecaj na imunomodulacijske učinke terapije cAD-MSC-a zbog uloge navedenog biljega u protuupalnim procesima. Gen koji kodira protein CD73 pokazuje smanjenu izražajnost, ali ta razlika nije statistički značajna. Svakako, smanjena izražajnost ovog biljega ukazuje na potrebu za pažljivim razmatranjem vremena provedenog u kulturi prije potencijalne primjene ovih stanica u terapijske svrhe. Ostali istraživani biljezi održavaju stabilnu izražajnost tijekom *in vitro* uzgoja, što ujedno potvrđuje njihovu važnost u identifikaciji cAD-MSC-a.

Drugi dio istraživanja, predstavljen u članku II, ukazuje na promjene u izražajnosti gena i sastavu sekretoma cAD-MSC-a tijekom starenja *in vitro*. Istraživanjem 84 gena ustanovili smo nižu izražajnost u 21 i pojačanu izražajnost u 10 gena, sa statistički značajnim smanjenjem *CD45/PTPRC* i *IL10*. Analizom sekretoma također je utvrđeno da postoji značajna razlika u sastavu proteina kod rane i kasne pasaže cAD-MSC-a, što čini 10% ukupno izlučenih proteina.

Tijekom procesa *in vitro* starenja, cAD-MSC-e su izgubile određene proteine povezane s regulacijom staničnog citoskeleta putem Rho GTPaze, ali i nikotinsko-acetilkolinskim receptorima, Wnt signalnim putem i CCKR signalizacijom, što su iznimno važni proteinski putevi za regenerativne funkcije matičnih stanica, a ujedno i inhibiciju apoptoze i diferencijaciju. Suprotno tome, proteini detektirani u *in vitro* ostarenim uzorcima (P6) ukazuju na povećano sudjelovanje u proteinskim putevima zgrušavanja krvi. Navedeni rezultati pokazuju kako je utjecaj *in vitro* uzgoja značajan te postoji mogućnost gubitka regenerativnog potencijala i nuspojave zgrušavanja krvi uslijed primjene kasnih pasaža cAD-MSC-a u terapiji.

Trećim dijelom istraživanja, predstavljenim u članku III, dokazujemo prijemljivost cAD-MSC infekciji CHV-om i opisujemo promjene u izražajnosti gena i sastavu sekretoma ovih stanica nakon infekcije. Uporabom autohtonog divljeg soja CHV-a, rezultati infekcije bolje opisuju prirodni odnos virusa i domaćina u usporedbi s laboratorijski adaptiranim sojevima. Rezultati pokazuju da su stanice prijemljive na infekciju CHV-om, no serijskim pasażama uočeno je kako se citopatogeni učinak gubi što je moguća posljedica abortivne infekcije. Međutim, kako bismo potvrdili tu hipotezu potrebna su daljnja istraživanja. Tijekom infekcije CHV-om opaženo je da dolazi do morfoloških promjena u cAD-MSC-ama s umanjenim preživljavanjem stanica. Istraživanjem izražajnosti gena inficiranih stanica otkriveno je značajno povećanje gena povezanih s proliferacijom, diferencijacijom i imunomodulacijom, poput *TNF* gena koji je najznačajnije promijenjen kod inficiranih cAD-MSC-a. *TNF* protein je ključan za razne stanične procese, uključujući imunosupresiju i diferencijaciju, no njegovo izlučivanje je najviše izraženo u pretečama adipocita, što je znak začetka adipogeneze posljedično infekciji CHV-om. Uz *TNF*, zabilježena je i povećana izražajnost gena poput *ADIPOQ* i *NOTCH1*, ključnih za inicijaciju adipogeneze, što dodatno potvrđuje da infekcija CHV-om može usmjeriti stanice prema diferencijaciji u adipocite. Stanice začetkom diferencijacije gube svojstvo multipotencije koje je po dosadašnjim istraživanjima ključno u regeneraciji tkiva. Gubitak regenerativnih svojstava također se potvrđuje i proteomskom analizom sekretoma cAD-MSC-a. Promatrano s proteomske strane, posljedično infekciji CHV-om dokazan je gubitak proteina uključenih u regenerativne procese i također preusmjeravanje cAD-MSCs prema adipogenezi. Ujedno je opaženo i povećanje proteina povezanih s glikolizom, što sugerira da virus koristi stanične resurse za vlastitu replikaciju, a također može dovesti do oštećenja stanica i smanjenja njihovih tipičnih funkcija. **ZAKLJUČCI:** Zaključci ovih triju znanstvenih članaka objavljenih u okviru doktorskog rada naglašavaju važnost različitih čimbenika koji utječu na terapijski potencijal cAD-MSCs.

Članci I i II pokazuju da starenje cAD-MSCs tijekom *in vitro* uzgoja značajno utječe na imunofenotip, izražajnost gena i sastav sekretoma. Rane pasaže (P1–P3) cAD-MSC-a značajno bolje podržavaju imunomodulatornu funkciju stanica u usporedbi s kasnijim pasažama. Suprotno rečenom, kasnije pasaže (P4-P6) ukazuju na smanjeni regenerativni potencijal i povećanu aktivnost koagulacijskih proteinskih putova, dodatno naglašavajući važnost odabira ranih pasaža za terapijsku primjenu. Članak III ukazuje kako su cAD-MSC prijemljive na infekciju autohtonim sojem CHV-a, te da infekcija značajno utječe na izražajnost gena i sastav sekretoma tih stanica, uzrokujući pomak prema adipogenom fenotipu i potencijalna funkcionalna oštećenja. Rezultati ovih triju članaka ističu nužnost obaveznog testiranja staničnih pripravaka cAD-MSC-a na prisutnost CHV-a i pažljivog umnažanja *in vitro* kako bi se očuvala sigurnost i terapijska učinkovitost cAD-MSC-a.

KLJUČNE RIJEČI: mezenhimske matične stanice porijeklom iz masnog tkiva pasa; trilinijska diferencijacija; imunofenotip; izražajnost gena; sekretom; pseći herpesvirus; Varicellovirus canidalpha 1; veterinarska regenerativna medicina; mikromrežna analiza; tekućinska kromatografija s tandemskom masenom spektrometrijom

ABBREVIATIONS

AD-MSCs	Adipose-Derived Mesenchymal Stem Cells
cAD-MSCs	Canine Adipose-Derived Mesenchymal Stem Cells
CD	Cluster of Differentiation
CHV	Canid alpha herpesvirus 1
CPE	Cytopathogenic Effect
DMEM Low Glucose	Dulbecco's Modified Eagle Medium with Low Glucose
FDR	False Discovery Rate
GO	Gene Ontology
IBD	Inflammatory Bowel Disease
ISCT	International Society for Cellular Therapy
ISSCR	International Society for Stem Cell Research
KCS	Keratoconjunctivitis sicca
LC-MS/MS	Liquid Chromatography with Tandem Mass Spectrometry
MDCK	Madin-Darby Canine Kidney Cell Culture
MFI	Median Fluorescence Intensity
MOI	Multiplicity Of Infection
MSC	Mesenchymal Stem Cell
NGS	Next-Generation Sequencing
OA	Osteoarthritis
P(number)	Passage (Number)
qPCR	Quantitative Polymerase Chain Reaction
RT-qPCR	Reverse Transcription-Quantitative Polymerase Chain Reaction
SVF	Stromal Vascular Fraction

TABLE OF CONTENTS

1. INTRODUCTION.....	1
1.1. cAD-MSCs extraction.....	1
1.2. cAD-MSCs characteristics.....	3
1.3. cAD-MSCs secretome.....	4
1.4. <i>In vitro</i> establishment of cAD-MSCs.....	5
1.5. Microbial sterility of <i>in vitro</i> established cAD-MSC cultures.....	5
1.6. cAD-MSCs in veterinary regenerative medicine.....	6
1.6.1. Orthopaedics.....	7
1.6.2. Neurology.....	7
1.6.3. Dermatology.....	8
1.6.4. Ophthalmology.....	8
1.6.5. Gastroenterology.....	9
1.6.6. Hepatology.....	9
1.6.7. Haematology.....	9
1.6.8. Urology.....	9
1.7. Current Advances and Status of Stem Cell Research in the Republic of Croatia....	10
2. HYPOTHESIS AND OBJECTIVES.....	11
3. MATERIAL AND METHODS.....	12
3.1. Canine adipose tissue donors.....	12
3.2. Extraction and propagation of cAD-MSCs <i>in vitro</i>	13
3.3. Immunophenotyping of cAD-MSCs during <i>in vitro</i> cultivation.....	14
3.4. Multipotency <i>in vitro</i> testing of cAD-MSCs during culture.....	14
3.5. Gene expression profiling of cAD-MSCs during <i>in vitro</i> cultivation.....	15
3.6. Proteomic analysis of the cAD-MSC secretome during <i>in vitro</i> culture.....	15
3.7. Infection of cAD-MSCs with CHV <i>in vitro</i>	16
3.7.1. Isolation and characterisation of autochthonous wild-type CHV.....	16
3.7.2. Verification of the autochthonous wild-type CHV strain by NGS.....	16
3.7.3. <i>In vitro</i> infection of cAD-MSCs with wild-type CHV.....	16
3.7.4. Quantification of CHV DNA with qPCR.....	17

3.7.5.	Gene expression profiling of <i>in vitro</i> CHV-infected cAD-MSCs.....	17
3.7.6.	Proteomic analysis of the <i>in vitro</i> CHV-infected cAD-MSCs secretome.....	17
3.8.	Statistical analysis	17
3.9.	Ethics approval and consent to participate.....	18
4.	RESULTS.....	19
4.1.	Paper I	19
4.2.	Paper II	19
4.3.	Paper III.....	20
5.	DISCUSSION	22
6.	CONCLUSIONS.....	29
7.	BIBLIOGRAPHY	30
8.	PUBLISHED SCIENTIFIC PAPERS.....	49
8.1.	Paper I: "The Expression Pattern of Surface Markers in Canine Adipose-Derived Mesenchymal Stem Cells"	49
8.2.	Paper II: " <i>In vitro</i> aging alters the gene expression and secretome composition of canine adipose-derived mesenchymal stem cells"	69
8.3.	Paper III: "Canid alphaherpesvirus 1 infection alters the gene expression and secretome profile of canine adipose-derived mesenchymal stem cells <i>in vitro</i> ".....	82
9.	BIOGRAPHY OF THE AUTHOR WITH BIBLIOGRAPHY OF PUBLISHED WORK	

1. INTRODUCTION

For more than 50 years, stem cells have been recognised for their regenerative capabilities, i.e., the replacement of damaged cells and the generation of new healthy ones. The most renowned application, bone marrow-stem cell transplantation, has become a standard practice for treating numerous human and animal diseases. However, many other degenerative and cancerous diseases still lack adequate treatment options. Given that most tissues in a living organism contain stem cells, from embryonic to adult, there is a significant potential to extract these cells and investigate their properties to improve treatment options and extend longevity. However, the extraction of stem cells involves subjecting a living organism to surgical procedures, raising numerous ethical concerns.

Nevertheless, adult tissue of mesenchymal origin, such as adipose tissue, has been shown to be abundant in stem cells. They are relatively easy to obtain and multiply rapidly compared to other types of stem cells, making them a promising source for therapeutic applications (RUSSELL et al., 2016; VILLATORO et al., 2019; HUMENIK et al., 2022). These cells, known as mesenchymal stem cells (MSCs) of adipose tissue origin (AD-MSCs), have demonstrated the capacity to regenerate tissue across numerous species, including canines (VOGA et al., 2020; EL-HUSSEINY et al., 2022; PRIŠLIN et al., 2022). In 2008, canine adipose-derived mesenchymal stem cells (cAD-MSCs) were first extracted and documented, marking an essential development in veterinary regenerative medicine (NEUPANE et al., 2008).

Since then, numerous case studies have been documented showing good therapeutic outcomes and a low incidence of side effects following the application of cAD-MSCs (PRIŠLIN et al., 2022). Furthermore, as cAD-MSCs exhibit the ability to modulate immune responses, it is increasingly documented that they promote regeneration by secreting relevant molecules, i.e., the secretome (VILLATORO et al., 2019; TESHIMA et al., 2021). This area is currently the focus of most research, as it could provide the benefits of cell therapy without the associated side effects.

1.1. cAD-MSCs extraction

cAD-MSCs are found within the stromal vascular fraction (SVF) of adipose tissue, a heterogeneous mixture of cells that include blood cells, endothelial precursors, endothelial and smooth muscle cells, preadipocytes, pericytes, macrophages, adipocytes, and AD-MSCs (GUO et al., 2016; BORA and MAJUMDAR, 2017; RAMAKRISHNAN and BOYD, 2018) (Figure

1). Although adipocytes account for more than 90% of adipose tissue volume, SVF constitutes the majority of the total cell population (COHEN and SPIEGELMAN, 2016). Isolation of SVF typically involves mechanical disruption of connective tissue followed by enzymatic digestion using collagenase (HENDAWY et al., 2021). These methods aim to preserve the viability of stem cells and the vascular compartment (stromal cell niche) to maintain the therapeutic potential of SVF products (ANDIA et al., 2019). Enzymatic digestion, considered the "gold standard," offers a higher yield of individual cells with enhanced viability, while mechanical extraction better preserves cell-matrix interactions (VAN DONGEN et al., 2016; SENESI et al., 2019). After enzyme digestion, centrifugation separates SVF cells from mature adipocytes, producing a sediment that is cultured *in vitro*. In these conditions, cAD-MSCs exhibit adherence to plastic surfaces, allowing their isolation from nonadherent SVF cells to establish a "pure" cAD-MSC population, which should be further characterised (DOMINICI et al., 2006).

Tissue harvesting significantly affects the viability of SVF and AD-MSC, cell yield, and immunophenotype. Recent findings identified the periovarian region as the optimal site for the harvest of cAD-MSC, as it contains the highest number of viable CD90+ cells per gramme of adipose tissue compared to subcutaneous and falciform ligament sites (HENDAWY et al., 2021). Similar findings were reported in another study (ASTOR et al., 2013), which observed significantly fewer viable cells per gramme in adipose tissue collected from the falciform ligament compared to the thoracic wall and inguinal sites. Furthermore, age and reproductive status were identified as influential factors, with higher viability of SVF cells observed in dogs younger than 4.5 years and in intact (non-spayed) dogs compared to spayed ones. Young donors also exhibited higher population doubling rates and differentiation potential (LEE et al., 2017). These findings emphasise the importance of considering multiple factors, including tissue harvesting site, donor age, and reproductive status, to optimise the therapeutic potential of cAD-MSCs.

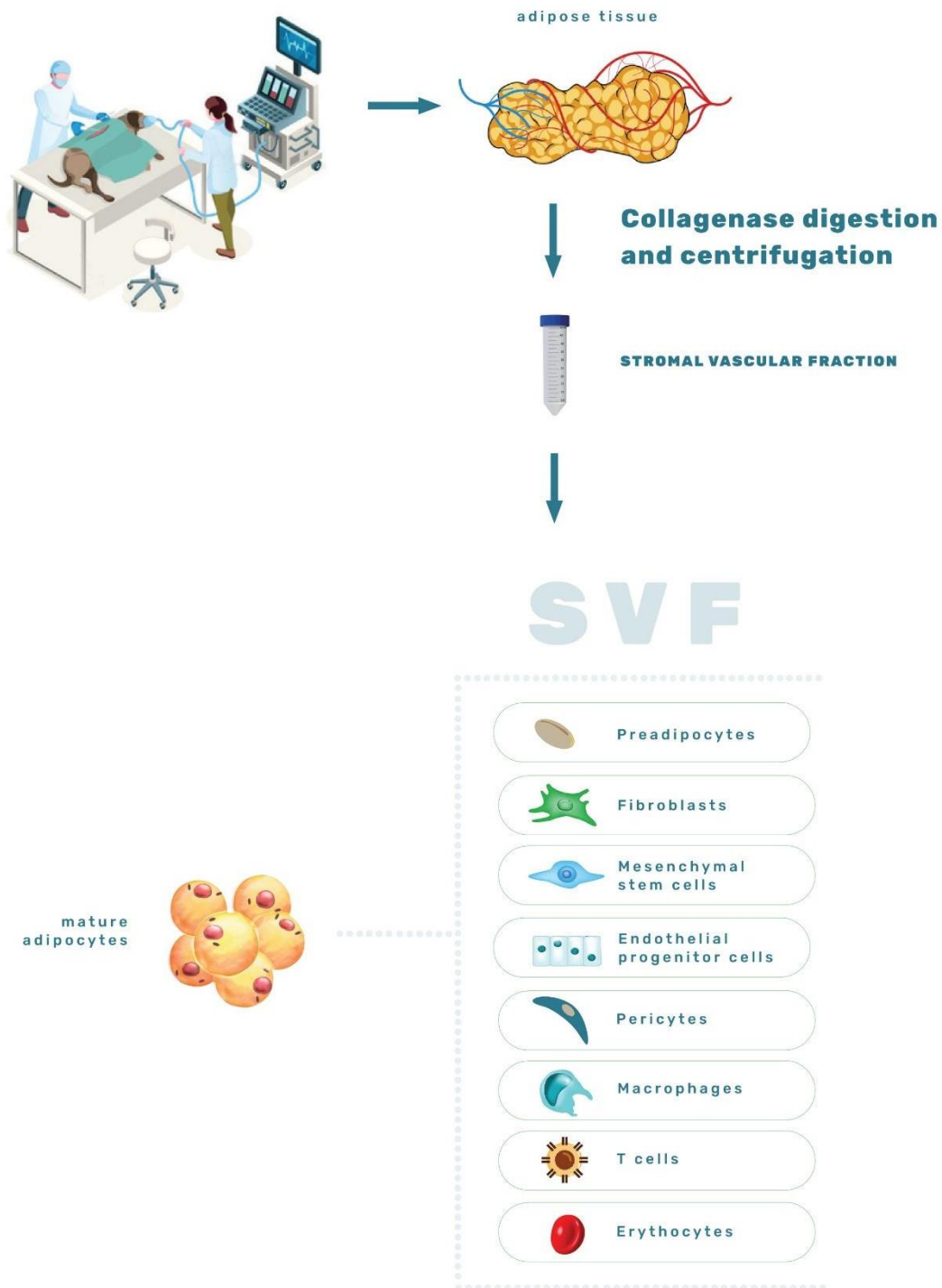


Figure 1. Graphical representation of the extraction and components of the stromal vascular fraction (PRIŠLIN et al., 2022).

1.2. cAD-MSCs characteristics

To establish the identity of mesenchymal stem cells (MSCs) in humans, the International Society for Cell Therapy (ISCT) has provided guidelines and recommendations (DOMINICI et

al., 2006). These criteria include the capacity for plastic adhesion and proliferation in culture, differentiation potential into osteogenic, chondrogenic, and adipogenic lineages *in vitro*, and the immunophenotypic presence of surface markers, i.e. clusters of differentiation (CDs) CD90, CD73, and CD105, while being negative for CD14, CD34, CD45, CD11b, CD19, and CD79 α . In 2023, the International Society for Stem Cell Research (ISSCR) further expanded these guidelines to include genomic characterisation, such as genome sequencing and karyotyping (LUDWIG et al., 2023). Despite the applicability of these criteria only to human stem cell research, there remains a pressing need to establish similar standards for canine MSCs. Until such criteria are developed, animal research will continue to adhere to the existing guidelines set for human MSCs.

The cAD-MSCs have repeatedly demonstrated their ability to adhere to plastic surfaces and proliferate under *in vitro* conditions (NEUPANE et al., 2008; VIEIRA et al., 2010). Additionally, it has been confirmed to differentiate into three lineages (RASHID et al., 2021). Several studies are extending their potential to differentiate into other cell types, including neuronal (BLECKER et al., 2017; PRPAR MIHEVC et al., 2020). However, there are discrepancies regarding the immunophenotype, specifically the proportion of positive cells within the culture and the lack of canine-specific antibodies for accurate detection. These immunophenotypic markers are associated with the promotion of growth, proliferation, migration, adhesion, differentiation, and cell survival (SANZ-RODRIGUEZ et al., 2004; JORDAN et al., 2015), as well as immunomodulation (TAN et al., 2019). All of these factors significantly contribute to the regenerative capacity and warrant further investigation in cAD-MSCs.

1.3. cAD-MSCs secretome

Based on most recent studies, the prospect of cellular regeneration is found in the paracrine activity of cAD-MSCs, called secretome (TRZYNA and BANAŚ-ZĄBCZYK, 2021; CHANDRA et al., 2022; MERLO and IACONO, 2023). The secretome encompasses soluble factors, including cytokines, growth factors, morphogens, chemokines, and nonsoluble factors, known as extracellular vesicles containing proteins, lipids, and RNAs (MERLO and IACONO, 2023). Formerly viewed as cellular debris, it is now established that these biomolecules play a pivotal role in modulating various biological processes such as cell proliferation, survival, differentiation, immunomodulation, anti-apoptosis, and angiogenesis (TRZYNA and BANAŚ-ZĄBCZYK, 2021). From the current point of view, the cAD-MSC secretome provides several advantages over cAD-MSC therapy, such as a lower risk of thrombosis and tumour formation

and easier manufacturing, handling and storage. Furthermore, the secretome could be mass-produced under controlled conditions, tailored for therapeutic effects, and stored for immediate use in acute conditions without the need for a donor or time-consuming cell expansion (VIZOSO et al., 2017; CHANDRA et al., 2022; MERLO and IACONO, 2023).

1.4. *In vitro* establishment of cAD-MSCs

To achieve and store therapeutic doses of cAD-MSCs and their secretome for therapy, *in vitro* culture is needed. The goal of successful expansion *in vitro* is to maintain stem cell identity and show repeated self-renewal, i.e., to undergo extensive proliferation while maintaining their multipotent differentiation potentials. However, throughout the long-term cultivation process, MSCs undergo replicative senescence, leading to a possible reduction or absence of positive therapeutic outcomes, as extensively reviewed in human research (YANG et al., 2018; LIU et al., 2020). Long-term cultivated MSCs undergo enlargement and adopt a hypertrophic morphology, aligning with significant changes in biological features, gene expression profile, differentiation, and immunomodulatory potential (LIU et al., 2020; WENG et al., 2022).

Unlike human MSCs, there has been limited research into the impact of *in vitro* ageing on the immunophenotype, gene expression and secretome profiles of cAD-MSCs. Previous research has contributed to a better understanding of gene expression changes during *in vitro* passages, albeit on a limited scale (KREŠIĆ et al., 2017), indicating the need for further investigation. To my knowledge, no data have been published on alterations in the secretome composition during the long-term culture of cAD-MSCs. To date, only two studies have focused on investigating the secretome of cAD-MSCs. The first study characterised soluble factors and exosomes, confirming their immunomodulatory potential (VILLATORO et al., 2019). The second study further demonstrated the immunosuppressive effects of cAD-MSCs secretome exosomes *in vitro* (TESHIMA et al., 2021). Therefore, the understanding of the effects of *in vitro* ageing on gene expression and secretome composition of cAD-MSCs remains to be fully elucidated.

1.5. Microbial sterility of *in vitro* established cAD-MSC cultures

Acquiring and storing cAD-MSCs and their secretomes in therapeutic quantities necessitates *in vitro* cultivation, a process that inherently introduces the risk of microbial contamination. Studies have indicated that stored MSC batches may become contaminated with bacteria, fungi, or viruses (MARTÍN et al., 2012; SZABŁOWSKA-GADOMSKA et al., 2023). Bacterial and fungal contamination can be effectively mitigated with antibiotics and

antimycotics (SZABŁOWSKA-GADOMSKA et al., 2023); however, mitigating potential viral contamination remains challenging. The available data indicate that MSCs can be permissive to infection with RNA and DNA viruses. Such infections may lead to a variety of adverse outcomes, including cell death, persistent infection, cellular transformation, and ultimately impairment of MSC functionality (SUNDIN et al., 2006; KHATRI et al., 2010; MA et al., 2011; NAZARI-SHAFTI et al., 2011; KHATRI and SAIF, 2013).

Viral infection of MSCs has been associated with inhibition of differentiation (ROY et al., 2020), increased secretion of pro-inflammatory cytokines (BEHZADI FARD et al., 2019), and loss of immunomodulatory function (MEISEL et al., 2014). In cAD-MSCs, a study reported the susceptibility to distemper virus (ALTAMIRANO-SAMANIEGO et al., 2022), and recent findings confirmed the possibility of viral contamination of cryobanked cAD-MSC batches by detecting canine parvovirus, influenza, parainfluenza, and canid alphaherpesvirus 1 (PEKKER et al., 2023).

Canid alphaherpesvirus 1 (CHV) belongs to the species *Varicellovirus canidalpha 1* within the *Orthoherpesviridae* family, whose genome consists of double-stranded DNA (ICTV, 2024). The latent and subclinical persistence of CHV in dogs poses a significant challenge, which could lead to infection oversight during routine clinical examination of cAD-MSC donors. Moreover, CHV is distributed globally, with seroprevalence ranging from 21.7% to 80% (DAHLBOM et al., 2009; KROGENÆS et al., 2012), and nearly one-third of dogs in Croatia have antibodies against CHV (GRACIN, 2020). The widespread prevalence of CHV poses a significant risk of transmission from donors or contamination during sampling and culturing processes.

Previous studies on human and equine MSCs have shown that herpesvirus infection can decrease the immunomodulatory effects of these cells (LA GARZA-RODEA et al., 2011; MEISEL et al., 2014; CLAESSEN et al., 2015). However, similar studies focusing on canine MSCs are currently lacking. Given the high seroprevalence of CHV and its potential to compromise the therapeutic efficacy of MSCs, it is imperative to explore the susceptibility and adaptability of cAD-MSCs to CHV. Such research could pave the way for the development of robust protocols to minimise viral contamination and preserve the functionality of MSCs in therapeutic applications.

1.6. cAD-MSCs in veterinary regenerative medicine

Stem cell therapy can be autologous, where the patient receives his own cells; allogeneic, where cells from a donor of the same species are used; or xenogeneic, where donor cells from

a different species are applied. The routes of administration (Figure 6) are varied, with intraarticular (IA), intravenous (IV), and acupuncture point-based methods being the most commonly used (BRONDEEL et al., 2021). A detailed description of the effects of cAD-MSC studies is provided in the following sections. These studies highlight the various therapeutic potentials of cAD-MSCs in different fields, including orthopaedics, neurology, dermatology, ophthalmology, and gastroenterology.

1.6.1. Orthopaedics

Numerous studies in this field suggest that the application of autologous and allogenic cAD-MSC reduces pain and lameness in dogs with osteoarthritis (OA) (YOON et al., 2012; VILAR et al., 2013; CUERVO et al., 2014; VILAR et al., 2016; YUN et al., 2016; SHAH et al., 2018; SRZENTIĆ DRAŽILOV et al., 2018; OLSEN et al., 2019; WITS et al., 2020; BRONDEEL et al., 2021). In 2018, scientists described the use of allogenic cAD-MSCs in 203 dogs, concluding that IA administration led to better outcomes compared to IV treatment in cases of polyarthritis. Age was found to be a factor, with most dogs under five years of age showing significant improvement (SHAH et al., 2018). Positive therapeutic outcomes were also observed in cases of chronic hip and elbow OA (GUERCIO et al., 2012; HARMAN et al., 2016; KRISTON-PÁL et al., 2017), and the application of cAD-MSCs significantly reduced symptoms of hip dysplasia in 60% of dogs one week after treatment (MARX et al., 2014). Furthermore, significant improvements were documented in semitendinosus myopathy after cAD-MSC therapy (BROWN et al., 2012; GIBSON et al., 2017), and improvement without side effects was also observed after long-term therapy with allogenic cAD-MSC in dog with rheumatoid arthritis (SEO et al., 2022). Recently, a study involving 245 dogs with various musculoskeletal pathologies, which had not been successfully treated with conventional therapy, resulted in statistically significant positive outcomes, including increased range of motion, reduced pain, and ultimately improved quality of life two years after local administration of autologous cAD-MSCs (ARMITAGE et al., 2023).

1.6.2. Neurology

In dogs with chronic spinal cord/intervertebral disc injury, percutaneous intraspinal transplantation of allogenic cAD-MSCs had no adverse effects or complications (infection, neuropathic pain, or worsening of neurological function) during the 16-week monitoring period. Furthermore, three dogs showed significant progress in movement and one dog walked completely without support (ESCALHÃO et al., 2017). In a study of lumbosacral spinal cord injury, allogeneic cAD-MSC transplantation in four dogs resulted in significant neurological

improvements with normal movement ability (4/4) and control of urine (3/4) three months after surgery and the first cAD-MSC transplant (CHEN et al., 2022). In cases of acute paraplegia, epidural cAD-MSC transplantation in conjunction with surgical decompression contributed to faster locomotor recovery and reduced postoperative hospitalisation (BACH et al., 2019). Furthermore, in cases of spontaneous degenerative lumbosacral stenosis in dogs with hindlimb paresis, the use of autologous cAD-MSCs cultured *in vitro* resulted in the return of independent walking for at least 4.5 years following cAD-MSC application, or for the duration of the study (SRZENTIĆ DRAŽILOV et al., 2018).

1.6.3. Dermatology

Stem cell treatment has also gained popularity in the treatment of skin pathologies. Systemic application of cAD-MSCs showed positive results in the treatment of drug-resistant atopic dermatitis for six months, without side effects (VILLATORO et al., 2018). The prospective role of cAD-MSCs was also evident in treating large acute skin defects where corrective surgery was not a viable option (ZUBIN et al., 2015). Furthermore, the healing of acute and chronic wounds in 24 dogs of various ages and breeds improved significantly in terms of contraction and reepithelialization in the cAD-MSC-treated group. Histopathological findings revealed a reduction in inflammatory infiltrates and the presence of multiple hair follicles seven days after cAD-MSC treatment (ENCISO et al., 2020). Furthermore, a double-blind, placebo-controlled evaluation of the efficacy of allogenic cAD-MSCs in treating atopic dermatitis in dogs did not show serious side effects in any patient, and treatment with high doses of cAD-MSCs was effective in alleviating clinical signs of atopic dermatitis for up to 30 days after the last subcutaneous application (KAUR et al., 2022).

1.6.4. Ophthalmology

Therapeutic applications of cAD-MSCs have been studied in dry keratoconjunctivitis (KCS). A study in 15 dogs with KCS revealed that a single application of cAD-MSCs to the lacrimal glands resulted in significant clinical improvement in all patients without side effects, and daily corticosteroid use was not required during the 12-month follow-up (BITTENCOURT et al., 2016). This result was further supported by another study applying cAD-MSCs to the conjunctival sac, further confirming the potential of cAD-MSCs as an adjunctive therapy in the treatment of KCS in both dogs and humans (SGRIGNOLI et al., 2019). In dogs diagnosed with deep corneal ulcers, subconjunctival application of cAD-MSCs resulted in complete healing of ulcerated wounds within 14 days in 22 out of 26 dogs, indicating that this therapy could be a simpler alternative to surgical intervention (FALCÃO et al., 2020). The use of allogenic cAD-

MSCs in chronic keratitis therapy also showed success, although more significant symptom improvement was observed in the control group treated with corticosteroids (PEREIRA et al., 2022).

1.6.5. Gastroenterology

In gastroenterological pathologies, cAD-MSC therapy has been tested for currently incurable inflammatory bowel disease (IBD). Administration of a single IV infusion of cAD-MSCs showed no side effects during the monitoring of 11 dogs, while nine out of 11 dogs were in clinical remission (PÉREZ-MERINO et al., 2015). Therefore, the study concluded that cAD-MSCs have a basis for clinical application in dogs with severe IBD. cAD-MSC therapy also showed success in treating immune-mediated chronic gastroenteropathies, with significant reductions in inflammatory markers, neutrophil count, lymphocytes, and platelets up to nine months after transplantation of allogenic cAD-MSCs (CRISTÓBAL et al., 2022).

1.6.6. Hepatology

Autologous transplantation of cAD-MSCs in dogs with liver diseases significantly improved liver function, reduced liver inflammatory biomarkers and exhibited effects associated with the stem cell immunomodulatory mechanisms (GARDIN et al., 2018; YAN et al., 2019). Furthermore, the reduction in inflammation was also observed following the application of allogenic cAD-MSCs in acute liver injury induced by carbon tetrachloride in dogs. After the first injection of cAD-MSC, the expression levels of pro-inflammatory cytokine genes decreased, while the expression of anti-inflammatory cytokine genes increased significantly, indicating a positive immunomodulatory effect of stem cells (TESHIMA et al., 2017).

1.6.7. Haematology

Recently, the use of allogenic cAD-MSCs has also been tested in the treatment of immune-mediated nonregenerative anaemia. The study was carried out on five dogs, all of whom showed significant improvement in red blood cell count after transplantation, without the need for further transfusions (MIZUNO et al., 2022).

1.6.8. Urology

A case of a two-year-old dog with a urethral fistula resulting from ureterolithiasis was treated using a combination of autologous micro-fragmented adipose tissue containing mesenchymal stem cells with platelet-rich plasma in addition to surgical repair (KARADJOLE et al., 2024). Treatment resulted in successful healing, highlighting its potential for implementation in urological procedures.

1.7. Current Advances and Status of Stem Cell Research in the Republic of Croatia

In the field of human regenerative medicine, Croatian researchers are actively investigating the therapeutic potential of stem cells. The Croatian Institute for Brain Research (CIBR) at the Faculty of Medicine of the University of Zagreb contributes significantly to the advancement of stem cell research, particularly within the domains of neuroscience and regenerative medicine. Current studies at CIBR focus on the regenerative capabilities of stem cells, with a highlight on the recently published studies of stem cell role in stroke recovery (STANČIN et al., 2023; LISJAK et al., 2024). Additionally, a collaborative effort with the Faculty of Veterinary Medicine of the University of Zagreb, focusses on Alzheimer's and Down syndrome diseases, with ongoing studies contributing to this critical field (ALIĆ et al., 2021; FERTAN et al., 2024). Significant advances have also been made in the research on human limbal stem cells, emphasising their characterisation, safety, and clinical effectiveness, particularly their mitotic processes and morphology (ZDRAVEVA et al., 2023a; ZDRAVEVA, et al., 2023b; ZEKUŠIĆ et al., 2023). They also investigated the potential of various scaffolds to support the adhesion and growth of limbal stem cells for corneal repair. Noteworthy progress has also been achieved in cancer and stem cell research (PERVAN et al., 2022; DERFI et al., 2024; SMOLJO et al., 2024) and dermatology as well (NANIĆ et al., 2022).

However, in Croatia, recent advances in veterinary regenerative medicine remain limited. Over the past five years, veterinary stem cell research has been conducted primarily at the Croatian Veterinary Institute, focussing on the properties of AD-MSCs (KREŠIĆ et al., 2017, 2019). This work has been further expanded through the Croatian Science Foundation Installation Project UIP-2019-04-2178, titled "Revealing the Mesenchymal Stem Cell Transcriptome and Secretome" which has generated valuable insights into AD-MSCs (KREŠIĆ et al., 2021; PRIŠLIN et al., 2022; PRIŠLIN et al., 2023; PRIŠLIN et al., 2024). At the Faculty of Veterinary Medicine, University of Zagreb, a limited number of studies have been carried out, including an *in vivo* study in hens and clinical research investigating autologous grafts of adipose tissue to treat bone fractures (ZEC GOSSAINN et al., 2023) and urethral fistula (KARADJOLE et al., 2024), respectively. These research gaps underscore the pressing need to establish robust research initiatives in veterinary regenerative medicine. Such efforts have significant potential not only for advancing animal health, but also for contributing to human medicine, as animals such as dogs serve as valuable models for studying human diseases.

2. HYPOTHESIS AND OBJECTIVES

The hypothesis of this doctoral dissertation posited that the molecular characteristics and secretome composition of cAD-MSCs will be maintained during both cultivation and infection with CHV in cell culture.

Given the lack of knowledge of the properties of cAD-MSCs during *in vitro* expansion, the general objective was to investigate the alterations in molecular characteristics and secretome composition of cAD-MSCs during cultivation and subsequent *in vitro* infection with CHV. Specific objectives of this study included:

1. Characterising the immunophenotypic and functional properties of cAD-MSCs *in vitro*.
2. Analysing the changes in gene expression and secretome composition of cAD-MSCs at two distinct time points *in vitro*.
3. Evaluating the susceptibility of cAD-MSCs to CHV infection *in vitro*.
4. Analysing the alterations in gene expression and secretome composition of cAD-MSCs following CHV infection *in vitro*.

3. MATERIAL AND METHODS

3.1. Canine adipose tissue donors

The dogs included in the research were clinically healthy and elective abdominal surgery was performed at the Faculty of Veterinary Medicine of the University of Zagreb and the Veterinary Clinic Buba in Zagreb. The doctoral dissertation encompassed a total of 20 samples of canine adipose tissue. Scientific Papers I, II, and III analysed eight, nine, and twelve samples, respectively, with the details of cAD-MSC donors outlined in Table 1. In Paper III, some donor cells from Paper II were utilised again, as the focus of Paper III was to investigate the effects of CHV infection on cAD-MSCs. This study did not necessitate freshly collected cells; therefore, previously extracted and cryopreserved donor cells were employed as well as the additional three donors. On the contrary, the cryopreserved donor cells from Paper I were not utilised, due to insufficient cAD-MSC stock. Abdominal adipose tissue samples were collected from postoperative biological waste in sterile screw-capped tubes. The samples were transported at 4°C within two hours of collection and subsequently subjected to extraction. Detailed information on the donors' adipose tissue collection site and/or adipose tissue mass can be found in Table 2 of Paper I and Table 1 of Papers II and III.

Table 1. Canine adipose tissue donor information.

No	DONOR	SEX	AGE (Months)	BREED	SCIENTIFIC PAPER
1	4/20	Female	12	Medium poodle	Paper I
2	5/20	Female	14,5	Ridgeback	Paper I
3	6/20	Female	6	Dachshund short- haired	Paper I
4	7/20	Female	9	Mixed breed	Paper I
5	8/20	Female	9	Beagle	Paper I
6	9/20	Female	9	Jack Russell Terrier	Paper I
7	11/20	Female	36	Belgian Shepherd	Paper I

8	13/20	Female	38	Mixed breed	Paper I
9	6/21	Female	12	German Spaniel	Paper II, III
10	7/21	Female	6	Miniature Schnauzer	Paper III
11	8/21	Female	12	Mixed	Paper III
12	9/21	Female	12	Labrador Retriever	Paper II, III
13	13/21	Female	7	Toy Poodle	Paper II, III
14	14/21	Female	7	Toy Poodle	Paper II, III
15	1/22	Female	10	Jack Russell Terrier	Paper II, III
16	2/22	Female	6	Lagotto Romagnolo	Paper II, III
17	3/22	Female	12	Medium Poodle	Paper II, III
18	6/22	Female	60	Portuguese Water Dog	Paper II, III
19	7/22	Female	36	Mixed	Paper II, III
20	8/22	Male	12	German Shepard	Paper III

3.2. Extraction and propagation of cAD-MSCs *in vitro*

Methods for extracting and propagating cAD-MSCs were detailed in Paper I, with modifications described in Papers II and III. Briefly, the adipose tissue sample was enzymatically degraded and centrifuged. The residue was resuspended in a basal medium consisting of 79% Dulbecco's Minimum Essential Medium with Low Glucose (DMEM Low Glucose) (Gibco, Gibco, Waltham, MA, USA, Cat. No. 31885049), 20% foetal bovine serum (FBS) (Gibco, Cat. No. 1027010) and 1% penicillin/streptomycin (Sigma-Aldrich, St. Louis, MO, USA, Cat. No. P4333-100ML) in cell culture flasks (Thermo Fisher Scientific, Waltham, MA, USA) at 37°C. Following extraction, the sterility of the cell supernatant was tested, specifically for aerobic and anaerobic bacteria, fungi, and mycoplasma. Furthermore, all cAD-MSCs used in Paper III were tested for CHV, with the full protocol described in the respective paper. Confluent adherent cells were designated as zero passage (P0) and were further passaged

until proliferation arrest. All donor cells were cryobanked following the standard cryobanking procedure with 10% dimethyl sulfoxide (Sigma–Aldrich, Cat. No. D2650-100ML) in P2 or P3.

3.3. Immunophenotyping of cAD-MSCs during *in vitro* cultivation

Immunophenotyping was thoroughly detailed in Paper I, with modifications and updates provided in Paper II. The procedures had to adhere to the stem cell identification criteria established by ISCT (DOMINICI et al., 2006). Briefly, to validate the immunophenotype of cAD-MSCs, Paper I assessed the immunophenotypic characteristics of undifferentiated cAD-MSCs from passages P1 to P6. Meanwhile, Papers II and III utilised immunophenotyping only in P3 to confirm stem cell identity. Using the BD FACSVerser instrument (BD, Franklin Lakes, NJ, USA), performance quality control was maintained using CS&T beads (BD, Cat. No. 656504) before each experiment. A single stain labelling approach was employed for immunophenotyping, and the antibody panel is detailed in Tables 3 of Paper I and 2 of Paper II. Experimental conditions were calibrated with unstained cells and kept consistent across all test tubes. Cell viability was assessed with a propidium iodide staining solution (BD, Cat. No. 556463). Data files were gated using the method described method in Paper I. The FACSuite software analysed 10,000 collected events, presenting results regarding median fluorescence intensity (MFI) and percentage of positive cells.

3.4. Multipotency *in vitro* testing of cAD-MSCs during culture

Multipotency testing was comprehensively described in Paper I, with subsequent modifications outlined in Paper II. Following the stem cell identification criteria of the ISCT (DOMINICI et al., 2006), multipotency testing of the cAD-MSCs was performed at P3 in Papers I, II, and III. As detailed in Paper I, the multipotency of established cAD-MSCs was evaluated through trilineage differentiation, which includes adipogenic, osteogenic, and chondrogenic lineages. In summary, cells were cultured in triplicate in a 24-well plate (Nunc, Thermo Fisher Scientific) with a basal medium. The medium was replaced with special differentiation media for each lineage after reaching confluence. Chondrogenic differentiation was induced in spheroid form within 15 mL conical polypropylene tubes (Deltalab, Barcelona, Spain). The control wells were maintained in basal media. Specialised staining methods were employed to detect lipid droplets, alkaline phosphatase activity, and aggrecan. Post-staining, slides or cells were examined using an Axio Observer D1 inverted microscope (Zeiss, Jena, Germany), with images captured by a Zeiss camera (AxioCam ER/105/208/HD, Zeiss) at total magnifications ranging from 50x to 200x.

3.5. Gene expression profiling of cAD-MSCs during *in vitro* cultivation

Gene expression analysis using a quantitative reverse transcription polymerase chain reaction (RT-qPCR) array was performed after total RNA extraction at two-time points during *in vitro* culture, P3 and P6. The experimental procedure adhered to the methodology outlined in Paper I, with certain modifications, described in Paper II. Briefly, total RNA extraction was performed using the RNeasy Mini Kit (Qiagen, Hilden, Germany, Cat. No. 74106). The RNA integrity score and the 28S:18S ratio were determined using the QIAxcel RNA QC Kit (Qiagen, Cat. No. 50-727-743) using the QIAxcel Advanced instrument (Qiagen) according to the manufacturer's instructions. Genomic DNA elimination and complementary DNA synthesis were performed using the RT2 First Strand kit (Qiagen, Cat. No. 330401) following the manufacturer's protocol on Biometra TRIO (Analytik Jena, Jena, Germany) thermal cycler.

Subsequently, a commercially available RT2 Profiler™ PCR Array for Dog Mesenchymal Stem Cells (PAFD-082ZR, Qiagen) with SYBR Green-optimised primer assays (Qiagen, Cat. No. 330603) was used for gene expression analysis, according to the manufacturer's instructions for Rotor-Gene Q (Qiagen). After data acquisition, normalisation and in-depth analysis were performed using the specialised RT2 Profiler PCR Array Data Analysis software, accessible online at <https://dataanalysis2.qiagen.com/pcr>. Gene expression profiling data are publicly available in the NCBI Gene Expression Omnibus (GEO) database (Accession Number GSE255585). The complete analysis report is attached as Supplementary Material 1 in Paper II.

3.6. Proteomic analysis of the cAD-MSC secretome during *in vitro* culture

As detailed in Paper II, the alterations in the proteome composition of the cAD-MSCs secretome during *in vitro* culture were assessed at two specific time points, P3 and P6, in six randomly selected donors (6/21, 9/21, 14/21, 1/22, 6/22, and 7/22). In summary, cells were conditioned in 2 mL of 100% DMEM Low Glucose. After 48 hours, the secretome was carefully collected, centrifuged, filtered, and preserved at -80°C until proteomic analysis. Following a previously published protocol (Isola et al., 2011), proteomic analysis was conducted using liquid chromatography with tandem mass spectrometry (LC-MS/MS). The secretome proteins were reduced and extracted from the culture medium. Protein concentrations were adjusted using the Bradford assay, followed by enzyme digestion and peptide separation using the EASY-nLC 1200 system (Thermo Fisher Scientific). The mass spectra were recorded using a Q Exactive Plus Hybrid Quadrupole-Orbitrap (Thermo Fisher Scientific) tandem mass spectrometer.

Raw data analysis was performed using Scaffold Quant Q+S 5.3.0, employing protein sequence data from the *Canis lupus familiaris* reference proteome. Statistical significance was verified via t-tests, with $p < 0.05$ considered significant. Mass spectrometry proteomics data was deposited with the ProteomeXchange consortium through the PRIDE partner repository (PEREZ-RIVEROL et al., 2022) with the dataset identifier PXD049324. Bioinformatic analysis of the detected proteins was performed using Gene Ontology (GO) Panther 18.0 bioinformatic tool.

3.7. Infection of cAD-MSCs with CHV *in vitro*

3.7.1. Isolation and characterisation of autochthonous wild-type CHV

The autochthonous wild-type CHV strain 29107 was obtained from the organs (liver, spleen, and lungs) of a 6-day-old golden retriever undergoing routine CHV diagnostics at the Croatian Veterinary Institute. The detailed protocol for the isolation and characterisation of autochthonous wild-type CHV is described in Paper III.

3.7.2. Verification of the autochthonous wild-type CHV strain by NGS

To verify autochthonous wild-type CHV strain 29107 and generate its whole genome sequence, next-generation sequencing (NGS) on the NextSeq 550 sequencer (Illumina Inc., Cat. No. SY-415-1002) platform was performed following the complete methodology detailed in Paper III. The genome sequence of the autochthonous wild-type CHV strain 29107 was deposited in NCBI GenBank under accession number PP349830.

3.7.3. In vitro infection of cAD-MSCs with wild-type CHV

To demonstrate successful CHV infection in cultured cAD-MSCs, a cohort of six donors (9/21, 13/21, 14/21, 2/22, 3/22, and 7/22) was randomly chosen for five consecutive viral passage experiments with the detailed methodology outlined in Paper III. Briefly, cryopreserved cAD-MSCs were utilised at passages P2 or P3 for CHV infection experiments. Following thawing and expansion, cells from each donor were distributed in 24-well plates at a density of 10^5 cells per well and cultured until they reached 90% confluence. Three wells per donor were inoculated with CHV at a multiplicity of infection (MOI) of 0.5. After a two-hour adsorption period, basal medium was added to the inoculum. The infection was monitored until the cytopathic effect (CPE) reached 80% or a maximum of 120 hours if CPE was minimal or absent. The plates were then frozen at -80°C . After centrifugation and filtration, supernatants were stored in cryovials. Subsequent CHV passages were initiated using 500 μL of the previous passage as inoculum. Five viral passages were performed for each cAD-MSC donor and control cell line (MDCK), with the progression of CPE documented using microscopy (Axio Observer

D1, Zeiss) and the live imaging Lux2 live imaging platform, Axion BioSystems, Atlanta, GA, USA). Supernatants from each passage, both CHV-infected and uninfected, were stored at -80°C for further qPCR analysis.

3.7.4. Quantification of CHV DNA with qPCR

To confirm successful CHV infection, viral DNA in the supernatant of infected cAD-MSCs was quantified as detailed in Paper III. CHV genome copies were measured by quantitative PCR (qPCR), using a 5-point standard curve. Additionally, the method's limits of detection (LOD) and quantification (LOQ) were defined.

3.7.5. Gene expression profiling of *in vitro* CHV-infected cAD-MSCs

Gene expression analysis via RT-qPCR array was conducted on P3 of CHV-infected and uninfected cAD-MSCs from 12 donors following the method described in Paper III. In brief, two T75 flasks were incubated until cAD-MSCs reached 90% confluence. A flask was inoculated with CHV stock at an MOI of 0.5, allowing a two-hour adsorption period, while the second flask served as a negative control. Twenty-four hours after infection, total RNA extraction and gene expression profiling and analysis were performed following the method described in Section 3.6. Gene expression profile data were publicly deposited in the NCBI Gene Expression Omnibus database under accession number GSE267402. The complete analysis report is attached as Supplementary Material 1 in Paper III.

3.7.6. Proteomic analysis of the *in vitro* CHV-infected cAD-MSCs secretome

The alterations in the proteomic composition of the secretome of cAD-MSCs were analysed in P3 under two conditions: uninfected and CHV-infected cAD-MSCs. This analysis was carried out using samples from six randomly selected donors (6/21, 9/21, 14/21, 1/22, 6/22 and 7/22). The methodology used was detailed in paragraph 3.7, with modifications described in Paper III. The results were further analysed using GO Panther and STRING bioinformatic tools. Mass spectrometry proteomics data have been deposited with the ProteomeXchange consortium via the PRIDE partner repository (PEREZ-RIVEROL et al., 2022) under the dataset identifier PXD052289.

3.8. Statistical analysis

Detailed descriptions of each statistical software, method, and criterion applied can be found in the respective individual papers. All data were visualised with GraphPad Prism 10 (v10). Statistical significance was defined at $p < 0.05$, and the results were presented as mean \pm SEM unless otherwise indicated.

3.9. Ethics approval and consent to participate

The scientific research included in the doctoral dissertation was evaluated and approved by the Ethics Board of the Croatian Veterinary Institute, approval code Z-IV-4-2022/19, May 9, 2019, and the Veterinary Ethics Committee at the Faculty of Veterinary Medicine, University of Zagreb, approval code 640-01/20-17/10, February 20, 2020, 640-01/20-17/55, September 28, 2020, and 640-01/22-02/07, April 20, 2022. The owners provided written informed consent before sampling.

4. RESULTS

4.1. Paper I

KREŠIĆ, N., M. PRIŠLIN, D. VLAHOVIĆ, P. KOSTEŠIĆ, I. LJOLJE, D. BRNIĆ, N. TURK, A. MUSULIN, B. HABRUN (2021): The Expression Pattern of Surface Markers in Canine Adipose-Derived Mesenchymal Stem Cells. *Int. J. Mol. Sci.* 22 (14), 7476:1-19. doi: 10.3390/ijms22147476

The results presented in Paper I (KREŠIĆ et al., 2021) address Specific Objective 1 by characterising the immunophenotypic and functional properties of cAD-MSCs *in vitro*. The functional properties were validated through trilineage differentiation, demonstrating adipogenic, osteogenic, and chondrogenic potential as presented in Figures 1-3. Additionally, this study provides the first comprehensive analysis of immunophenotypic markers in cAD-MSCs throughout the entire *in vitro* cultivation process, examining eight key markers: CD90, CD44, CD73, CD29, CD271, CD105, CD45, and CD14. The expression results, illustrated in Figures 4 and 5, reveal several alterations in the expression of the surface markers. In particular, only CD73 expression demonstrated significant changes in later passages (P4, P5 and P6). In general, in Paper I, cAD-MSCs met the criteria recommended by ISCT and were comprehensively characterised in terms of their immunophenotype and trilineage differentiation potential.

4.2. Paper II

PRIŠLIN, M., A. BUTORAC, R. BERTOŠA, V. KUNIĆ, I. LJOLJE, P. KOSTEŠIĆ, D. VLAHOVIĆ, Š. NALETILIĆ, N. TURK, D. BRNIĆ (2024): In vitro aging alters the gene expression and secretome composition of canine adipose-derived mesenchymal stem cells. *Front. Vet. Sci.* 11, 1387174:1-12. doi: 10.3389/fvets.2024.1387174

The findings in Paper II (PRIŠLIN et al., 2024) address Specific Objective 2 by analysing changes in gene expression and secretome composition changes in cAD-MSCs at two distinct *in vitro* time points. Gene expression analysis showed a significant down-regulation of the *IL10* and *PTPRC* between P3 and P6, with non-significant fluctuations in stemness, MSC-specific, MSC-associated, and MSC-differentiation gene categories, as depicted in Figure 2.

The analysis of secretome composition identified notable alterations, with nine biologically significant downregulated proteins and 12 upregulated proteins as presented in Figure 4. Furthermore, 63 and 52 proteins were unique to P3 and P6, respectively, as detailed in the Supplementary Material Data Sheet 2. GO Panther Pathways analysis of the distinct protein groups revealed critical pathways affected by *in vitro* ageing. Proteins in Group P3, which were lost during *in vitro* ageing, were significantly associated with pathways such as cytoskeletal regulation by Rho GTPase, inflammation mediated by chemokine and cytokine signalling, and Wnt signalling. On the contrary, proteins secreted in Group P6, representing the secretome of aged cAD-MSCs *in vitro*, were linked to pathways related to metabolic salvage and blood coagulation. Summarily, *in vitro* cultivation of cAD-MSCs, as published in the results of Paper II, led to alterations in gene expression and secretome composition.

4.3. Paper III

PRIŠLIN ŠIMAC, M., Š. NALETILIĆ, V. KOSTANIĆ, V. KUNIĆ, T. M. ZOREC, M. POLJAK, D. VLAJ, R. KOGOJ, N. TURK, D. BRNIĆ (2024): Canid alphaherpesvirus 1 infection alters the gene expression and secretome profile of canine adipose-derived mesenchymal stem cells in vitro. Virol. J., 21, 335:1-18. doi: 10.1186/s12985-024-02603-8

The results presented in Paper III (PRIŠLIN ŠIMAC et al., 2024) contribute to Specific Objectives 3 and 4 by evaluating the susceptibility of cAD-MSCs to CHV infection *in vitro* and analysing the subsequent alterations in gene expression and secretome composition following CHV infection. Paper III demonstrated that CHV infects cAD-MSCs from all 12 experimental donors, as shown in Figure 2C. Canine AD-MSCs exhibited similar cytopathogenic effects (CPE), with focal cell rounding and clustering, creating empty spaces between the cells. CPE developed within 24-48 hours post-infection (p.i.), with the typical CPE observed in 100% of the cell monolayer at 72-96 hours p.i., as illustrated in Figure 2B and Additional file 4. Gene expression analysis after CHV infection *in vitro* revealed significant alterations in 20.9% (18/85) of the genes assessed, with specific changes in 16.7% (1/6) of the stemness genes, 33.3% (6/18) of the MSC-specific genes, 25.8% (8/31) of the MSC-associated genes, and 9.7% (3/31) of the MSC differentiation genes as presented in Figure 4. Analysis of the cAD-MSC secretome revealed that, among commonly secreted proteins, 10 were significantly down-regulated, while 66 were significantly up-regulated (Figure 5D and Additional file 6). Of the proteins with distinctive secretion patterns, 13.2% of the total proteins showed unique

expression: 105 proteins were specific to uninfected samples and 51 proteins were specific to CHV-infected samples as detailed in Additional File 6. Bioinformatic analyses, including GO enrichment and STRING analysis, were performed to explore the involvement of these proteins in various pathways. The results of the GO enrichment analysis are presented in Table 2, while the findings of the STRING analysis are provided in Table 3 and Figure 5F. Overall, the results presented in Paper III demonstrate that cAD-MSCs are susceptible to CHV infection *in vitro*. Subsequent analysis of gene expression and secretome composition revealed significant alterations following infection.

5. DISCUSSION

In vitro culture is crucial for obtaining and preserving therapeutic quantities of cAD-MSCs and their secretome. However, this process carries certain risks, such as cellular alterations and microbial contamination. Prolonged primary cultures usually result in cellular senescence, which may impair the regenerative and immunomodulatory functions of cAD-MSCs. There is a significant gap in understanding how *in vitro* propagation affects both cAD-MSCs and their secretory products, such as the secretome. Furthermore, every transplantation procedure poses the risk of transmitting microorganisms. Although bacterial and fungal contamination can typically be controlled with antibiotics and antifungals, viral contamination remains a significant challenge. To address this knowledge gap, this doctoral dissertation aimed to investigate the alterations in molecular characteristics and secretome composition of cAD-MSCs during cultivation and subsequent *in vitro* infection with CHV. The hypothesis proposed that cAD-MSCs would retain their regenerative properties under these conditions. However, the results presented in Papers I, II, and III collectively refute this hypothesis.

Initially, isolated cells in all three studies had to comply with the criteria stipulated by the ISCT for the identification of human stem cells (DOMINICI et al., 2006), given the absence of standardised criteria for verifying canine stem cells. The criteria of plastic adherence and *in vitro* proliferation have been proven in previous studies (KREŠIĆ et al., 2017; VOGA et al., 2021) and in all three studies conducted in this doctoral dissertation. However, the immunophenotype and multipotency remained insufficiently explored, necessitating further investigation to establish the reproducibility and standardisation of cAD-MSCs. Paper I addressed this gap by focussing on one of the specific objectives of this dissertation: the characterisation of the immunophenotypic and functional properties of cAD-MSCs *in vitro*. This was achieved by investigating the surface marker expression of cAD-MSCs up to the passage in which proliferation arrest is typically observed, which was the first study of the immunophenotype of cAD-MSCs conducted in all passages during *in vitro* ageing. Paper II further corroborated the effects of *in vitro* ageing on cAD-MSCs, which addressed another specific objective of this doctoral dissertation: analysing changes in gene expression and secretome composition of cAD-MSCs at two distinct time points *in vitro*.

The study presented in Paper I confirmed the trilineage differentiation potential of cAD-MSCs (Figures 1–3, Paper I) and identified alterations in the expression of several surface markers during *in vitro* culture. During *in vitro* culture, cAD-MSCs undergo proliferation arrest, which is marked by morphological changes such as increased cell size and granularity (KREŠIĆ

et al., 2017). According to our results, cAD-MSCs showed insignificant alterations of CD90, CD44, CD29, CD271, CD105, CD45, and CD14 markers, while the expression of CD73 significantly decreased during later passages (P4-P6) of *in vitro* cultivation (Figure 4, Paper I). Considering cell enlargement during *in vitro* ageing, a study found that CD73+ AD-MSCs are mainly small cells, whereas CD73- AD-MSCs are large cells (LI et al., 2013). Therefore, this finding warrants further investigation into the correlation between cell size and surface marker expression. Nevertheless, the expression of CD73 could aid the immunomodulatory effects of MSC therapies (TAN et al., 2019). Consequently, the expression pattern of CD73 under our conditions indicates the need to carefully consider the time that cells spend *in vitro* and the time in which cells are transplanted into patients or animal models.

Apart from notable changes in the CD73 expression pattern, other ISCT-recommended surface markers showed insignificant but attention-worthy variability. The CD90, associated with stemness (MORAES et al., 2016) showed a slight overall increase in protein expression during *in vitro* ageing, mainly due to donor 13/20 (Figure 4, Paper I). Other donors exhibited decreased expression of CD90, similar to the study by MORAES et al., 2016. The observed differences in cellular proliferation may explain this variability since donor 13/20 showed prolonged proliferation. Furthermore, the expression of the *CD90* gene was down-regulated, although no statistical differences were observed. In Paper II, where a different set of nine donors was involved, a nonsignificant upregulation of the *CD90/THY1* gene was found in subsequent passages. These discrepancies could probably be intraspecies variabilities, highlighting the need for more breed-specific studies.

Another ISCT marker, CD105, whose gene expression was shown to be stable, decreased during *in vitro* propagation (Figure 4, Paper I), which is in line with findings in murine MSCs, where it was negatively affected by passage number (ANDERSON et al., 2013). However, CD105 is highly involved in angiogenesis and could benefit regenerating tissue (DUFF et al., 2003), indicating that earlier passages could be more favourable for therapy. Additionally, the surface markers CD44 and CD29 were highly and consistently expressed during *in vitro* culture (Figure 4, Paper I), and had a slight increase at the gene expression level. These findings are in correlation with the high expression of CD44 in canine umbilical cord-derived MSCs (LEE et al., 2013) and corroborate previous findings of CD29 observed in both canine bone marrow MSCs and cAD-MSCs (TAKEMITSU et al., 2012; KREŠIĆ et al., 2017).

Although CD271, like CD44 and CD29, is not proposed to conform to the ISCT immunophenotype guidelines, it is proposed as a universal marker for the extraction of human bone marrow and AD-MSCs (ÁLVAREZ-VIEJO, 2015). Furthermore, this marker is suggested

as a primary choice for tissue regeneration and autologous stem cell therapies in human subjects (CUEVAS-DIAZ DURAN et al., 2013). In cAD-MSCs, low levels of CD271 through *in vitro* culture demonstrate that this rule cannot be attributed to the canine population (Figure 4, Paper I).

The ISCT-negative markers CD14 and CD45 were very low or undetectable during *in vitro* expansion (Figure 4, Paper I), with less than 5% of the cells expressing the markers, adhering to ISCT criteria. Moreover, the expression of the *CD45 / PTPRC* gene was also not significantly altered as reported in Paper I (Table 1, Paper I). However, in Paper II, *CD45 / PTPRC* gene expression was shown to be significantly down-regulated even though immunophenotyping in a Paper II study revealed the absence of CD45 protein on the surface of cAD-MSCs in all donors during the P3 stage. The possible cause for this discrepancy could be in the initial heterogeneity of adipose tissue SVF, which can lead to variabilities in surface marker expression, including *CD45/PTPRC*, at the beginning of *in vitro* expansion (HENDAWY et al., 2021). The CD45⁺ cells in SVF cannot adequately proliferate during *in vitro* expansion, so the expression could decrease or even diminish with *in vitro* ageing and lead to natural purification of cAD-MSCs. Furthermore, the appearance of this gene in earlier cAD-MSC passage could be explained by another hypothesis, which is based on the fact that CD34⁺ cells can express *PTPRC/CD45* gene (AYABE et al., 2022). The CD34⁺ marker was additionally investigated in Paper II during standard *in vitro* immunophenotype tests in P3. It was revealed that 4% of the extracted cells were CD34⁺, which is consistent with similar observations reported elsewhere (SCREVEN et al., 2014; VOGA et al., 2021). Nevertheless, both of these hypotheses should be further explored during *in vitro* ageing, depending on the availability of canine-specific antibodies.

As detailed in Paper II, the analysis of 84 genes revealed that 21 genes were downregulated, while 10 genes were upregulated. Among these, only the previously mentioned *CD45/PTPRC* and *IL10* showed statistically significant downregulation (Figure 2, Paper II). Both are not proven to be expressed by MSCs and may originate from various cell types within the SVF (HENDAWY et al., 2021). Therefore, down-regulation of these two genes in later passages, such as P6, may result from the absence of these cells. *IL10* is an immune regulatory cytokine with profound anti-inflammatory functions produced by various immune and non-immune cells (IYER and CHENG, 2012). Moreover, coexpression of *IL10* in MSCs was shown to be beneficial, contributing to anti-inflammatory activity in humans and canines (CHOI et al., 2008; NAKAJIMA et al., 2017; SONG et al., 2019; NITAHARA-KASAHARA et al., 2021; HERVÁS-SALCEDO et al., 2023; KUANG et al., 2023). Therefore, these findings suggest that

the observed expression of *IL10* in earlier passages, such as P3, may confer beneficial effects on inflammation, which could disappear with *in vitro* ageing.

The influence of *in vitro* ageing was further expanded to the secretome composition of cAD-MSCs in Paper II, which revealed significant alterations. To the best of my knowledge, the study in Paper II represents the first investigation into the impact of prolonged passages of cAD-MSCs on secretome composition. Furthermore, it significantly contributes to expanding the limited database on the secretome of cAD-MSCs. Most detected proteins and their functional characteristics were shared between early and late passages (P3 and P6) (Figure 3, Paper II). Similar observations were documented in the secretome and exosomes of feline AD-MSCs (VILLATORO et al., 2021), canine bone marrow MSCs, and cAD-MSCs comparative study (VILLATORO et al., 2019). However, a notable functional difference was observed for the group of distinctively expressed proteins (10% of detected proteins) in each passage (Group P3 and Group P6) (Supplementary Material Data Sheet, Paper II).

First, proteins detected in Group P3 exhibited substantial involvement in Rho GTPase cytoskeletal regulation, which plays pivotal roles in diverse cellular processes, encompassing gene expression, cytoskeletal dynamics, survival, cell division, cell adhesion, polarity, and vesicle trafficking (ZHANG et al., 2021). As cells age, these events decrease, consistent with the cellular quiescence observed in the later passage of the Paper II study (P6). Furthermore, Group P3 proteins displayed a significant association with the nicotinic acetylcholine receptor, Wnt, and CCKR signalling pathways, which play crucial roles in MSC regenerative function (ALQAHTANI et al., 2023), cell proliferation/apoptosis inhibition (MA et al., 2019), and adipocyte differentiation (PLAZA et al., 2018), respectively. The last but significant finding within Group P3 proteins is associated with inflammation mediated by the chemokine and cytokine signalling, regulating the trafficking and migration of immune cells (NATIONAL, 2024). On the other hand, Group P6 proteins were significantly associated with the blood coagulation pathway. Given the apparent pro-thrombotic role, it is imperative to emphasise stringent control of culture passages prior to administration to prevent adverse coagulation events (GUILLAMAT-PRATS, 2022).

In addition to analysing groups of distinctive proteins detected in P3 or P6, our investigation revealed significant modifications in a subset of shared proteins across both passages, comprising 21 entities that exhibited significant up- or down-regulation (Figure 4, Paper II). In particular, the down-regulated proteins in P6 (HSP70, SRSF1, SERPINB1 and COQ10B), solely, were intricately associated with stem cell regenerative pathways in the treatment of various diseases (CHEN et al., 2015; OUAAMARI et al., 2016; LI et al., 2019;

WANG et al., 2022; PLESA et al., 2023). The results of the studies from Papers I and II, coupled with corroborating evidence on human MSCs (YANG et al., 2018; LIU et al., 2020), underscore the need for caution when extending cAD-MSCs to later passages.

The caution regarding *in vitro* cultivation was further reinforced in Paper III, since the expansion of cAD-MSCs poses a potential risk of microbial contamination, including viral pathogens. Therefore, the study in Paper III aimed to evaluate the susceptibility of cAD-MSCs to CHV infection *in vitro* and further analyse the alterations in gene expression and secretome composition of cAD-MSCs after CHV infection *in vitro*. To the best of my knowledge, this study represents the first investigation of the effects of viral infection on the gene expression and secretome profile of cAD-MSCs. To achieve this aim, an autochthonous CHV strain was established. This strain should reflect the natural virus-host interplay more accurately than CHV strains *in vitro*. The novel complete genome sequence of the autochthonous CHV strain from Croatia contributes to the knowledge of the complete genome diversity of CHV. Before this contribution, the GenBank database contained 22 complete CHV genome sequences, with only five sequences from Europe, three from the United Kingdom, and two from Italy.

In vitro susceptibility to CHV, as indicated by the characteristic CPE of *Orthoherpesviridae* viruses (SUCHMAN and BLAIR, 2007), was observed in cAD-MSCs and MDCK cells (Figure 2A-B; Additional files 2 and 4, Paper III). However, successive passages of CHV in cAD-MSCs exhibited a gradual reduction and disappearance of CPE. This observation was supported by the decrease in, yet persistent, CHV genome copy numbers (Figure 2C, Paper III) in the supernatants of cell lysates, suggesting abortive infection. Abortive infection has recently been documented in *in vitro* research on herpes simplex virus (COHEN et al., 2020), which proves that herpesviruses can infect non-neuronal cells, remain quiescent, and be reactivated, challenging the current paradigm of herpesvirus latency. Our results resemble the above scenario, but further experimental validation is needed to assign abortive infection status to this specific virus-host interaction.

The effects of CHV infection on cAD-MSCs were further explored at the gene expression level, and the results revealed that CHV infection significantly affected the expression of researched genes (Figure 4, Paper III). Up-regulated genes were associated with proliferation (HAN et al., 2014), differentiation (PARK et al., 2019), and immunosuppressive response (RUBTSOV et al., 2017; YANG et al., 2018; DENG et al., 2022). Similar alterations in gene expression attributed to virus infections have been documented in previous studies on human stem cells infected with Parvovirus B19 and Cytomegalovirus (LI et al., 2014; BEHZADI FARD et al., 2019). The most significantly upregulated gene in infected cAD-MSCs, *TNF*

(Figure 4C, Paper III), encodes a protein responsible for various cellular processes, including proliferation, differentiation, and, interestingly, immune suppression in MSCs (YAN et al., 2018; YANG et al., 2018). It remains unclear whether canine MSCs can produce TNF; however, in human MSCs, there is clear evidence of their inability to produce TNF (BERK et al., 2010). Nevertheless, cAD-MSCs are progenitors of adipocytes, and adipocytes and their progenitors are well known for secreting TNF (CAWTHORN and SETHI, 2008). In this study, high *TNF* production combined with alterations in other genes primarily suggested increased adipocyte differentiation in CHV-infected cells. Moreover, the upregulation of *ADIPOQ* and *NOTCH1* (NEDVÍDKOVÁ et al., 2005; SHAN et al., 2017) coupled with the downregulation of several genes related to stemness and regenerative capacity (TANABE et al., 2016; ENCISO et al., 2018; WANG et al., 2018; CAO et al., 2020) further support the initiation of differentiation processes, predominantly adipogenesis, in CHV-infected cAD-MSCs. These findings indicate that CHV infection can drive cAD-MSC differentiation, affecting its regenerative potential and altering its typical stem cell properties.

The proteomic composition of the cAD-MSC secretomes further corroborated the initiation of adipogenesis in CHV-infected cells observed at the RNA level. The GO enrichment analysis of the uninfected group revealed that proteins significantly involved in the WNT signalling pathway were absent in CHV-infected cells (Table 2, Paper III). This finding suggests that CHV infection leads to the loss of the WNT signalling pathway, and its deactivation in MSCs is considered crucial for inducing adipogenesis (LING et al., 2009; VISWESWARAN et al., 2015). Furthermore, both GO enrichment and STRING analyses (Tables 2 and 3, Paper III) revealed the presence of essential protein pathways involved in cell self-renewal, structure, survival, homing, and migration (ZHANG et al., 2021; ALQAHTANI et al., 2023) in the uninfected group, which were lost after CHV infection. These losses at the proteomic level align with the microscopically observed loss of cellular structure, survival, and migration following the development of CPE (Figure 2; Additional files 2 and 4, Paper III).

The observed microscopic reduction in cell survival was further supported by GO enrichment and STRING findings from the cAD-MSC secretomes of the CHV-infected group. These findings revealed upregulated glycolysis and elevated levels of proteins associated with the enolase and pyruvate metabolism pathways (Tables 2 and 3, Paper III). The takeover of the host cell's resources and metabolic machinery by this virus prioritises the production of viral particles over normal cellular functions, ultimately leading to cell damage and death. Similar alterations were previously documented in studies on viral host interactions in other

Orthoherpesviridae infections, such as human cytomegalovirus infections (MORENO et al., 2022) and herpes simplex virus (ZHUO et al., 2017; KUN-VARGA et al., 2023) infections.

Apart from providing valuable results and insights, the findings of this doctoral dissertation open some questions warranting further research and validation. The results presented in Paper I suggest that additional studies are required to explore interspecies variability and the involvement of other unexplored markers such as CD34 during *in vitro* ageing. The proteomic analyses in Papers II and III are currently limited by the availability of canine-specific reagents, such as monoclonal antibodies, which will be essential to confirm the significant proteomic alterations occurring in the cAD-MSCs secretome as they become available. Furthermore, Paper III underscores the need for a deeper investigation of the interactions of cAD-MSC and CHV, particularly focusing on transcriptomic and secretomic changes between serial passages, testing the abortive infection hypothesis, and exploring the occurrence of viral genome variants after infection of cAD-MSCs. Nevertheless, standardising the identity of cAD-MSCs *in vitro* remains crucial, much like the ISCT (DOMINICI et al., 2006) and ISSCR (LUDWIG et al., 2023) guidelines for human MSCs, to fully understand regenerative mechanisms and therapeutic possibilities.

As the role of canines as valued companions continues to grow, advancing research on cAD-MSCs is essential, laying the groundwork for future investigations that will ultimately improve stem cell therapies for canines and humans. By deepening our understanding of their properties and therapeutic potential, we can improve treatments for a wide range of canine and human health conditions, ensuring more effective and customised regenerative medicine.

6. CONCLUSIONS

1. The immunophenotypic and functional properties of *in vitro* cultured cAD-MSCs remain stable for surface markers CD90, CD105, CD44 and CD29 except for CD73, while the expression of CD45, CD14, and CD271 was not detected. The decreased CD73 expression due to *in vitro* ageing suggests that earlier passages may be more optimal for therapeutic applications.
2. *In vitro* ageing significantly alters the gene expression and proteomic profile of the cAD-MSC secretome. The early passages (P3) show enriched regenerative and immunomodulatory proteins, while the late passages (P6) exhibit increased coagulation pathway activity and reduced regenerative proteins. These findings highlight the importance of selecting early passages to maintain the regenerative potential and safety of cAD-MSCs.
3. The susceptibility of cAD-MSCs, as indicated by the characteristic CPE of Orthoherpesviridae viruses, to autochthonous CHV strain was confirmed in all infected donors. However, successive passages of CHV on cAD-MSCs exhibited a gradual reduction and disappearance of CPE, indicating abortive infection, which should be further explored.
4. CHV infection significantly alters the gene expression and secretome composition of cAD-MSCs, with genomic variations suggesting potential impacts on their stemness, migration, and functional properties. Gene expression and secretome analyses indicate a shift toward an adipogenic phenotype, which could impair its regenerative capacity. These findings underscore the importance of screening batches of cAD-MSC for CHV before therapeutic use.

7. BIBLIOGRAPHY

- ALIĆ, I., P.A. GOH, A. MURRAY, E. PORTELIUS, E. GKANATSIU, G. GOUGH, K.Y. MOK, D. KOSCHUT, R. BRUNMEIR, Y.J. YEAP, N.L. O'BRIEN, J. GROET, X. SHAO, S. HAVLICEK, N.R. DUNN, H. KVARTSBERG, G. BRINKMALM, R. HITHERSAY, C. STARTIN, S. HAMBURG, M. PHILLIPS, K. PERVUSHIN, M. TURMAINE, D. WALLON, A. ROVELET-LECRUX, H. SOININEN, E. VOLPI, J.E. MARTIN, J.N. FOO, D.L. BECKER, A. ROSTAGNO, J. GHISO, Ž. KRŠNIK, G. ŠIMIĆ, I. KOSTOVIĆ, D. MITREČIĆ, A. STRYDOM, E. FISHER, F. WISEMAN, D. NIZETIC, J. HARDY, V. TYBULEWICZ, A. KARMILOFF-SMITH, P.T. FRANCIS, K. BLENNOW, A. STRYDOM, J. HARDY, H. ZETTERBERG and D. NIŽETIĆ (2021): Patient-specific Alzheimer-like pathology in trisomy 21 cerebral organoids reveals BACE2 as a gene dose-sensitive AD suppressor in human brain. *Mol. Psychiatry* 26, 5766–5788. doi:10.1038/s41380-020-0806-5
- ALQAHTANI, S., M.C. BUTCHER, G. RAMAGE, M.J. DALBY, W. MCLEAN and C.J. NILE (2023): Acetylcholine Receptors in Mesenchymal Stem Cells. *Stem Cells Dev.* 32, 47–59. doi:10.1089/scd.2022.0201
- ALTAMIRANO-SAMANIEGO, F., J. ENCISO-BENAVIDES, N. ROJAS, J.M. IGLESIAS-PEDRAZ, N. ENCISO, M. FOSSATTI and J. ENCISO (2022): First report of canine morbillivirus infection of adipose tissue-derived stem cells from dogs with distemper. *Vet. World* 15, 1835–1842. doi:10.14202/vetworld.2022.1835-1842
- ÁLVAREZ-VIEJO, M. (2015): CD271 as a marker to identify mesenchymal stem cells from diverse sources before culture. *World J. Stem Cells* 7, 470. doi:10.4252/wjsc.v7.i2.470
- ANDERSON, P., A.B. CARRILLO-GÁLVEZ, A. GARCÍA-PÉREZ, M. COBO and F. MARTÍN (2013): CD105 (Endoglin)-Negative Murine Mesenchymal Stromal Cells Define a New Multipotent Subpopulation with Distinct Differentiation and Immunomodulatory Capacities. *PLoS One* 8, 1–13. doi:10.1371/journal.pone.0076979
- ANDIA, I., N. MAFFULLI and N. BURGOS-ALONSO (2019): Stromal vascular fraction technologies and clinical applications. *Expert Opin. Biol. Ther.* 19, 1289–1305. doi:10.1080/14712598.2019.1671970
- ARMITAGE, A.J., J.M. MILLER, T.H. SPARKS, A.E. GEORGIU and J. REID (2023): Efficacy of autologous mesenchymal stromal cell treatment for chronic degenerative musculoskeletal conditions in dogs: A retrospective study. *Front. Vet. Sci.* 9, 1014687. doi: 10.3389/fvets.2022.1014687

- ASTOR, D.E., M.G. HOELZLER, R. HARMAN and R.P. BASTIAN (2013): Patient factors influencing the concentration of stromal vascular fraction (SVF) for adipose-derived stromal cell (ASC) therapy in dogs. *Can. J. Vet. Res.* 77, 177–182.
- AYABE, T., M. HISASUE, Y. YAMADA, S. NITTA, K. KIKUCHI, S. NEO, Y. MATSUMOTO, R. HORIE and K. KAWAMOTO (2022): Characterisation of canine CD34+/CD45 diminished cells by colony-forming unit assay and transcriptome analysis. *Front. Vet. Sci.* 9, 936623:1–11. doi:10.3389/fvets.2022.936623
- BACH, F.S., C.L.K. REBELATTO, L. FRACARO, A.C. SENEGAGLIA, F.Y.I. FRAGOSO, D.R. DAGA, P.R.S. BROFMAN, C.T. PIMPÃO, J.R. ENGRACIA FILHO, F. MONTIANI-FERREIRA and J.A. VILLANOVA (2019): Comparison of the Efficacy of Surgical Decompression Alone and Combined With Canine Adipose Tissue-Derived Stem Cell Transplantation in Dogs With Acute Thoracolumbar Disk Disease and Spinal Cord Injury. *Front. Vet. Sci.* 6, 1–11. doi:10.3389/fvets.2019.00383
- BEHZADI FARD, M., S. KAVIANI and A. ATASHI (2019): Parvovirus B19 Infection in Human Bone Marrow Mesenchymal Stem Cells Affects Gene Expression of IL-6 and TNF- α and also Affects Hematopoietic Stem Cells Differentiation. *Indian J. Hematol. Blood Transfus.* 35, 765–772. doi:10.1007/s12288-019-01097-7
- BERK, L.C.J. VAN DEN, B.J.H. JANSEN, K.G.C. SIEBERS-VERMEULEN, H. ROELOFS, C.G. FIGDOR, G.J. ADEMA and R. TORENSMA (2010): Mesenchymal stem cells respond to TNF but do not produce TNF. *J. Leukoc. Biol.* 87, 283–289. doi:10.1189/jlb.0709467
- BITTENCOURT, M.K.W., M.A. BARROS, J.F.P. MARTINS, J.P.C. VASCONCELLOS, B.P. MORAIS, C. POMPEIA, M.D. BITTENCOURT, K.D.S. EVANGELHO, I. KERKIS and C. V. WENCESLAU (2016): Allogeneic Mesenchymal Stem Cell Transplantation in Dogs with Keratoconjunctivitis Sicca. *Cell Med.* 8, 63–77. doi:10.3727/215517916x693366
- BLECKER, D., M.I. ELASHRY, M. HEIMANN, S. WENISCH and S. ARNHOLD (2017): New Insights into the Neural Differentiation Potential of Canine Adipose Tissue-Derived Mesenchymal Stem Cells. *J. Vet. Med. Ser. C Anat. Histol. Embryol.* 46, 304–315. doi:10.1111/ahe.12270
- BORA, P. and A.S. MAJUMDAR (2017): Adipose tissue-derived stromal vascular fraction in regenerative medicine: A brief review on biology and translation. *Stem Cell Res. Ther.* 8, 1–10. doi:10.1186/s13287-017-0598-y
- BRONDEEL, C., G. PAUWELYN, E. DE BAKKER, J. SAUNDERS, Y. SAMOY and J.H.

- SPAAS (2021): Review: Mesenchymal Stem Cell Therapy in Canine Osteoarthritis Research: “Experientia Docet” (Experience Will Teach Us). *Front. Vet. Sci.* 8, 1–13. doi:10.3389/fvets.2021.668881
- BROWN, G.S., J.R. HARMAN and L.L. BLACK (2012): Adipose-derived stem cell therapy for severe muscle tears in working German shepherds: Two case reports. *Stem Cell Discov.* 02, 41–44. doi:10.4236/scd.2012.22007
- CAO, Z., Y. XIE, L. YU, Y. LI and Y. WANG (2020): Hepatocyte growth factor (HGF) and stem cell factor (SCF) maintained the stemness of human bone marrow mesenchymal stem cells (hBMSCs) during long-term expansion by preserving mitochondrial function via the PI3K/AKT, ERK1/2, and STAT3 signaling pathways. *Stem Cell Res. Ther.* 11, 329. doi:10.1186/s13287-020-01830-4
- CAWTHORN, W.P. and J.K. SETHI (2008): TNF- α and adipocyte biology. *FEBS Lett.* 582, 117–131. doi:10.1016/j.febslet.2007.11.051
- CHANDRA, V., P. MANKUZHY and T. SHARMA G (2022): Mesenchymal Stem Cells in Veterinary Regenerative Therapy: Basic Physiology and Clinical Applications. *Curr. Stem Cell Res. Ther.* 17, 237–251. doi:10.2174/1574888x16666210804112741
- CHEN, C.C., S.F. YANG, I.K. WANG, S.Y. HSIEH, J.X. YU, T.L. WU, W.J. HUANG, M.H. SU, H.L. YANG, P.C. CHANG, A.C. TENG, C. CHIA-YI and S.L. LIANG (2022): The Long-Term Efficacy Study of Multiple Allogeneic Canine Adipose Tissue-Derived Mesenchymal Stem Cells Transplantations Combined With Surgery in Four Dogs With Lumbosacral Spinal Cord Injury. *Cell Transplant.* 31, 9636897221081487. doi:10.1177/09636897221081487
- CHEN, Y. Bin, Y.W. LAN, L.G. CHEN, T.T. HUANG, K.B. CHOO, W.T.K. CHENG, H.S. LEE and K.Y. CHONG (2015): Mesenchymal stem cell-based HSP70 promoter-driven VEGFA induction by resveratrol alleviates elastase-induced emphysema in a mouse model. *Cell Stress Chaperones* 20, 979–989. doi:10.1007/s12192-015-0627-7
- CHOI, J.J., S.A. YOO, S.J. PARK, Y.J. KANG, W.U. KIM, I.H. OH and C.S. CHO (2008): Mesenchymal stem cells overexpressing interleukin-10 attenuate collagen-induced arthritis in mice. *Clin. Exp. Immunol.* 153, 269–276. doi:10.1111/j.1365-2249.2008.03683.x
- CLAESSEN, C., H. FAVOREEL, G. MA, N. OSTERRIEDER, C. DE SCHAUWER, S. PIEPERS and G.R. VAN DE WALLE (2015): Equid herpesvirus 1 (EHV1) infection of equine mesenchymal stem cells induces a pUL56-dependent downregulation of select cell surface markers. *Vet. Microbiol.* 176, 32–39. doi:10.1016/j.vetmic.2014.12.013

- COHEN, E.M., N. AVITAL, M. SHAMAY and O. KOBILER (2020): Abortive herpes simplex virus infection of nonneuronal cells results in quiescent viral genomes that can reactivate. *Proc. Natl. Acad. Sci. U. S. A.* 117, 635–640. doi:10.1073/pnas.1910537117
- COHEN, P. and B.M. SPIEGELMAN (2016): Cell biology of fat storage. *Mol. Biol. Cell* 27, 2523–2527. doi:10.1091/mbc.e15-10-0749
- CRISTÓBAL, J.I., F.J. DUQUE, J. USÓN-CASAÚS, R. BARRERA, E. LÓPEZ and E.M. PÉREZ-MERINO (2022): Complete Blood Count-Derived Inflammatory Markers Changes in Dogs with Chronic Inflammatory Enteropathy Treated with Adipose-Derived Mesenchymal Stem Cells. *Animals* 12, 2798. doi:10.3390/ani12202798
- CUERVO, B., M. RUBIO, J. SOPENA, J.M. DOMINGUEZ, J. VILAR, M. MORALES, R. CUGAT and J.M. CARRILLO (2014): Hip osteoarthritis in dogs: A randomized study using mesenchymal stem cells from adipose tissue and plasma rich in growth factors. *Int. J. Mol. Sci.* 15, 13437–13460. doi:10.3390/ijms150813437
- CUEVAS-DIAZ DURAN, R., M.T. GONZÁLEZ-GARZA, A. CARDENAS-LOPEZ, L. CHAVEZ-CASTILLA, D.E. CRUZ-VEGA and J.E. MORENO-CUEVAS (2013): Age-related yield of adipose-derived stem cells bearing the low-affinity nerve growth factor receptor. *Stem Cells Int.* 2013, 372164. doi: 10.1155/2013/372164
- DAHLBOM, M., M. JOHNSON, V. MYLLYS, J. TAPONEN and M. ANDERSSON (2009): Seroprevalence of canine herpesvirus-1 and *Brucella canis* in Finnish breeding kennels with and without reproductive problems. *Reprod. Domest. Anim.* 44, 128–131. doi:10.1111/j.1439-0531.2007.01008.x
- DENG, J., D. LI, X. HUANG, W. LI, F. ZHAO, C. GU, L. SHEN, S. CAO, Z. REN, Z. ZUO, J. DENG and S. YU (2022): Interferon- γ enhances the immunosuppressive ability of canine bone marrow-derived mesenchymal stem cells by activating the TLR3-dependent IDO/kynurenine pathway. *Mol. Biol. Rep.* 49, 8337–8347. doi:10.1007/s11033-022-07648-y
- DERFI, K.V., T. VASILJEVIC, T. DRAGICEVIC and T.M. GLAVAN (2024): Mithramycin targets head and neck cancer stem cells by inhibiting Sp1 and UFMylation. *Cancer Cell Int.* 24, 412. doi:10.1186/s12935-024-03609-6
- DOMINICI, M., K. LE BLANC, I. MUELLER, I. SLAPER-CORTENBACH, F.C. MARINI, D.S. KRAUSE, R.J. DEANS, A. KEATING, D.J. PROCKOP and E.M. HORWITZ (2006): Minimal criteria for defining multipotent mesenchymal stromal cells. The International Society for Cellular Therapy position statement. *Cytotherapy* 8, 315–317. doi:10.1080/14653240600855905

- DONGEN, J.A. VAN, H.P. STEVENS, M. PARVIZI, B. VAN DER LEI and M.C. HARMSSEN (2016): The fractionation of adipose tissue procedure to obtain stromal vascular fractions for regenerative purposes. *Wound Repair Regen.* 24, 994–1003. doi:10.1111/wrr.12482
- DUFF, S.E., C. LI, J.M. GARLAND and S. KUMAR (2003): CD105 is important for angiogenesis: evidence and potential applications. *FASEB J.* 17, 984–992. doi:10.1096/fj.02-0634rev
- EL-HUSSEINY, H.M., E.A. MADY, M.A.Y. HELAL and R. TANAKA (2022): The Pivotal Role of Stem Cells in Veterinary Regenerative Medicine and Tissue Engineering. *Vet. Sci.* 9, 648. doi:10.3390/vetsci9110648
- ENCISO, N., L. AVEDILLO, M.L. FERMÍN, C. FRAGÍO and C. TEJERO (2020): Cutaneous wound healing: Canine allogeneic ASC therapy. *Stem Cell Res. Ther.* 11, 1–14. doi:10.1186/s13287-020-01778-5
- ENCISO, N., L.L.K. OSTRONOFF, G. MEJÍAS, L.G. LEÓN, M.L. FERMÍN, E. MERINO, C. FRAGIO, L. AVEDILLO and C. TEJERO (2018): Stem cell factor supports migration in canine mesenchymal stem cells. *Vet. Res. Commun.* 42, 29–38. doi:10.1007/s11259-017-9705-x
- ESCALHÃO, C.C.M.I., I.P. RAMOS, C. HOCHMAN-MENDEZ, T.H.K. BRUNSWICK, S.A.L. SOUZA, B. GUTFILEN, R.C. DOS SANTOS GOLDENBERG and T. COELHO-SAMPAIO (2017): Safety of allogeneic canine adipose tissue-derived mesenchymal stem cell intraspinal transplantation in dogs with chronic spinal cord injury. *Stem Cells Int.* 2017, 3053759. doi: 10.1155/2017/3053759
- FALCÃO, M.S.A., H. dos S.S. BRUNEL, M.A.S. PEIXER, B.S.L. DALLAGO, F.F. COSTA, L.M. QUEIROZ, P. CAMPBELL and P.F. MALARD (2020): Effect of allogeneic mesenchymal stem cells (MSCs) on corneal wound healing in dogs. *J. Tradit. Complement. Med.* 10, 440–445. doi:10.1016/j.jtcme.2019.04.006
- FERTAN, E., D. BÖKEN, A. MURRAY, J.S.H. DANIAL, J.Y.L. LAM, Y. WU, P.A. GOH, I. ALIĆ, M.R. CHEETHAM, E. LOBANOVA, Y.P. ZHANG, D. NIŽETIĆ and D. KLENERMAN (2024): Cerebral organoids with chromosome 21 trisomy secrete Alzheimer's disease-related soluble aggregates detectable by single-molecule-fluorescence and super-resolution microscopy. *Mol. Psychiatry* 29, 369–386. doi:10.1038/s41380-023-02333-3
- GARDIN, C., L. FERRONI, G. BELLIN, G. RUBINI, S. BAROSIO and B. ZAVAN (2018): Therapeutic potential of autologous adipose-derived stem cells for the treatment of liver disease. *Int. J. Mol. Sci.* 19, 1–27. doi:10.3390/ijms19124064

- GIBSON, M.A., S.G. BROWN and N.O. BROWN (2017): Semitendinosus myopathy and treatment with adipose-derived stem cells in working German shepherd police dogs. *Can. Vet. J.* 58, 241–246.
- GRACIN, K. (2020): Dijagnostika herpesvirusne infekcije u pasa u Republici Hrvatskoj i njezin utjecaj na poremećaje reprodukcije. Ph.D. Thesis. University of Zagreb, Veterinary Faculty
- GUERCIO, A., P. DI MARCO, S. CASELLA, V. CANNELLA, L. RUSSOTTO, G. PURPARI, S. DI BELLA and G. PICCIONE (2012): Production of canine mesenchymal stem cells from adipose tissue and their application in dogs with chronic osteoarthritis of the humeroradial joints. *Cell Biol. Int.* 36, 189–194. doi:10.1042/cbi20110304
- GUILLAMAT-PRATS, R. (2022): Role of Mesenchymal Stem/Stromal Cells in Coagulation. *Int. J. Mol. Sci.* 23, 10393:1–10. doi:10.3390/ijms231810393
- GUO, J., A. NGUYEN, D.A. BANYARD, D. FADAVI, J.D. TORANTO, G.A. WIRTH, K.Z. PAYDAR, G.R.D. EVANS and A.D. WIDGEROW (2016): Stromal vascular fraction: A regenerative reality? Part 2: Mechanisms of regenerative action. *J. Plast. Reconstr. Aesthetic Surg.* 69, 180–188. doi:10.1016/j.bjps.2015.10.014
- HAN, S.H., G. JANG, B.K. BAE, S.M. HAN, Y.R. KOH, J.O. AHN, W.S. JUNG, S.K. KANG, J.C. RA, H.W. LEE and H.Y. YOUN (2014): Effect of ectopic OCT4 expression on canine adipose tissue-derived mesenchymal stem cell proliferation. *Cell Biol. Int.* 38, 1163–1173. doi:10.1002/cbin.10295
- HARMAN, R., K. CARLSON, J. GAYNOR, S. GUSTAFSON, S. DHUPA, K. CLEMENT, M. HOELZLER, T. MCCARTHY, P. SCHWARTZ and C. ADAMS (2016): A prospective, randomized, masked, and placebo-controlled efficacy study of intraarticular allogeneic adipose stem cells for the treatment of osteoarthritis in dogs. *Front. Vet. Sci.* 3, 1–10. doi:10.3389/fvets.2016.00081
- HENDAWY, H., A. UEMURA, D. MA, R. NAMIKI, H. SAMIR, M.F. AHMED, A. ELFADADNY, H.M. EL-HUSSEINY, C. CHIEH-JEN and R. TANAKA (2021): Tissue harvesting site effect on the canine adipose stromal vascular fraction quantity and quality. *Animals* 11, 460:1–14. doi:10.3390/ani11020460
- HERVÁS-SALCEDO, R., M. FERNÁNDEZ-GARCÍA, M. HERNANDO-RODRÍGUEZ, C. SUÁREZ-CABRERA, J.A. BUEREN and R.M. YÁÑEZ (2023): Improved efficacy of mesenchymal stromal cells stably expressing CXCR4 and IL-10 in a xenogeneic graft versus host disease mouse model. *Front. Immunol.* 14, 1062086:1–15. doi:10.3389/fimmu.2023.1062086

- HUMENIK, F., M. MALOVESKA, N. HUDAKOVA, P. PETROUSKOVA, L. HORNAKOVA, M. DOMANIZA, D. MUDRONOVA, S. BODNAROVA and D. CIZKOVA (2022): A Comparative Study of Canine Mesenchymal Stem Cells Isolated from Different Sources. *Animals* 12, 1502. doi:10.3390/ani12121502
- ICTV (2024): *Varicellovirus* Taxonomy. <https://ictv.global/report/chapter/orthoherpesviridae/orthoherpesviridae/varicellovirus>; accessed: 03/25/2024
- IYER, S.S. and G. CHENG (2012): Role of interleukin 10 transcriptional regulation in inflammation and autoimmune disease. *Crit. Rev. Immunol.* 32, 23–63. doi:10.1615/critrevimmunol.v32.i1.30
- JORDAN, A.R., R.R. RACINE, M.J.P. HENNIG and V.B. LOKESHWAR (2015): The Role of CD44 in Disease Pathophysiology and Targeted Treatment. *Front. Immunol.* 6, 182. doi:10.3389/fimmu.2015.00182
- KARADJOLE, T., I. BUTKOVIĆ, A. DIMOVA, V. MOLNAR, J. ŠAVORIĆ, G. BAČIĆ and D. PRIMORAC (2024): Stone-induced urethral fistula treatment with microfragmented adipose tissue containing mesenchymal stem cells: a case report from veterinary medicine with potential application in humans. *Croat. Med. J.* 65, 288–293. doi:10.3325/cmj.2024.65.288
- KAUR, G., A. RAMIREZ, C. XIE, D. CLARK, C. DONG, C. MAKI, T. RAMOS, F. IZADYAR, S.O.L. NAJERA, J. HARB and J. HAO (2022): A double-blinded placebo-controlled evaluation of adipose-derived mesenchymal stem cells in treatment of canine atopic dermatitis. *Vet. Res. Commun.* 46, 251–260. doi:10.1007/s11259-021-09853-9
- KHATRI, M., T.D. O'BRIEN, S.M. GOYAL and J.M. SHARMA (2010): Isolation and characterization of chicken lung mesenchymal stromal cells and their susceptibility to avian influenza virus. *Dev. Comp. Immunol.* 34, 474–479. doi:10.1016/j.dci.2009.12.008
- KHATRI, M. and Y.M. SAIF (2013): Influenza virus infects bone marrow mesenchymal stromal cells in vitro: Implications for bone marrow transplantation. *Cell Transplant.* 22, 461–468. doi:10.3727/096368912x656063
- KREŠIĆ, N., M. PRIŠLIN, D. VLAHOVIĆ, P. KOSTEŠIĆ, I. LJOLJE, D. BRNIĆ, N. TURK, A. MUSULIN and B. HABRUN (2021): The Expression Pattern of Surface Markers in Canine Adipose-Derived Mesenchymal Stem Cells. *Int. J. Mol. Sci.* 22, 7476. doi:10.3390/ijms22147476
- KREŠIĆ, N., I. ŠIMIĆ, I. LOJKIĆ and T. BEDEKOVIĆ (2017): Canine Adipose Derived Mesenchymal Stem Cells Transcriptome Composition Alterations: A Step towards

- Standardizing Therapeutic. Stem Cells Int. 2017, 4176292,1–12. doi:10.1155/2017/4176292
- KREŠIĆ, N., I. ŠIMIĆ, I. LOJKIĆ and T. BEDEKOVIĆ (2019): Mezenhimske matične stanice u veterinarskoj medicini. Vet. stanica 50, 149–154.
- KRISTON-PÁL, É., Á. CZIBULA, Z. GYURIS, G. BALKÁ, A. SEREGI, F. SÜKÖSD, M. SÜTH, E. KISS-TÓTH, L. HARACSKA, F. UHER and É. MONOSTORI (2017): Characterization and therapeutic application of canine adipose mesenchymal stem cells to treat elbow osteoarthritis. Can. J. Vet. Res. 81, 73–78.
- KROGENÆS, A., V. ROOTWELT, S. LARSEN, E.K. SJØBERG, B. AKSELSEN, T.M. SKÅR, S.S. MYHRE, L.H.M. RENSTRÖM, B. KLINGEBORN and A. LUND (2012): A serologic study of canine herpes virus-1 infection in the Norwegian adult dog population. Theriogenology 78, 153–158. doi:10.1016/j.theriogenology.2012.01.031
- KUANG, P.P., X.Q. LIU, C.G. LI, B.X. HE, Y.C. XIE, Z.C. WU, C.L. LI, X.H. DENG and Q.L. FU (2023): Mesenchymal stem cells overexpressing interleukin-10 prevent allergic airway inflammation. Stem Cell Res. Ther. 14, 369:1–15. doi:10.1186/s13287-023-03602-2
- KUN-VARGA, A., B. GUBÁN, V. MIKLÓS, S. PARVANEH, M. GUBA, D. SZÚCS, T. MONOSTORI, J. VARGA, Á. VARGA, Z. RÁZGA, Z. BATA-CSÖRGŐ, L. KEMÉNY, K. MEGYERI and Z. VERÉB (2023): Herpes Simplex Virus Infection Alters the Immunological Properties of Adipose-Tissue-Derived Mesenchymal-Stem Cells. Int. J. Mol. Sci. 24, 11989. doi:10.3390/ijms241511989
- LA GARZA-RODEA, A.S. DE, M.C. VERWEIJ, H. BOERSMA, I. VAN DER VELDE-VAN DIJKE, A.A.F. DE VRIES, R.C. HOEBEN, D.W. VAN BEKKUM, E.J.H.J. WIERTZ and S. KNAÄN-SHANZER (2011): Exploitation of herpesvirus immune evasion strategies to modify the immunogenicity of human mesenchymal stem cell transplants. PLoS One 6, e14493. doi:10.1371/journal.pone.0014493
- LEE, J., K.S. LEE, C.L. KIM, J.S. BYEON, N.Y. GU, I.S. CHO and S.H. CHA (2017): Effect of donor age on the proliferation and multipotency of canine adipose-derived mesenchymal stem cells. J. Vet. Sci. 18, 141–148. doi:10.4142/jvs.2017.18.2.141
- LEE, K.S., S.H. CHA, H.W. KANG, J.Y. SONG, K.W. LEE, K.B. KO and H.T. LEE (2013): Effects of serial passage on the characteristics and chondrogenic differentiation of canine umbilical cord matrix derived mesenchymal stem cells. Asian-Australasian J. Anim. Sci. 26, 588–595. doi:10.5713/ajas.2012.12488
- LI, Q., L.J. QI, Z.K. GUO, H. LI, H.B. ZUO and N.N. LI (2013): CD73+ adipose-derived

- mesenchymal stem cells possess higher potential to differentiate into cardiomyocytes in vitro. *J. Mol. Histol.* 44, 411–422. doi:10.1007/s10735-013-9492-9
- LI, Q., P. YU, W. WANG, P. ZHANG, H. YANG, S. LI and L. ZHANG (2014): Gene expression profiles of various cytokines in mesenchymal stem cells derived from umbilical cord tissue and bone marrow following infection with human cytomegalovirus. *Cell. Mol. Biol. Lett.* 19, 140–157. doi:10.2478/s11658-014-0187-3
- LI, X., J. ZHAN, Y. HOU, Y. HOU, S. CHEN, D. LUO, J. LUAN, L. WANG and D. LIN (2019): Coenzyme Q10 Regulation of Apoptosis and Oxidative Stress in H₂O₂ Induced BMSC Death by Modulating the Nrf-2/NQO-1 Signaling Pathway and Its Application in a Model of Spinal Cord Injury. *Oxid. Med. Cell. Longev.* 2019. doi:10.1155/2019/6493081
- LING, L., V. NURCOMBE and S.M. COOL (2009): Wnt signaling controls the fate of mesenchymal stem cells. *Gene* 433, 1–7. doi:10.1016/j.gene.2008.12.008
- LISJAK, D., I. ALIĆ, I. ŠIMUNIĆ and D. MITREČIĆ (2024): Transplantation of neural stem cells improves recovery of stroke-affected mice and induces cell-specific changes in GSDMD and MLKL expression. *Front. Mol. Neurosci.* 17, 1439994:1–11. doi:10.3389/fnmol.2024.1439994
- LIU, J., Y. DING, Z. LIU and X. LIANG (2020): Senescence in Mesenchymal Stem Cells: Functional Alterations, Molecular Mechanisms, and Rejuvenation Strategies. *Front. Cell Dev. Biol.* 8, 258. doi:10.3389/fcell.2020.00258
- LUDWIG, T.E., P.W. ANDREWS, I. BARBARIC, N. BENVENISTY, A. BHATTACHARYYA, J.M. CROOK, L.M. DAHERON, J.S. DRAPER, L.E. HEALY, M. HUCH, M.S. INAMDAR, K.B. JENSEN, A. KURTZ, M.A. LANCASTER, P. LIBERALI, M.P. LUTOLF, C.L. MUMMERY, M.F. PERA, Y. SATO, N. SHIMASAKI, A.G. SMITH, J. SONG, C. SPITS, G. STACEY, C.A. WELLS, T. ZHAO and J.T. MOSHER (2023): ISSCR standards for the use of human stem cells in basic research. *Stem Cell Reports* 18, 1744–1752. doi:10.1016/j.stemcr.2023.08.003
- MA, R., Q. XING, L. SHAO, D. WANG, Q. HAO, X. LI, L. SAI and L. MA (2011): Hepatitis B virus infection and replication in human bone marrow mesenchymal stem cells. *Virology* 438, 486. doi:10.1016/j.virus.2011.08.017
- MA, T., B. FU, X. YANG, Y. XIAO and M. PAN (2019): Adipose mesenchymal stem cell-derived exosomes promote cell proliferation, migration, and inhibit cell apoptosis via Wnt/ β -catenin signaling in cutaneous wound healing. *J. Cell. Biochem.* 120, 10847–10854. doi:10.1002/jcb.28376

- MARTÍN, P.G., M.B. GONZÁLEZ, A.R. MARTÍNEZ, V.G. LARA and B.C. NAVEROS (2012): Isolation and characterization of the environmental bacterial and fungi contamination in a pharmaceutical unit of mesenchymal stem cell for clinical use. *Biologicals* 40, 330–337. doi:10.1016/j.biologicals.2012.06.002
- MARX, C., M.D. SILVEIRA, I. SELBACH, A.S. DA SILVA, L.M.G.D.M. BRAGA, M. CAMASSOLA and N.B. NARDI (2014): Acupoint injection of autologous stromal vascular fraction and allogeneic adipose-derived stem cells to treat hip dysplasia in dogs. *Stem Cells Int.* 2014, 391274. doi: 10.1155/2014/391274
- MEISEL, R., K. HESELER, J. NAU, S.K. SCHMIDT, M. LEINEWEBER, S. PUDELKO, J. WENNING, A. ZIMMERMANN, H. HENGEL, C. SINZGER, Ö. DEGISTIRICI, R. VOLKER SORG and W. DÄUBENER (2014): Cytomegalovirus infection impairs immunosuppressive and antimicrobial effector functions of human multipotent mesenchymal stromal cells. *Mediators Inflamm.* 2014, 898630. doi:10.1155/2014/898630
- MERLO, B. and E. IACONO (2023): Beyond Canine Adipose Tissue-Derived Mesenchymal Secretome Characterization and Applications. *Animals* 2023, 3571. doi:10.3390/ani13223571
- MIZUNO, T., M. INOUE, T. KUBO, Y. IWAKI, K. KAWAMOTO, K. ITAMOTO, S. KAMBAYASHI, M. IGASE, K. BABA and M. OKUDA (2022): Improvement of anemia in five dogs with nonregenerative anemia treated with allogeneic adipose-derived stem cells. *Vet. Anim. Sci.* 17, 100264. doi:10.1016/j.vas.2022.100264
- MORAES, D.A., T.T. SIBOV, L.F. PAVON, P.Q. ALVIM, R.S. BONADIO, J.R. DA SILVA, A. PIC-TAYLOR, O.A. TOLEDO, L.C. MARTI, R.B. AZEVEDO and D.M. OLIVEIRA (2016): A reduction in CD90 (THY-1) expression results in increased differentiation of mesenchymal stromal cells. *Stem Cell Res. Ther.* 7, 1–14. doi:10.1186/s13287-016-0359-3
- MORENO, I., I. RODRÍGUEZ-SÁNCHEZ, X. SCHAFFER and J. MUNGER (2022): Human cytomegalovirus induces neuronal enolase to support virally mediated metabolic remodeling. *Proc. Natl. Acad. Sci.* 119, e2205789119. doi:10.1073/pnas.2205789119
- NAKAJIMA, M., C. NITO, K. SOWA, S. SUDA, Y. NISHIYAMA, A. NAKAMURA-TAKAHASHI, Y. NITAHARA-KASAHARA, K. IMAGAWA, T. HIRATO, M. UEDA, K. KIMURA and T. OKADA (2017): Mesenchymal Stem Cells Overexpressing Interleukin-10 Promote Neuroprotection in Experimental Acute Ischemic Stroke. *Mol. Ther. - Methods Clin. Dev.* 6, 102–111. doi:10.1016/j.omtm.2017.06.005
- NANIĆ, L., A. CEDILAK, N.Š. VIDAČEK, F. GRUBER, M. HUZAK, M. BADER and I.

- RUBELJ (2022): In Vivo Skin Regeneration and Wound Healing Using Cell Micro-Transplantation. *Pharmaceutics* 14, 1955. doi:10.3390/pharmaceutics14091955
- NATIONAL, C. for B.I. (2024): PubChem Pathway Summary for Pathway P00031, Inflammation mediated by chemokine and cytokine signaling pathway. <https://pubchem.ncbi.nlm.nih.gov/pathway/PANTHER:P00031>; accessed: 02/05/2024
- NAZARI-SHAFTI, T.Z., E. FREISINGER, U. ROY, C.T. BULOT, C. SENST, C.L. DUPIN, A.E. CHAFFIN, S.K. SRIVASTAVA, D. MONDAL, E.U. ALT and R. IZADPANA (2011): Mesenchymal stem cell derived hematopoietic cells are permissive to HIV-1 infection. *Retrovirology* 8, 3. doi:10.1186/1742-4690-8-3
- NEDVÍDKOVÁ, J., K. SMITKA, V. KOPSKÝ and V. HAINER (2005): Adiponectin, an Adipocyte-Derived Protein. *Physiol. Res.* 54, 133–140. doi:10.1161/01.cir.102.11.1296
- NEUPANE, M., C.-C. CHANG, M. KIUPEL and V. YUZBASIYAN-GURKAN (2008): Isolation and Characterization of Canine Adipose-Derived Mesenchymal Stem Cells. *Tissue Eng. Part A* 14, 1007–1015. doi:10.1089/tea.2007.0207
- NITAHARA-KASAHARA, Y., M. KURAOKA, Y. ODA, H. HAYASHITA-KINOH, S. TAKEDA and T. OKADA (2021): Enhanced cell survival and therapeutic benefits of IL-10-expressing multipotent mesenchymal stromal cells for muscular dystrophy. *Stem Cell Res. Ther.* 12, 105:1–15. doi:10.1186/s13287-021-02168-1
- OLSEN, A., V. JOHNSON, T. WEBB, K.S. SANTANGELO, S. DOW and F.M. DUERR (2019): Evaluation of Intravenously Delivered Allogeneic Mesenchymal Stem Cells for Treatment of Elbow Osteoarthritis in Dogs: A Pilot Study. *Vet. Comp. Orthop. Traumatol.* 32, 173–181. doi:10.1055/s-0039-1678547
- OUAAMARI, A. EL, E. DIRICE, N. GEDEON, J. HU, J.Y. ZHOU, J. SHIRAKAWA, L. HOU, J. GOODMAN, C. KARAMELIAS, G. QIANG, J. BOUCHER, R. MARTINEZ, M.A. GRITSENKO, D.F. DE JESUS, S. KAHRAMAN, S. BHATT, R.D. SMITH, H.D. BEER, P. JUNGTRAKOON, Y. GONG, A.B. GOLDFINE, C.W. LIEW, A. DORIA, O. ANDERSSON, W.J. QIAN, E. REMOLD-O'DONNELL and R.N. KULKARNI (2016): SerpinB1 Promotes Pancreatic β Cell Proliferation. *Cell Metab.* 23, 194–205. doi:10.1016/j.cmet.2015.12.001
- PARK, S.R., A. CHO, J.W. KIM, H.Y. LEE and I.S. HONG (2019): A Novel Endogenous Damage Signal, CSF-2, Activates Multiple Beneficial Functions of Adipose Tissue-Derived Mesenchymal Stem Cells. *Mol. Ther.* 27, 1087–1100. doi:10.1016/j.ymthe.2019.03.010

- PEKKER, E., K. PRISKIN, É. SZABÓ-KRISTON, B. CSÁNYI, O. BUZÁS-BERECZKI, L. ADORJÁN, V. SZUKACSOV, L. PINTÉR, M. RUSVAI, P. COOPER, E. KISS-TÓTH and L. HARACSKA (2023): Development of a Large-Scale Pathogen Screening Test for the Biosafety Evaluation of Canine Mesenchymal Stem Cells. *Biol. Proced. Online* 25, 33. doi:10.1186/s12575-023-00226-x
- PEREIRA, A.L., M.K.W. BITTENCOURT, M.A. BARROS, R. MALAGO, J.F.M. PANATTONI, B.P. DE MORAIS, F. MONTIANI-FERREIRA and J.P.C. VASCONCELLOS (2022): Subconjunctival use of allogeneic mesenchymal stem cells to treat chronic superficial keratitis in German shepherd dogs: Pilot study. *Open Vet. J.* 12, 744–753. doi:10.5455/ovj.2022.v12.i5.20
- PÉREZ-MERINO, E.M., J.M. USÓN-CASAÚS, C. ZARAGOZA-BAYLE, J. DUQUE-CARRASCO, L. MARIÑAS-PARDO, M. HERMIDA-PRIETO, R. BARRERA-CHACÓN and M. GUALTIERI (2015): Safety and efficacy of allogeneic adipose tissue-derived mesenchymal stem cells for treatment of dogs with inflammatory bowel disease: Clinical and laboratory outcomes. *Vet. J.* 206, 385–390. doi:10.1016/j.tvjl.2015.08.003
- PEREZ-RIVEROL, Y., J. BAI, C. BANDLA, D. GARCÍA-SEISDEDOS, S. HEWAPATHIRANA, S. KAMATCHINATHAN, D.J. KUNDU, A. PRAKASH, A. FRERICKS-ZIPPER, M. EISENACHER, M. WALZER, S. WANG, A. BRAZMA and J.A. VIZCAÍNO (2022): The PRIDE database resources in 2022: A hub for mass spectrometry-based proteomics evidences. *Nucleic Acids Res.* 50, D543–D552. doi:10.1093/nar/gkab1038
- PERVAN, M., S. MARIJAN, A. MARKOTIĆ, L.I. PILKINGTON, N.A. HAVERKATE, D. BARKER, J. REYNISSON, L. MEIĆ, M. RADAN and V. ČIKEŠ ČULIĆ (2022): Novel Thieno [2,3-b]pyridine Anticancer Compound Lowers Cancer Stem Cell Fraction Inducing Shift of Lipid to Glucose Metabolism. *Int. J. Mol. Sci.* 23, 11457. doi:10.3390/ijms231911457
- PLAZA, A., B. MERINO, A. SÁNCHEZ-PERNAUTE, A.J. TORRES-GARCÍA, M.A. RUBIO-HERRERA and M. RUIZ-GAYO (2018): Expression analysis of a cholecystokinin system in human and rat white adipose tissue. *Life Sci.* 206, 98–105. doi:10.1016/j.lfs.2018.05.036
- PLESA, A.M., S. JUNG, H.H. WANG, F. OMAR and M. SHADPOUR (2023): Transcriptomic reprogramming screen identifies SRSF1 as rejuvenation factor Measuring aging using gene expression. *bioRxiv*. doi: 10.1101/2023.11.13.566787 doi:
- PRIŠLIN, M., A. BUTORAC, R. BERTOŠA, V. KUNIĆ, I. LJOLJE, P. KOSTEŠIĆ, D.

- VLAHOVIĆ, Š. NALETILIĆ, N. TURK and D. BRNIĆ (2024): In vitro aging alters the gene expression and secretome composition of canine adipose-derived mesenchymal stem cells. *Front. Vet. Sci.* 11, 1387174. doi:10.3389/fvets.2024.1387174
- PRIŠLIN, M., D. VLAHOVIĆ, P. KOSTEŠIĆ, I. LJOLJE, D. BRNIĆ, N. TURK, I. LOJKIĆ, V. KUNIĆ, T. KARADJOLE and N. KREŠIĆ (2022): An Outstanding Role of Adipose Tissue in Canine Stem Cell Therapy. *Animals* 12, 1088. doi:10.3390/ani12091088
- PRIŠLIN, M., D. VLAHOVIĆ, I. LJOLJE, P. KOSTEŠIĆ, N. TURK, Š. NALETILIĆ, D. BRNIĆ and N. KREŠIĆ (2023): Influence of In Vitro Cultivation on Differentiation Gene Expressions in Canine Adipose-Derived Mesenchymal Stem Cells. *Advances in Biomedical and Veterinary Engineering. BioMedVetMech 2022. IFMBE Proceedings*, 90, 1–18. doi: 10.1007/978-3-031-42243-0_1
- PRIŠLIN ŠIMAC, M., Š. NALETILIĆ, V. KOSTANIĆ, V. KUNIĆ, T. M. ZOREC, M. POLJAK, D. VLAJ, R. KOGOJ, N. TURK, D. BRNIĆ (2024): Canid alphaherpesvirus 1 infection alters the gene expression and secretome profile of canine adipose-derived mesenchymal stem cells in vitro. *Virology*, 21, 335:1-18. doi: 10.1186/s12985-024-02603-8
- PRPAR MIHEVC, S., V. KOKONDOSKA GRGICH, A.N. KOPITAR, L. MOHORIČ and G. MAJDIČ (2020): Neural differentiation of canine mesenchymal stem cells/multipotent mesenchymal stromal cells. *BMC Vet. Res.* 16, 1–12. doi:10.1186/s12917-020-02493-2
- RAMAKRISHNAN, V.M. and N.L. BOYD (2018): The Adipose Stromal Vascular Fraction as a Complex Cellular Source for Tissue Engineering Applications. *Tissue Eng. - Part B Rev.* 24, 289–299. doi:10.1089/ten.teb.2017.0061
- RASHID, U., A. YOUSAF, M. YAQOUB, E. SABA, M. MOAEEN-UD-DIN, S. WASEEM, S.K. BECKER, G. SPONDER, J.R. ASCHENBACH and M.A. SANDHU (2021): Characterization and differentiation potential of mesenchymal stem cells isolated from multiple canine adipose tissue sources. *BMC Vet. Res.* 17, 1–12. doi:10.1186/s12917-021-03100-8
- ROY, E., W. SHI, B. DUAN and S.P. REIDA (2020): Chikungunya Virus Infection Impairs the Function of Osteogenic Cells. *mSphere* 5, e00347-20. doi:10.1128/msphere.00347-20
- RUBTSOV, Y., K. GORYUNOV, A. ROMANOV, Y. SUZDALTSEVA, G. SHARONOV and V. TKACHUK (2017): Molecular Mechanisms of Immunomodulation Properties of Mesenchymal Stromal Cells: A New Insight into the Role of ICAM-1. *Stem Cells Int.* 2017, 6516854. doi:10.1155/2017/6516854
- RUSSELL, K.A., N.H.C. CHOW, D. DUKOFF, T.W.G. GIBSON, J. LA MARRE, D.H.

- BETTS and T.G. KOCH (2016): Characterization and immunomodulatory effects of canine adipose tissue- and bone marrow-derived mesenchymal stromal cells. *PLoS One* 11, e0167442. doi:10.1371/journal.pone.0167442
- SANZ-RODRIGUEZ, F., M. GUERRERO-ESTEO, L.-M. BOTELLA, D. BANVILLE, C.P.H. VARY and C. BERNABÉU (2004): Endoglin Regulates Cytoskeletal Organization through Binding to ZRP-1, a Member of the Lim Family of Proteins. *J. Biol. Chem.* 279, 32858–32868. doi:10.1074/jbc.m400843200
- SCREVEN, R., E. KENYON, M.J. MYERS, H.F. YANCY, M. SKASKO, L. BOXER, E.C. BIGLEY, D.L. BORJESSON and M. ZHU (2014): Immunophenotype and gene expression profile of mesenchymal stem cells derived from canine adipose tissue and bone marrow. *Vet. Immunol. Immunopathol.* 161, 21–31. doi:10.1016/j.vetimm.2014.06.002
- SENESI, L., F. DE FRANCESCO, L. FARINELLI, S. MANZOTTI, G. GAGLIARDI, G.F. PAPALIA, M. RICCIO and A. GIGANTE (2019): Mechanical and enzymatic procedures to isolate the stromal vascular fraction from adipose tissue: Preliminary results. *Front. Cell Dev. Biol.* 7, 1–9. doi:10.3389/fcell.2019.00088
- SEO, M.G., S. PARK, S. HAN, A.Y. KIM, E.J. LEE, K.S. JEONG and I.H. HONG (2022): Long-term treatment of allogeneic adipose-derived stem cells in a dog with rheumatoid arthritis. *J. Vet. Sci.* 23, e61. doi:10.4142/jvs.22069
- SGRIGNOLI, M.R., D.A. SILVA, F.F. NASCIMENTO, D.A.M. SGRIGNOLI, G.A. NAI, M.G. DA SILVA, M.A. DE BARROS, M.K.W. BITTENCOURT, B.P. DE MORAIS, H.R. DINALLO, B.T.D. FOGLIA, W.B. CABRERA, E.C. FARES and S.F. ANDRADE (2019): Reduction in the inflammatory markers CD4, IL-1, IL-6 and TNF α in dogs with keratoconjunctivitis sicca treated topically with mesenchymal stem cells. *Stem Cell Res.* 39, 101525. doi:10.1016/j.scr.2019.101525
- SHAH, K., T. DRURY, I. ROIC, P. HANSEN, M. MALIN, R. BOYD, H. SUMER and R. FERGUSON (2018): Outcome of allogeneic adult stem cell therapy in dogs suffering from osteoarthritis and other joint defects. *Stem Cells Int.* 2018, 7309201. doi:10.1155/2018/7309201
- SHAN, T., J. LIU, W. WU, Z. XU and Y. WANG (2017): Roles of Notch Signaling in Adipocyte Progenitor Cells and Mature Adipocytes. *J. Cell. Physiol.* 232, 1258–1261. doi:10.1002/jcp.25697
- SMOLJO, T., H. LALIC, V. DEMBITZ, B. TOMIC, J. BATINIC, R. VRHOVAC, A. BEDALOV and D. VISNJIC (2024): Bone marrow stromal cells enhance differentiation of acute myeloid leukemia induced by pyrimidine synthesis inhibitors. *Am. J. Physiol.*

- Physiol. 327, C1202–C1218. doi:10.1152/ajpcell.00413.2024
- SONG, W.J., Q. LI, M.O. RYU, A. NAM, J.H. AN, Y.C. JUNG, J.O. AHN and H.Y. YOUN (2019): Canine adipose tissue-derived mesenchymal stem cells pre-treated with TNF-alpha enhance immunomodulatory effects in inflammatory bowel disease in mice. *Res. Vet. Sci.* 125, 176–184. doi:10.1016/j.rvsc.2019.06.012
- SRZENTIĆ DRAŽILOV, S., J. MRKOVAČKI, V. SPASOVSKI, A. FAZLAGIĆ, S. PAVLOVIĆ and G. NIKČEVIĆ (2018): The use of canine mesenchymal stem cells for the autologous treatment of osteoarthritis. *Acta Vet. Hung.* 66, 376–389. doi:10.1556/004.2018.034
- STANČIN, P., M.S. SONG, I. ALAJBEG and D. MITREČIĆ (2023): Human Oral Mucosa Stem Cells Increase Survival of Neurons Affected by In Vitro Anoxia and Improve Recovery of Mice Affected by Stroke Through Time-limited Secretion of miR-514A-3p. *Cell. Mol. Neurobiol.* 43, 1975–1988. doi:10.1007/s10571-022-01276-7
- SUCHMAN, E. and C. BLAIR (2007): Cytopathic Effects of Viruses. ASM Conference for Undergraduate Educators 2007. American Society for Microbiology, 1–13
- SUNDIN, M., C. ÖRVELL, I. RASMUSSEN, B. SUNDBERG, O. RINGDÉN and K. LE BLANC (2006): Mesenchymal stem cells are susceptible to human herpesviruses, but viral DNA cannot be detected in the healthy seropositive individual. *Bone Marrow Transplant.* 37, 1051–1059. doi:10.1038/sj.bmt.1705368
- SZABŁOWSKA-GADOMSKA, I., M. HUMI and J. PŁACZKOWSKA (2023): Microbiological Aspects of Pharmaceutical Manufacturing of Adipose-Derived Stem Cell-Based Medicinal Products. *cells* 2023, 680. doi:/10.3390/cells12050680
- TAKEMITSU, H., D. ZHAO, I. YAMAMOTO, Y. HARADA, M. MICHISHITA and T. ARAI (2012): Comparison of bone marrow and adipose tissue-derived canine mesenchymal stem cells. *BMC Vet. Res.* 8, 150. doi:10.1186/1746-6148-8-150
- TAN, K., H. ZHU, J. ZHANG, W. OUYANG, J. TANG, Y. ZHANG, L. QIU, X. LIU, Z. DING and X. DENG (2019): CD73 expression on mesenchymal stem cells dictates the reparative properties via its anti-inflammatory activity. *Stem Cells Int.* 2019, 8717694. doi: 10.1155/2019/8717694
- TANABE, S., T. KAWABATA, K. AOYAGI, H. YOKOZAKI and H. SASAKI (2016): Gene expression and pathway analysis of CTNNA1 in cancer and stem cells. *World J. Stem Cells* 8, 384–395. doi:10.4252/wjsc.v8.i11.384
- TESHIMA, T., H. MATSUMOTO, M. MICHISHITA, A. MATSUOKA, M. SHIBA, T. NAGASHIMA and H. KOYAMA (2017): Allogenic adipose tissue-derived mesenchymal

- stem cells ameliorate acute hepatic injury in dogs. *Stem Cells Int.* 2017, 3892514:1–12. doi:10.1155/2017/3892514
- TESHIMA, T., Y. YASUMURA, R. SUZUKI and H. MATSUMOTO (2022): Antiviral Effects of Adipose Tissue-Derived Mesenchymal Stem Cells Secretome against Feline Calicivirus and Feline Herpesvirus Type 1. *Viruses* 14, 1687. doi:10.3390/v14081687
- TESHIMA, T., Y. YUCHI, R. SUZUKI, H. MATSUMOTO and H. KOYAMA (2021): Immunomodulatory effects of canine adipose tissue mesenchymal stem cell-derived extracellular vesicles on stimulated cd4+t cells isolated from peripheral blood mononuclear cells. *J. Immunol. Res.* 2021, 2993043. doi:10.1155/2021/2993043
- TRZYNA, A. and A. BANAŚ-ZĄBCZYK (2021): Adipose-derived stem cells secretome and its potential application in “stem cell-free therapy.” *Biomolecules* 11, 878. doi:10.3390/biom11060878
- VIEIRA, N.M., V. BRANDALISE, E. ZUCCONI, M. SECCO, B.E. STRAUSS and M. ZATZ (2010): Isolation, characterization, and differentiation potential of canine adipose-derived stem cells. *Cell Transplant.* 19, 279–289. doi:10.3727/096368909x481764
- VILAR, J.M., B. CUERVO, M. RUBIO, J. SOPENA, J.M. DOMÍNGUEZ, A. SANTANA and J.M. CARRILLO (2016): Effect of intraarticular inoculation of mesenchymal stem cells in dogs with hip osteoarthritis by means of objective force platform gait analysis: Concordance with numeric subjective scoring scales. *BMC Vet. Res.* 12, 1–10. doi:10.1186/s12917-016-0852-z
- VILAR, J.M., M. MORALES, A. SANTANA, G. SPINELLA, M. RUBIO, B. CUERVO, R. CUGAT and J.M. CARRILLO (2013): Controlled, blinded force platform analysis of the effect of intraarticular injection of autologous adipose-derived mesenchymal stem cells associated to PRGF-Endoret in osteoarthritic dogs. *BMC Vet. Res.* 9, 131. doi: 10.1186/1746-6148-9-131
- VILLATORO, A.J., C. ALCOHOLADO, M.C. MARTÍN-ASTORGA, V. FERNÁNDEZ, M. CIFUENTES and J. BECERRA (2019): Comparative analysis and characterization of soluble factors and exosomes from cultured adipose tissue and bone marrow mesenchymal stem cells in canine species. *Vet. Immunol. Immunopathol.* 208, 6–15. doi:10.1016/j.vetimm.2018.12.003
- VILLATORO, A.J., M. HERMIDA-PRIETO, V. FERNÁNDEZ, F. FARIÑAS, C. ALCOHOLADO, M. ISABEL RODRÍGUEZ-GARCÍA, L. MARIÑAS-PARDO and J. BECERRA (2018): Allogeneic adipose-derived mesenchymal stem cell therapy in dogs with refractory atopic dermatitis: Clinical efficacy and safety. *Vet. Rec.* 183, 654.

doi:10.1136/vr.104867

- VILLATORO, A.J., M.D.C. MARTÍN-ASTORGA, C. ALCOHOLADO, M.D.M. SÁNCHEZ-MARTÍN and J. BECERRA (2021): Proteomic analysis of the secretome and exosomes of feline adipose-derived mesenchymal stem cells. *Animals* 11, 295:1–15. doi:10.3390/ani11020295
- VISWESWARAN, M., S. POHL, F. ARFUSO, P. NEWSHOLME, R. DILLEY, S. PERVAIZ and A. DHARMARAJAN (2015): Multi-lineage differentiation of mesenchymal stem cells - To Wnt, or not Wnt. *Int. J. Biochem. Cell Biol.* 68, 139–147. doi:10.1016/j.biocel.2015.09.008
- VIZOSO, F.J., N. EIRO, S. CID, J. SCHNEIDER and R. PEREZ-FERNANDEZ (2017): Mesenchymal stem cell secretome: Toward cell-free therapeutic strategies in regenerative medicine. *Int. J. Mol. Sci.* 18, 1852. doi:10.3390/ijms18091852
- VOGA, M., N. ADAMIC, M. VENGUST and G. MAJDIC (2020): Stem Cells in Veterinary Medicine—Current State and Treatment Options. *Front. Vet. Sci.* 7, 278. doi:10.3389/fvets.2020.00278
- VOGA, M., V. KOVAČ and G. MAJDIC (2021): Comparison of Canine and Feline Adipose-Derived Mesenchymal Stem Cells/Medicinal Signaling Cells With Regard to Cell Surface Marker Expression, Viability, Proliferation, and Differentiation Potential. *Front. Vet. Sci.* 7, 610240:1–13. doi:10.3389/fvets.2020.610240
- WANG, H., J. HUA, S. CHEN and Y. CHEN (2022): SERPINB1 overexpression protects myocardial damage induced by acute myocardial infarction through AMPK/mTOR pathway. *BMC Cardiovasc. Disord.* 22, 1–11. doi:10.1186/s12872-022-02454-7
- WANG, S., M. MO, J. WANG, S. SADIA, B. SHI, X. FU, L. YU, E.E. TREDGET and Y. WU (2018): Platelet-derived growth factor receptor beta identifies mesenchymal stem cells with enhanced engraftment to tissue injury and pro-angiogenic property. *Cell. Mol. Life Sci.* 75, 547–561. doi:10.1007/s00018-017-2641-7
- WENG, Z., Y. WANG, T. OUCHI, H. LIU, X. QIAO, C. WU, Z. ZHAO, L. LI and B. LI (2022): Mesenchymal Stem/Stromal Cell Senescence: Hallmarks, Mechanisms, and Combating Strategies. *Stem Cells Transl. Med.* 11, 356–371. doi:10.1093/stcltm/szac004
- WITS, M.I., G.C. TOBIN, M.D. SILVEIRA, K.G. BAJA, L.M.M. BRAGA, P. SESTERHEIM, M. CAMASSOLA and N.B. NARDI (2020): Combining canine mesenchymal stromal cells and hyaluronic acid for cartilage repair. *Genet. Mol. Biol.* 43, 1–8. doi:10.1590/1678-4685-gmb-2019-0275
- YAN, L., D. ZHENG and R.-H. XU (2018): Critical Role of Tumor Necrosis Factor Signaling

- in Mesenchymal Stem Cell-Based Therapy for Autoimmune and Inflammatory Diseases. *Front. Immunol.* 9, 1658. doi:10.3389/fimmu.2018.01658
- YAN, Y., J. FANG, X. WEN, X. TENG, B. LI, Z. ZHOU, S. PENG, A.H. ARISHA, W. LIU and J. HUA (2019): Therapeutic applications of adipose-derived mesenchymal stem cells on acute liver injury in canines. *Res. Vet. Sci.* 126, 233–239. doi:10.1016/j.rvsc.2019.09.004
- YANG, H.M., W.J. SONG, Q. LI, S.Y. KIM, H.J. KIM, M.O. RYU, J.O. AHN and H.Y. YOUN (2018): Canine mesenchymal stem cells treated with TNF- α and IFN- γ enhance anti-inflammatory effects through the COX-2/PGE 2 pathway. *Res. Vet. Sci.* 119, 19–26. doi:10.1016/j.rvsc.2018.05.011
- YANG, Y.H.K., C.R. OGANDO, C. WANG SEE, T.Y. CHANG and G.A. BARABINO (2018): Changes in phenotype and differentiation potential of human mesenchymal stem cells aging in vitro. *Stem Cell Res. Ther.* 9, 1–14. doi:10.1186/s13287-018-0876-3
- YOON, H.-Y., J. LEE and S. JEONG (2012): Long-term follow-up after implantation of autologous adipose tissue derived mesenchymal stem cells to treat a dog with stifle joint osteoarthritis. *J. Vet. Clin.* 29, 82–86.
- YUN, S., S.K. KU and Y.S. KWON (2016): Adipose-derived mesenchymal stem cells and platelet-rich plasma synergistically ameliorate the surgical-induced osteoarthritis in Beagle dogs. *J. Orthop. Surg. Res.* 11, 1–12. doi:10.1186/s13018-016-0342-9
- ZDRAVEVA, E., K. BENDELJA, L. BOČKOR, T. DOLENEC and B. MIJOVIĆ (2023): Detection of Limbal Stem Cells Adhered to Melt Electrospun Silk Fibroin and Gelatin-Modified Polylactic Acid Scaffolds. *Polymers (Basel)*. 15, 777. doi:10.3390/polym15030777
- ZDRAVEVA, E., T. DOLENEC, M. TOMINAC TRCIN, E. GOVORČIN BAJSIĆ, T. HOLJEVAC GRGURIĆ, A. TOMLJENOVIĆ, I. DEKARIS, J. JELIĆ and B. MIJOVIC (2023): The Reliability of PCL/Anti-VEGF Electrospun Scaffolds to Support Limbal Stem Cells for Corneal Repair. *Polymers (Basel)*. 15, 2663. doi:10.3390/polym15122663
- ZEC GOSSAINN, D., O. SMOLEC, I.C. ŠOŠTARIĆ ZUCKERMAN, M. HOHŠTETER, M. PEĆIN, I. VLAHEK, E. OSTER, S. FARAGUNA, D. CVITKOVIĆ and M. LIPAR (2023): Critical diaphyseal bone defect healing in hens by autologous free transplant of adipose tissue. *Vet. stn.* 54, 407–415. doi:10.46419/vs.54.4.5
- ZEKUŠIĆ, M., M. BUJIĆ MIHICA, M. SKOKO, K. VUKUŠIĆ, P. RISTESKI, J. MARTINČIĆ, I.M. TOLIĆ, K. BENDELJA, S. RAMIĆ, T. DOLENEC, I. VRGOČ ZIMIĆ, D. PULJIĆ, I. PETRIC VICKOVIĆ, R. IVEKOVIĆ, I. BATARILO, U.

- PROSENC ZMRZLJAK, A. HOFFMEISTER and T. VUČEMILO (2023): New characterization and safety evaluation of human limbal stem cells used in clinical application: fidelity of mitotic process and mitotic spindle morphologies. *Stem Cell Res. Ther.* 14, 368. doi:10.1186/s13287-023-03586-z
- ZHANG, Z., M. LIU and Y. ZHENG (2021): Role of Rho GTPases in stem cell regulation. *Biochem. Soc. Trans.* 49, 2941–2955. doi:10.1042/bst20211071
- ZHUO, C., D. ZHENG, Z. HE, J. JIN, Z. REN, F. JIN and Y. WANG (2017): HSV-1 enhances the energy metabolism of human umbilical cord mesenchymal stem cells to promote virus infection. *Future Virol.* 12, 349–360. doi:10.2217/fvl-2017-0038
- ZUBIN, E., V. CONTI, F. LEONARDI, S. ZANICHELLI, R. RAMONI and S. GROLLI (2015): Regenerative therapy for the management of a large skin wound in a dog. *Clin. Case Reports* 3, 598–603. doi:10.1002/ccr3.253

8. PUBLISHED SCIENTIFIC PAPERS

8.1. Paper I: "The Expression Pattern of Surface Markers in Canine Adipose-Derived Mesenchymal Stem Cells"

The article was published in the International Journal of Molecular Sciences, 2021: 7476, in July 2021. The DOI number of the article is 10.3390/ijms22147476 (WoS JCR (2021) IF 6.208, Q1 in Biochemistry and Molecular Biology; Scopus SJR (2023) 1.18, h-index 269, Q1 in Medicine (miscellaneous)). The full paper, along with its supplementary material, is available via open access at the following link: <https://doi.org/10.3390/ijms22147476>.



Article

The Expression Pattern of Surface Markers in Canine Adipose-Derived Mesenchymal Stem Cells

Nina Krešić ^{1,*}, Marina Prišlin ^{1,†}, Dunja Vlahović ², Petar Kostešić ³, Ivana Ljolje ⁴, Dragan Brnić ¹, Nenad Turk ⁵, Andrija Musulin ³ and Boris Habrun ⁶

- ¹ Virology Department, Croatian Veterinary Institute, Savska Cesta 143, 10 000 Zagreb, Croatia; prislin@veinst.hr (M.P.); brnic@veinst.hr (D.B.)
 - ² Department of Veterinary Pathology, Faculty of Veterinary Medicine, University of Zagreb, Heinzelova 55, 10 000 Zagreb, Croatia; dvlahovic@vef.hr
 - ³ Surgery, Orthopaedics and Ophthalmology Clinic, Faculty of Veterinary Medicine, University of Zagreb, Heinzelova 55, 10 000 Zagreb, Croatia; kostesic@vef.hr (P.K.); musulin@vef.hr (A.M.)
 - ⁴ Veterinary Clinic for Small Animals Buba, Dore Pfanove 11, 10 000 Zagreb, Croatia; ivana.ljolje@gmail.com
 - ⁵ Department of Microbiology and Infectious Diseases with Clinic, Faculty of Veterinary Medicine, University of Zagreb, Heinzelova 55, 10 000 Zagreb, Croatia; turk@vef.hr
 - ⁶ Department for Bacteriology and Parasitology, Croatian Veterinary Institute, Savska Cesta 143, 10 000 Zagreb, Croatia; habrun@veinst.hr
- * Correspondence: lemo@veinst.hr
† These authors contributed equally to this work.



Citation: Krešić, N.; Prišlin, M.; Vlahović, D.; Kostešić, P.; Ljolje, I.; Brnić, D.; Turk, N.; Musulin, A.; Habrun, B. The Expression Pattern of Surface Markers in Canine Adipose-Derived Mesenchymal Stem Cells. *Int. J. Mol. Sci.* **2021**, *22*, 7476. <https://doi.org/10.3390/ijms22147476>

Academic Editor: Maria Grazia Cifone

Received: 8 June 2021
Accepted: 9 July 2021
Published: 12 July 2021

Publisher's Note: MDPI stays neutral with regard to jurisdictional claims in published maps and institutional affiliations.



Copyright: © 2021 by the authors. Licensee MDPI, Basel, Switzerland. This article is an open access article distributed under the terms and conditions of the Creative Commons Attribution (CC BY) license (<https://creativecommons.org/licenses/by/4.0/>).

Abstract: The influence of cultivation on the expression pattern of canine adipose-derived mesenchymal stem cells (cAD-MSCs) surface markers, contributing to, among others, the promotion of growth, proliferation, differentiation and immunomodulatory mechanisms of an excellent therapeutic, is still unknown. To fill the gap, we investigated CD90, CD44, CD73, CD29, CD271, CD105, CD45 and CD14 patterns of expression at the protein level with flow cytometry and mRNA level using a real-time polymerase chain reaction array. Gentle variations of expression occurred during cultivation, along with increased CD90, CD44 and CD29 expression, low and decreasing CD271 and CD73 expression and a decrease of initially high CD105. As expected, CD45 and CD14 were not expressed by cAD-MSCs. Interestingly, we discovered a significant decrease of CD73 expression, compared to early (P1–P3) to late (P4–P6) passages, although the CD73 gene expression was found to be stable. The percentage of positive cells was found to be higher for all positive markers up to P4. As CD73's one important feature is a modulation from a pro-inflammatory environment to an anti-inflammatory milieu, the expression of CD73 in our conditions indicate the need to consider the time cells spend in vitro before being transplanted into patients, since it could impact their favourable therapeutical properties.

Keywords: stem cells; in vitro cultivation; immunophenotype; gene expression; flow cytometry; canine

1. Introduction

The International Society for Cellular Therapy (ISCT) established minimum criteria for the definition of MSCs: adherence to tissue culture plastic; multipotency as demonstrated by in vitro differentiation into osteoblasts, adipocytes and chondroblasts; expression of surface markers CD73, CD90 and CD105 and negative for CD34, CD45, CD14 or CD11b, C79 α or CD19 and HLA-DR [1]. Many studies demonstrated that cells meeting the ISCT criteria possessed heterogeneous phenotypes and functionalities, heavily influenced by culture conditions [2].

The goal of successful expansion in vitro is to maintain stem cell phenotype and show repeated self-renewal, i.e., undergo extensive proliferation while maintaining their multipotent differentiation potentials [3]. The widespread lack of culture condition homogeneity

between laboratories has made it difficult to reach unequivocal consensus even on basic MSCs properties, leading to discrepancies at the basic research level and adding biases to the evaluation of stem cell-based clinical study outcomes [2]. Despite that, isolated culture-expanded cells have been applied in both preclinical and clinical settings in animals with variable but mostly positive results. Further intensive research on the cell properties and application are certainly needed.

Cultivation *in vitro* also affects the characteristic MSCs membrane markers used to confirm the identity of isolated cells. Therefore, the expression of established MSCs markers, clusters of differentiation (CD), may be influenced by factors secreted by accessory cells in the initial passages (P). Additionally, the *in vitro* expression of some MSCs markers does not always correlate with their expression patterns *in vivo* [4].

The importance of MSCs markers is the promotion of growth, proliferation, differentiation and survival of cells in stem cell habitat. Currently, there is no unique cell marker capable of solely isolating and defining MSCs, but THY1 (CD90), a glycoprotein present in the MSCs membranes, is related to the state of cellular non-differentiation [5]. CD90 is an anchored cell surface protein usually expressed on thymocytes, MSC, natural killer cells, neurons, endothelial cells, renal glomerular mesangial cells, follicular dendritic cells, fibroblasts and myofibroblasts. It has been found to regulate cell adhesion, migration, apoptosis, axon growth, cell–cell and cell–matrix interactions, T-cell activation and fibrosis [6]. Besides the specific expression pattern and functions of CD90 that were described in normal tissues, increasing evidence is currently highlighting the possible involvement of CD90 in cancer [7].

Another marker involved in migration and adhesion is CD44, a glycoprotein widely expressed on the surface endothelial cells, epithelial cells, fibroblasts, keratinocytes and leukocytes. CD44 has important functions in cell–cell and cell–matrix interactions, including proliferation, hematopoiesis and lymphocyte activation, homing and extravasation [8]. CD44 is essential for maintaining cartilage homeostasis, influences the production of collagen II and aggrecan and influences the chondrodifferentiation of amniotic MSCs [9]. CD44 has been implicated in cancer, arthritis, interstitial lung disease, vascular disease, wound-healing and infections by pathogens [8].

CD73, ecto-5-nucleotidase, is a membrane protein that dephosphorylates extracellular AMP to bioactive adenosine that leads a shift from an ATP-driven pro-inflammatory environment to an anti-inflammatory milieu [10]. CD73 expression is heterogeneous in MSCs derived from various sources: with MSCs from human umbilical cord blood at the highest and bone-marrow-derived MSC at the lowest, suggesting that nonuniform expression of CD73 is a ubiquitous phenomenon in the MSC pool [4]. One important feature of CD73-positive cells is their ability to modulate the immune response. Transplantation of CD73-positive cells suppressed fibrosis and inflammation in pulmonary fibrosis model mice. Although the clinical translation of these results requires further detailed research, CD73-positive cells might provide a new strategy for treating and managing pulmonary fibrosis. Furthermore, interstitial pneumonia after COVID-19 infection should be considered for the candidate disease [11].

CD29, or integrin $\beta 1$, is a cell surface receptor involved in the interaction of cells with extracellular matrix proteins such as collagen, laminin and fibronectin. Integrin family members are membrane receptors involved in cell adhesion and recognition in a variety of processes, including embryogenesis, hemostasis, tissue repair, immune response and metastatic diffusion of tumour cells [12]. Among all, it has been shown that CD29 is strongly expressed by adipocyte progenitors [13,14].

CD271, low-affinity nerve growth factor receptor (LNGFR), nerve growth factor receptor (NGFR) or p75NTR (neurotrophin receptor), belongs to the tumour necrosis factor superfamily. CD271 has been proposed as a versatile marker to selectively isolate and expand multipotent mesenchymal stem cells with immunosuppressive and lymphohematopoietic-engraftment-promoting properties. In the case of bone marrow or adipose tissue, CD271 could be considered a suitable marker for MSCs isolation [15].

Endoglin (ENG), or CD105, is a type I membrane glycoprotein located on cell surfaces and is part of the TGF beta receptor complex [16]. Endoglin may be involved in the cytoskeletal organization affecting cell morphology and migration [17]. Bearden et al. (2017) found that ~60% of cAD-MSCs were positive for CD105 [18]. Furthermore, the expression of CD105 in murine and human AD-MSCs was induced by the exposure of cells to culture plastic and was further affected by passage number and confluence [19].

The expression patterns of surface markers specific for canine adipose-derived MSCs (cAD-MSCs) and changes in the percentages of positive cells during cultivation and serial passaging are still unknown. Thus, we aimed to analyse the expression pattern and percentage of positive cells for selected CDs (CD90, CD44, CD73, CD29, CD271, CD45 and CD14) during *in vitro* cultivation. Furthermore, we investigated changes in the expression of selected markers on mRNA level between P3 and P6 using array technology. We performed the comparison of surface marker expression pattern and positivity percentage between early (P1–P3) and late passages (P4–P6). The study encompassed freshly isolated cAD-MSCs originating from young, healthy donors. For the first time, comprehensive analysis of cAD-MSCs markers dynamics during *in vitro* cultivation is presented with a final contribution to understanding their therapeutic potential.

2. Results

2.1. cAD-MSCs Terminate Proliferation at the Sixth and Successfully Differentiate in the Third Passage

Since cAD-MSCs characteristics during *in vitro* expansion are heavily influenced by culturing conditions, we aimed to reveal the expansion, functional and immunophenotype characteristics of cells in each passage until their proliferation arrest.

For the cAD-MSCs isolation, we employed our previously published protocol [20] based on collagenase digestion of adipose tissue samples which resulted in the successful isolation of cAD-MSCs from all donors. Similarly to our previous results, isolated cells were spindle-shaped, and successfully proliferated *in vitro* up to P6. Although the cells of most donors managed to survive only up to P6, the 13/20 cells showed excellent proliferative capacity and reached P8. During cultivation time, well-known changes in cellular morphology and proliferation capacity occurred [21,22], resulting in a prolonged time needed to reach 80% confluence.

The functionality of cAD-MSCs *in vitro* was well preserved, as demonstrated by successful differentiation into adipocytes (Figure 1), osteoblasts (Figure 2) and chondrocytes (Figure 3). Representative differentiation results from one experiment are shown in Figures 1–3.

During the differentiation experiments, microscopic changes in cellular phenotype became visible in the form of lipid droplets in the cytoplasm of rounded cells induced to differentiate into adipocytes.

Within this study, we improved the ability to detect lipid droplets accumulated within the cell during adipose-differentiation and reduced loss of lipid commonly occurring with the use of methanol. Although alcohol fixatives are considered for better-preserved morphology [23], the use of formaldehyde overcome the loss of lipid from the cells. Unfortunately, both of them are toxic products, methanol neurotoxic and formaldehyde mutagen.

The cell phenotype in osteodifferentiating wells was in the form of elongated cells. Cells in negative control wells preserved characteristic undifferentiated morphology.

2.2. CD73 Expression Significantly Changed between Early and Late Passages

Driven by the lack of information on the changes in expression of specific markers, we analysed their pattern of expression during cultivation in standard conditions. Given the very important function of each of these markers, it is to be expected that changes in their expression could affect the therapeutic properties of cells that have been propagated *in vitro*.

Besides surface markers expression pattern, we aimed to analyse the changes occurring in the cell population during extensive passaging in vitro reflected as changes of the percentage of positive cells. To achieve our aims, we performed serial investigations on protein and mRNA levels. This study, for the first time, brings comprehensive immunophenotyping of cAD-MSCs comprising a set of eight characteristic markers (CD90, CD44, CD73, CD29, CD271, CD105, CD45 and CD14). To avoid any influence on the pattern of expression and changes within the cellular population, we analysed cells without freezing. During the analysis, we managed to maintain high cellular viability as the manipulation with cells was very careful, and reading was performed immediately after the staining and washing step.

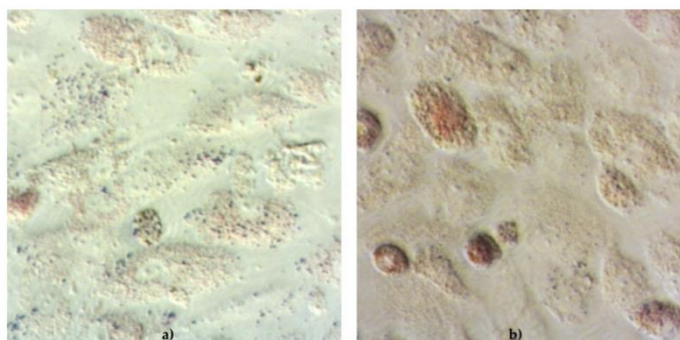


Figure 1. Functionality of canine adipose-derived mesenchymal stem cells (cAD-MSCs) demonstrated by successful differentiation into adipocytes. Microscopic images (40 \times) of cAD-MSCs after adipodifferentiation stained with Oil O Red for detection of lipid droplets within cell. Cells cultivated for 21 days in basal medium (negative control) (a) and stained with Oil O Red, showing lack of red staining. cAD-MSCs cultivated for 21 days in StemMACS AdipoDiff Media (b) successfully differentiated into adipocytes. When stained with Oil O Red, accumulated lipid droplets show high-intensity red staining within cell.

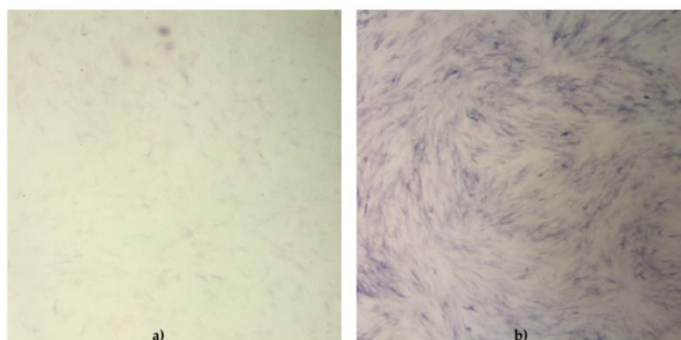


Figure 2. Functionality of canine adipose-derived mesenchymal stem cells (cAD-MSCs) demonstrated by successful differentiation into osteoblasts. Microscopic images (18 \times) of cAD-MSCs after osteodifferentiation. Cells were stained with SIGMAFAST(TM) BCIP (R)/NTB substrate to detect alkaline phosphatase activity. Cells were cultivated for 21 days in basal medium (negative control) (a) and stained with SIGMAFAST(TM) BCIP (R)/NTB, showing low-intensity staining. cAD-MSCs cultivated for 21 days in StemMACS OsteoDiff Media (b) and stained with SIGMAFAST(TM) BCIP (R)/NTB, showing high-intensity staining for alkaline phosphatase activity. The cells were examined under a stereomicroscope (Stereo Discovery, V20, CL1500 ECO, Zeiss).

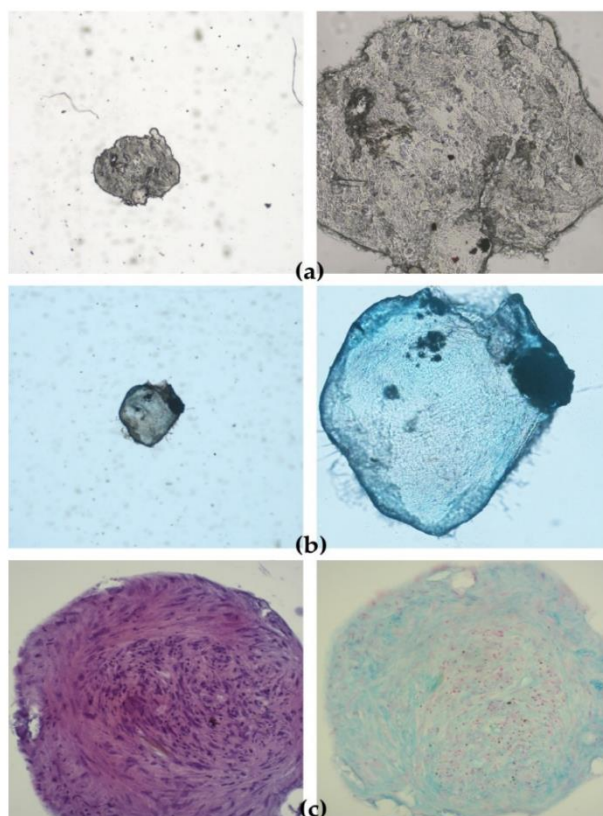


Figure 3. Functionality of canine adipose-derived mesenchymal stem cells (cAD-MSCs) demonstrated by successful chondrodifferentiation. Microscopic images of spheroids cultivated for 24 days in basal medium (negative control) stained with Alcian Blue showing lack of staining for extracellular matrix (ECM) aggrecan, 5 \times and 20 \times (a). Spheroids cultivated for 24 days in StemMACS ChondroDiff Media, stained with Alcian Blue, showing staining for ECM aggrecan, 5 \times and 20 \times (b). Images of histological sections of paraffin-embedded spheroids stained with hematoxylin-eosin (H&E) and Alcian Blue 20 \times (c).

Overall expression results are presented in Figure 4. Changes in the percentage of positive cells between passages are shown in Figures 5–7.

The obtained results encouraged us to investigate whether there was any statistically significant difference between early (P1–P3) and late passages (P4–P6). We observed that cells passaged up to P4 had a more favourable phenotype as investigated by microscopy and the expression of specific markers. Furthermore, we also observed that the percentage of positive cells was higher in early passages. No statistically significant differences in expression and percentage of positive cells were found between early (P1–P3) and late passages (P4–P6) for all of the analysed markers except for CD73. Changes in expression of CD73 were found to be statistically significant ($p = 0.0049$) as well as changes in percentage of CD73⁺ cells ($p = 0.0023$). Change in percentage CD105⁺ was found to be almost statistically significant ($p = 0.054$).

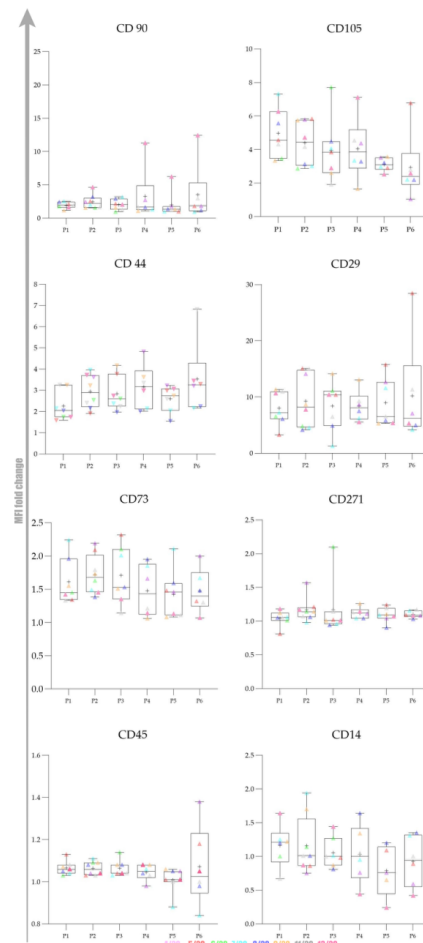


Figure 4. Canine adipose-derived mesenchymal stem cells (cAD-MSCs) surface markers expression pattern during in vitro cultivation. cAD-MSCs. The expression pattern was analysed by calculation of fold change of median fluorescence intensity (MFI). The results are based on eight biological replicates, young female canines referred to as elective surgery procedures with no obvious signs of disease. Flow cytometry assessment of positive and negative cAD-MSCs markers showed no statistically significant changes in the expression of the following positive markers: CD90, CD44, CD29, CD105 and CD271. A statistically significant change in expression was observed for CD73 between early (P1–P3) and late (P4–P6) passages. The X-axis represents the passage number (from P1 to P6), whereas the Y-axis displays the average fold change of MFI. MFI fold change was calculated by dividing the median of the appropriate antibody with the median of isotype control. The Whisker box plot was created to present the dynamics of changes between passages. Centerlines denote the median, plus the mean, box limits indicate the twenty-fifth and seventy-fifth percentiles; whiskers represent the maximum and minimum of the acquired values. Individual values are shown in colours to reveal changes for each donor included in the study. Donor 4/20 is presented in light pink, 5/20 in red, 6/20 in green, 7/20 in light blue, 8/20 in purple, 9/20 in orange, 11/20 in grey and 13/20 in dark pink.

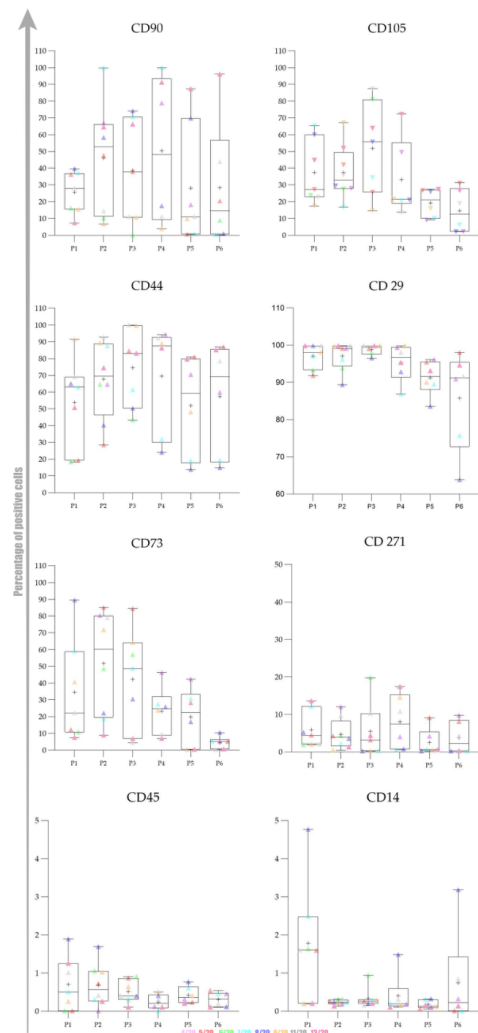


Figure 5. Changes in the percentage of positivity of canine adipose-derived mesenchymal stem cells (cAD-MSCs) during in vitro cultivation. The results are based on eight biological replicates, young female canines referred to an elective surgery procedure with no obvious signs of disease. Flow cytometry assessment of surface marker positive cAD-MSCs showed no statistically significant changes in the percentage of positive cells for the following markers: CD90, CD44, CD29, CD105 and CD271. Statistically significant changes were observed for CD73 between early (P1–P3) and late (P4–P6) passages. The X-axis represents the passage number (from P1 to P6), whereas the Y-axis displays the average positivity percentage. The Whisker box plot was created to present the dynamics of changes between passages. Centerlines denote the median, plus the mean, box limits indicate the twenty-fifth and seventy-fifth percentiles; whiskers represent the maximum and minimum of the average positivity percentage. Individual values are shown in colours to reveal changes for each donor included in the study. Donor 4/20 is presented in light pink, 5/20 in red, 6/20 in green, 7/20 in light blue, 8/20 in purple, 9/20 in orange, 11/20 in grey and 13/20 in dark pink.

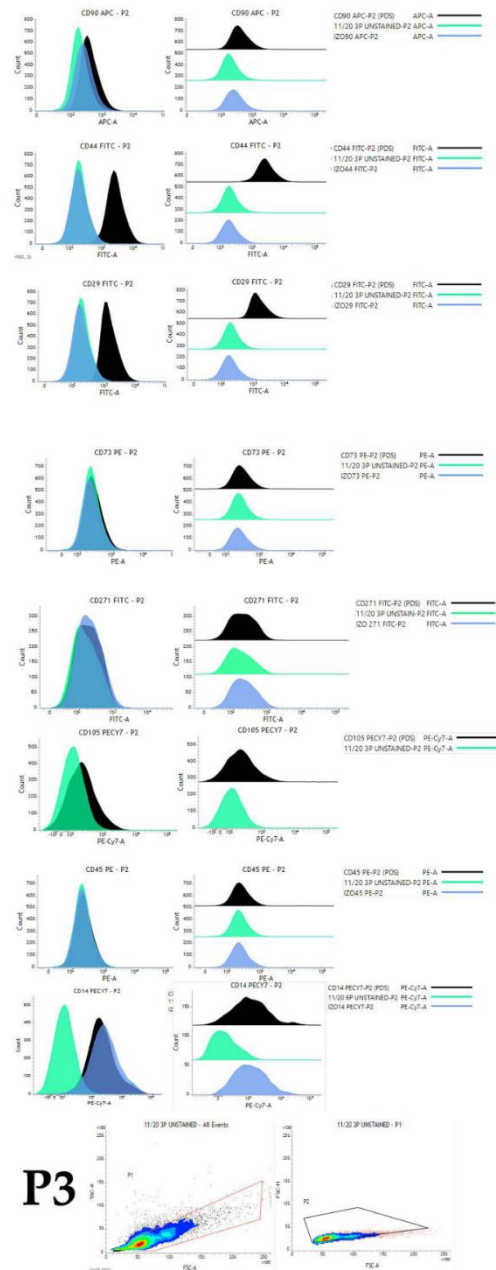


Figure 6. Histogram representation of immunophenotyping results obtained by flow cytometry analysis of cells in passage 3 originating from representative young female canine donor. Histogram presents overlaid unstained population (green), appropriate isotype control (blue) and fully stained population of cells (black).

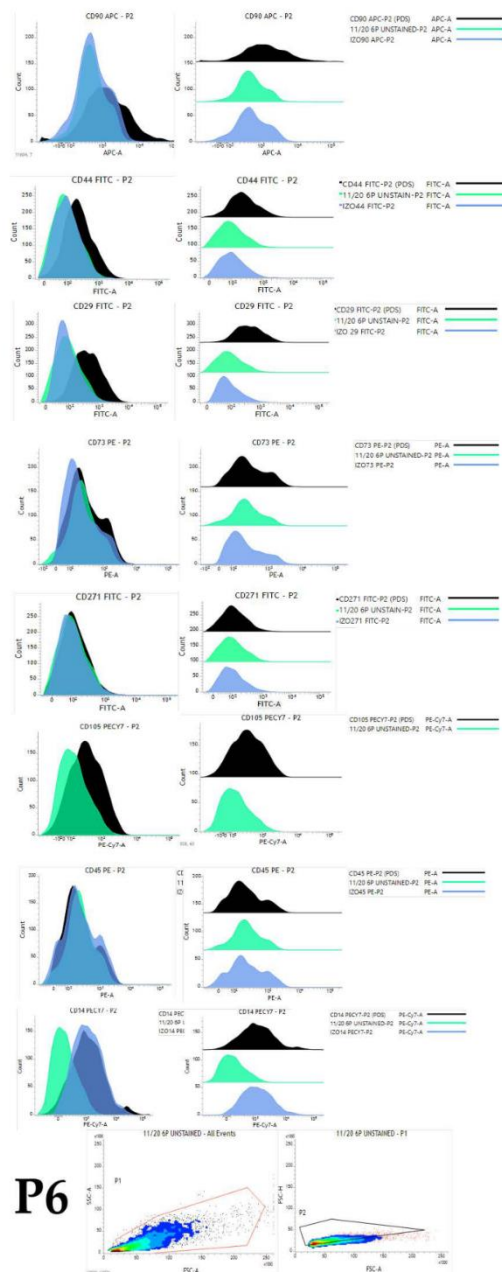


Figure 7. Histogram representation of immunophenotyping results obtained by flow cytometry analysis of cells in passage 6 originating from representative young female canine donor. Histogram presents overlaid unstained population (green), appropriate isotype control (blue) and fully stained population of cells (black).

2.3. Gene Expression

We also aimed to investigate gene expression changes between early (P3) and late passage (P6). We used commercially available array as it enables quick, reliable gene expression analysis. The array encompasses laboratory-verified qPCR assays, with integrated, patented controls to ensure a successful experiment. The results obtained by analysis of RNA integrity and purity matched the criteria needed for the downstream application of RNA prescribed by the array manufacturer ($A_{260}:A_{230}$ ratio greater than 1.7; $A_{260}:A_{230}$ ratio 1.8–2.0; concentration determined by $A_{260} > 40 \mu\text{g/mL}$). Integrity analysis showed the absence of ribosomal RNA degradation with a 28 S/18 S rRNA amount ratio of approximately 2 for all samples.

Our gene expression analysis revealed upregulation of CD44, CD29 and CD45, down-regulation of CD90, while CD73 expression was stable: Figures 5 and 6. Ct values, p values and fold regulation are demonstrated in Table 1.

Table 1. Changes in gene expression between passage 3 and passage 6.

Symbol	AVG Ct		Standard Deviation		AVG Delta(Ct) (Ct(GOI)— Ave Ct(HKG))		Standard Deviation		$2^{(-\text{Avg.}(\Delta\text{Ct}))}$		Fold Change (Compar- ing to Control Group)	p -Value (Compar- ing to Control Group)	Up-Down Regulation (Comparing to Control Group)
	P3	P6	P3	P6	P3	P6	P3	P6	P3	P6			
CD44	19.36	16.99	6.716420	1.548428	4.56	0.76	7.026048	2.686248	0.042306	0.588725	13.92	0.337119	13.92
CD105	20.39	22.01	3.632936	5.497423	5.59	5.78	3.893338	7.179577	0.020694	0.018228	0.88	0.345515	−1.14
CD29	16.54	15.13	3.526914	1.812936	1.74	−1.10	3.361122	2.769505	0.299093	2.147017	7.18	0.331704	7.18
CD73	23.74	25.84	4.609488	4.044292	8.94	9.61	4.350983	3.909274	0.002037	0.001282	0.63	0.507992	−1.59
CD45	27.65	27.69	1.551907	6.902877	12.85	11.46	4.233130	6.742563	0.000135	0.000356	2.62	0.368872	2.62
CD90	17.11	21.58	3.441485	4.568415	2.31	5.35	1.028564	8.537819	0.201242	0.024473	0.12	0.348287	−8.22

3. Discussion

Since stem cell therapy involves cellular manipulation and in vitro cultivation, it is necessary to reveal relevant surface markers expression dynamics during cultivation to predict how cultivation affects the expression and consequently stem cell desirable therapeutic properties.

The influence of cultivation on morphology, phenotype and gene expression changes is the subject of investigation in human MSCs [2,24,25]. However, similar studies involving canine stem cells are lacking. This study, for the first time, revealed changes in the percentage of positivity and surface markers expression dynamics of cAD-MSCs during cultivation. By that, we contributed to their proper cAD-MSCs characterisation and demonstrated the timeframe in which cAD-MSCs cultivated in vitro possess optimal phenotypes for transplantation.

The role of canines as companion animals is on the rise, and research on cAD-MSCs is important as it will provide basic knowledge about cAD-MSCs properties. It will make the foundation for future studies, basic and applied, to ensure excellent stem cell therapies for canines for various conditions.

The expression of CD90/Thy-1 is demonstrated in different cells at different locations in the body but also highly expressed in the aggressive high malignancy grade basal-like breast tumour cell line (Hs578T), pointing to this molecule as a promising breast tumour marker [26]. CD90 is also highly expressed in all MSCs, which is related to the undifferentiated status of MSCs, and a decrease in CD90 level can be correlated with the temporal lineage commitment in vitro [27,28]. The expression pattern for CD90 in canine umbilical cord MSCs was negatively correlated with the number of passages [29]. CD90 expression in our study gently varied during cultivation but generally slightly increased at the protein level. The increase in P4 and P6 was mainly due to high fold change values in P4 and P6 in cells originating from donor 13/20, the oldest donor among all in the study whose cells managed to reach P8. The average fold change of CD90 in P6 of remaining

donors in the study was very low (1.74). The reasons for such variable CD90 expression between 13/20 and the rest of the donors can be explained with intraspecies variability, an important feature of the canine population. The origin of adipose tissue probably could not have an impact on CD90 expression since we found no correlation between MFI values and the area of cAD-MSCs origin (ligament falciform, mesenteric and periovarian area).

Since CD90 appears to influence cell proliferation, differentiation, migration and survival [28], the decrease in its expression during cultivation in cells originating from the other seven donors could be contributing to cellular proliferation arrest that occurred in P6 as well as prolonged proliferation in the case of 13/20 donor.

Downregulation of CD90 gene expression is in line with flow cytometry data after exclusion of 13/20 extreme donor values. Such a discrepancy between CD90 expression at protein and mRNA level as in the case of 13/20 is not a surprise due to the known poor overall correlation between mRNAs and their protein products. The demonstrated decrease in the percentage of CD90⁺ cells is not a surprise since it has already been reported in our previous research [20].

High CD44 expression in our conditions is in line with the high and rising expression of CD44 in canine umbilical cord MSCs [29] and human AD-MSCs (hAD-MSCs) [25]. Gharibi et al. (2014) reported persistent expression of surface markers including CD146, CD105, CD44, CD90 and CD71 by flow cytometry throughout, and expression of these putative stem cell markers persisted even after the loss of differentiation potentials. The expression of CD44 is important from the aspect of possible influence on chondrodifferentiation. Newly published evidence shows that the deficiency of CD44 could inhibit the formation of type II collagen and significantly decrease the production of aggrecan, and CD44 could affect the differentiation of hAD-MSCs into chondrocytes [9]. High expression of CD44 in later passages could indicate preservation of important stem cell features that this molecule is implied to be involved with, such as homing and proliferation. Our gene expression results revealed CD44 upregulation, which can be considered a beneficial finding.

CD45 is a hematopoietic lineage-restricted antigen that is expressed on all hematopoietic cells except for some mature cell types [30]. With passages, the culture of mesenchymal stem cells is decontaminated, and CD45 expression decrease. The expression of CD45 at the mRNA level was very low, which is in line with our protein expression results.

CD73 expression in different subpopulations has the highest inconsistency, indicating that CD73 is a sensitive characteristic of MSCs [31]. Biological characteristics and differentiation potential of CD73⁺ and CD73⁻ cAD-MSCs show that CD73⁺ AD-MSCs are mainly small-sized cells, whereas CD73⁻ AD-MSCs are big-sized cells; both subpopulations can equally differentiate into adipocytes and osteoblasts in vitro [31].

According to our results, cAD-MSCs show low CD73 expression that significantly decreased during in vitro cultivation. The expression pattern of CD73 in our conditions indicate the need to carefully consider the time cells spent in vitro and at which cells are transplanted into patients or model animals, since it could impact their favourable properties and therapeutical effects.

We demonstrated that cAD-MSCs express CD271 at low levels similarly to placenta-derived MSCs while it is not expressed in the synovial membrane [32]. Barilani et al., 2018, detected the highest number of CD271⁺ MSCs soon after isolation in serum-based culture conditions. On the contrary to cAD-MSCs, human bone marrow, adipose-derived and periodontal ligament MSCs show a high level of CD271 expression. CD271⁺ AD-MSCs were proposed as the primary choice for tissue regeneration and autologous stem cell therapies in older subjects [33].

Our data also revealed high and rising expression of CD29 during cultivation time. CD29 proved to be highly expressed on cAD-MSCs, and more than 95% of cells in culture expressed CD29, similar to bone marrow and hAD-MSCs [34].

CD105 expression by cAD-MSCs demonstrated here is in line with murine and hAD-MSCs, where it was induced by exposure of cells to tissue culture plastic and was further affected by passage number and confluence [19].

This study revealed no statistically significant changes in the expression pattern of selected markers or percentage of positive cAD-MSCs, except for CD73. Generally, early passages seem to have a more favourable immunophenotype. However, there are reports on preserved immunophenotype during cultivation up to P6 for hAD-MSCs [25]. More research would be beneficial to reveal the real impact of cultivation on the nature of cultivated cells.

Furthermore, there is a trend towards early termination of AD-MSCs cultures in vitro, usually before the second or third passage. This short-term culturing may, in turn, lead to low, suboptimal cell titer for downstream applications of AD-MSCs. Those obstacles need to be overcome for using cAD-MSCs in the best condition for therapy, and by that, raising the positive therapeutic effect in canines.

In conclusion, one of the most important insights this study brought is the timeframe in which cAD-MSCs cultivated in vitro possess optimal immunophenotype for use in therapy.

The important limitation of the study is the lack of in vivo implication that is clearly needed. The investigations of stem cell effectiveness are obligatory as it reliably provides evidence on the cellular effectiveness and reveals whether demonstrated changes in expression affect their therapeutical properties.

Nevertheless, the peculiarities of cells originating from older donors also remain to be addressed in future research.

4. Materials and Methods

4.1. Ethics

The animal protocols used in this work were evaluated and approved by the by Veterinary Ethics Committee at the Faculty of Veterinary Medicine, University of Zagreb, approval code 640-01/20-17/10, 20 February 2020 and 640-01/20-17/55, 28 September 2020 and Ethics Board of Croatian Veterinary Institute, approval code Z-IV-4-2022/19, 9 May 2019. Owners of all canine donors included in this study provided written informed consent for the use of the biological materials of their pets in research.

4.2. Animals

This study encompasses 8 healthy canine (*Canis lupus familiaris*) female donors aged 6–38 months referred to elective surgical procedures. The donors' details are presented in Table 2.

Table 2. Donor data.

Donor	Species	Age (Months)	Breed	Surgical Procedure	Anatomical Origin of Adipose Tissue Used as a Source of cAD-MSCs	Health Status before Procedure
4/20	Canine	12	Medium poodle	Ovariohysterectomy	Mesenteric	No detectable signs of illness
5/20	Canine	14.5	Ridgeback	Ovariectomy	Periovarian area	No detectable signs of illness
6/20	Canine	6	Dachshund short-haired	Ovariectomy	Periovarian area	No detectable signs of illness
7/20	Canine	9	Mixed breed	Ovariectomy	Periovarian area	No detectable signs of illness
8/20	Canine	9	Beagle	Ovariectomy	Ligament falciform	No detectable signs of illness
9/20	Canine	9	Jack Russell Terrier	Ovariectomy	Periovarian area	No detectable signs of illness
11/20	Canine	36	Belgian Shepherd	Gastropexy	Ligament falciform	No detectable signs of illness
13/20	Canine	38	Mixed breed	Ovariectomy	Ligament falciform	No detectable signs of illness

Considering the diversity of the canine population, we aimed to eliminate other possible influencing factors such as age and sex and included young female donors in our study. The donors can further be divided into three age subgroups (6–9 months, 12–14 months and 36–38 months) decently representing young canines.

The applied criteria hold both an advantage and a disadvantage, as age up to 3 years holds a significant timespan in canine species while at the same time, dogs within that age frame can be considered as young. Furthermore, we decided to characterise cAD-MSCs from young canines because it is important from the banking aspect as the elective surgical procedure is the opportunity to collect the sample and bank the cells for use in adult age.

4.2.1. Adipose Tissue Collection

Adipose tissue was collected as medical waste after surgery. The origin of adipose tissue was the periovarian area, mesentery or falciform ligament (Table 1).

The dogs were sedated with an intramuscular cocktail of 0.3 mg/kg methadone (Comfortan, Genera dd, Croatia) and 2–3 µg/kg dexmedetomidine (Dexdomitor, Zoetis, Parsippany-Troy Hills, NJ, USA). Upon the onset of sedation, an intravenous catheter was placed in the antebrachial vein, and 2–5 mg/kg intravenous propofol (Propofol 1% (10 mg/1 mL) MCT Fresenius emulsion for injection or infusion, Fresenius Kabi, Bad Homburg, Germany) was applied for induction of general anaesthesia. An endotracheal tube was placed in the trachea, and anaesthesia was maintained via an inhalational mixture of 1–2% isoflurane (Forane, Abbott, Chicago, IL, USA) and oxygen. Intraoperative analgesia was provided by applying a bolus dose of fentanyl (1 mg/kg) followed by continuous intravenous administration of fentanyl 0.2 mg/kg/min (Fentanyl injections, Janssen Pharmaceutica N.V., Antwerp, Belgium). Postoperative analgesia was provided with meloxicam (Movalis, Boehringer Ingelheim, Zagreb, Croatia) in an initial bolus dose of 0.2 mg/kg intramuscular followed by a dose of 0.1 mg/kg orally, once a day, for at least 3 days. The surgical site was strichotomised and antiseptically prepared by cleaning with a 2% chlorhexidine soap solution for 5 min (Plivasept pjenušavi, Pliva d.o.o., Zagreb, Croatia). The final skin preparation was completed by applying a light coat of antiseptic surgical solution (70% alcohol) with a spray bottle and allowed to air dry. The surgical site was draped, and a midline celiotomy was performed. After ovariectomy or ovariohysterectomy, the periovarian, mesenteric or falciform adipose tissue (3–10 g) was collected into a sterile Falcon tube (without medium) and placed into a refrigerator until transport to the laboratory.

4.2.2. cAD-MSCs Isolation and Expansion

All collected samples were stored at 4 °C and subjected to isolation protocol within 2 h after sample collection. Isolation of the cAD-MSCs was performed according to the protocol we previously published [30] using 5–8 g of abdominal adipose tissue for isolation. Adipose tissue samples were washed with sterile PBS (in house reagent) with the addition of 1% penicillin/streptomycin antibiotic (p/s; Sigma-Aldrich, St. Louis, MO, USA), minced and placed in 0.2% collagenase type I solution (ThermoFisher Scientific, Waltham, MA, USA) in 50 mL sterile closed tube for digestion during 50 min at 37 °C, 5% CO₂ and 95% humidity, briefly stirring every 10 min. After the incubation period, foetal bovine serum (10%) (FBS, ThermoFisher Scientific, Waltham, MA, USA) was added to digested tissue to block collagenase activity; the suspension was filtered through 70 µm cell strainer (BD Biosciences, Franklin Lakes, NJ, USA) and centrifuged (Hettich Rotina 420, Tutlingen, Germany) 5 min at 2000 rpm (1400 × g). The cell pellet was resuspended in 10 mL Dulbecco's Modified Eagle's Medium (DMEM) Low Glucose (ThermoFisher Scientific, Waltham, MA, USA) and centrifuged a second time at the same conditions. Finally, pellet was resuspended in prewarmed 79% DMEM Low Glucose + 20% FBS + 1% p/s (basal medium) and incubated at 37 °C, 5% CO₂, 95% humidity. The medium was changed 24 h later, and all nonadherent cells were eliminated.

4.2.3. cAD-MSCs Cultivation

Confluent, adherent cells were designated P0. Passaging was performed in a T25 cell culture flask (Nunc, ThermoFisher Scientific, Waltham, MA, USA) using the basal medium. All experiments were performed on freshly, not thawed cells cultivated in vitro and continuously passaged until proliferation arrest. Passaging was performed at a confluence of 80% to 90% up to proliferation arrest. A portion of cells was cryopreserved in P2 and P3 in basal medium + 10% DMSO (Sigma-Aldrich, St. Louis, MO, USA) at -80°C using an alcohol-free freezing container (Corning, Corning, NY, USA) and then placed in liquid nitrogen. The cAD-MSCs suspensions were culture-negative for bacteria and fungi and polymerase chain reaction (PCR) was negative for *Mycoplasma* spp.

4.3. Differentiation Assay

Cells in P2 were passaged and used for the differentiation experiments as previously described [20] with significant improvements related to adipocytes and chondrocyte detection. Cells were induced to differentiate toward trilineage (adipogenic, osteogenic and chondrogenic). In brief, adipodifferentiation and osteodifferentiation tests were performed using a 24-microwell plate (Nunc, ThermoFisher Scientific, Waltham, MA, USA) by seeding 5×10^4 cells per well in a basal medium. After 48 h, cells reached confluence and the basal medium was aspirated and 1 mL of StemMACS AdipoDiff (Miltenyi Biotec, Bergisch Gladbach, Germany). Media for adipocytes, StemMACS OsteoDiff. Media for osteoblasts, (Miltenyi Biotec, Bergisch Gladbach, Germany) were added to particular wells except for control wells which were further cultivated in basal medium. Differentiation and basal media were changed every 48–72 h, and plates were microscopically (Zeiss, Oberkochen, Germany) examined ($\times 10$). Differentiation was performed for 21 days.

Chondrodifferentiation was performed in 15 mL conical polypropylene tubes with a cap according to Miltenyi Biotec protocol with minor modifications. In total, 10^5 cells resuspended in the basal medium was added to the control and test tube and centrifuged at $235 \times g$ for 10 min. Basal medium was aspirated from the test tube for chondrodifferentiation, cells were resuspended in 1 mL of ChondroDiff Media (Miltenyi Biotec, Bergisch Gladbach, Germany) and the centrifugation step was repeated. Control tube containing cell pellet in basal medium and chondrodifferentiation test tube caps were slightly opened, and tubes were incubated at 37°C , 5% CO_2 , 95% humidity 21 days. Media were changed every 48–72 h.

4.3.1. Detection of Adipocytes

Detection of adipocytes was performed by removing StemMACS AdipoDiff Media and washing the cells twice with 300 μL of sterile PBS (in house reagent). Cells were fixed with 300 μL of 10% buffered formalin and incubated for 10 min at room temperature (RT). Formalin was aspirated completely, cells were washed twice with deionised H_2O and 300 μL of Oil Red O (Sigma-Aldrich, St. Louis, MO, USA) was added to all wells. Plates were incubated for 20 min at RT. Oil Red O (Sigma-Aldrich, St. Louis, MO, USA) was aspirated, cells were washed $2 \times$ with deionised H_2O and finally, 100 μL of deionised H_2O was added to keep cells moisture. Immediately after staining, cells were examined under a microscope and pictures were taken with the camera (Zeiss, Oberkochen, Germany). Red colour stained cells were considered to be positive.

4.3.2. Detection of Osteoblasts

Detection of osteoblasts was performed by removing StemMACS OsteoDiff. Media (Miltenyi Biotec, Bergisch Gladbach, Germany), and washing the cells twice with 300 μL of sterile PBS (in house reagent). Cells were fixed by adding 300 μL 10% buffered formalin and incubated 10 min at RT. Formalin was aspirated completely, cells were washed twice with deionised H_2O and 300 μL of SIGMAFAST BCIP/NBT substrate (Sigma-Aldrich, St. Louis, MO, USA) was added to all wells. Plates were incubated for 10 min at RT. The substrate was aspirated, cells were washed $2 \times$ with deionised H_2O and finally, 100 μL

of deionised H₂O was added to keep cells moisture. Immediately after staining, stained cells were examined under a microscope and pictures were taken with the camera (Zeiss, Oberkochen, Germany). Purple-stained cells were considered to be positive.

4.3.3. Detection of Chondrocytes

Detection of chondrocytes was performed by carefully removing StemMACS ChondroDiff. Media (Miltenyi Biotec, Bergisch Gladbach, Germany) without aspirating spheroids and washing the spheroids twice with 300 µL of sterile PBS (in house reagent). Spheroids were carefully aspirated and placed in wells in a 24-microwell plate. Spheroids were fixed by adding 300 µL of neutral buffered formalin (3.7%) (in-house reagent) and incubated for 16 h at RT in the dark. Formalin was aspirated, and spheroids were washed twice with deionised H₂O. Spheroids were dehydrated in ethanol series (2 × 30 min 70% ethanol, 2 × 30 min 80% ethanol, 2 × 30 min 96% ethanol, 2 × 30 min 100% ethanol) and placed in xylol.

Alcian Blue 8GX (Sigma-Aldrich, St. Louis, MO, USA) stain was used to detect proteoglycan aggrecan in the extracellular matrix (ECM) produced by chondrocytes in 3D micromass culture (i.e., chondrocyte nodule or spheroid) of cAD-MSCs cultivated for 21 days in StemMACS ChondroDiff Media (Miltenyi Biotec, Bergisch Gladbach, Germany). Only cAD-MSCs spheroids from the same donor cultivated in StemMACS Expansion Media were used as a negative control. Counterstaining was performed with Nuclear fast red-aluminium sulfate solution 0.1% (Sigma Aldrich, St. Louis, MO, USA), which stains cell nuclei pink to red.

Formalin-fixed paraffin-embedded spheroids were sectioned at 5 µm thickness and transferred onto positively charged glass slides.

After deparaffinisation in xylene (3 × 5 min.) and rehydration in decreasing ethanol concentrations (100% 5 min., 96% 5 min., 75% 5 min.) ending with deionised H₂O (2 min.) slides were immersed in 3% acetic acid for 3 min, then in 1% Alcian Blue (Sigma-Aldrich, St. Louis, MO, USA) for 30 min, followed by rinsing a few times in 3% acetic acid and immersing in running tap water (10 min). Slides were rinsed a few times in deionised H₂O before and after counterstaining with Nuclear fast red-aluminium sulfate (Sigma-Aldrich, St. Louis, MO, USA). After dehydration in increasing ethanol concentrations (70% and 96% 1 min., 100% 2 × 1 min.) and coverslipping, the slides were examined under a microscope Nikon Eclipse E600 (Nikon, Tokyo, Japan) and photographs were taken with Olympus DP20 (Olympus, Tokyo, Japan) camera.

4.4. Immunophenotyping

To reveal the expression pattern and percentage of positive cells for selected markers, cAD-MSCs were analysed in passages P1 to P6. For the flow cytometry experiments, we created an antibody panel (Table 3) based on the following criteria: antibodies have to be raised against a canine antigen or have to be cross-reactive with canines; antibodies have to be labelled with an appropriate fluorophore that can be detected with two BD FACSVerser (serial number Z6511540253, BD Biosciences, Franklin Lakes, NJ, USA) lasers (blue or red) and there has to be an appropriate isotype control with the same fluorophore as the belonging antibody.

Prior to each experiment, daily performance QC was performed using CS & T beads (BD Biosciences, Franklin Lakes, NJ, USA) lot number 92,323 and characterisation QC was performed every 6 months.

Cells were detached using a cell scraper and carefully resuspended and centrifuged at 235 × g for 10 min. The medium was aspirated, and cells were resuspended in a 1 mL cell wash (BD Biosciences, Franklin Lakes, NJ, USA). Cell number was obtained using an automated cell counter (Corning, Corning, NY, USA). Cell number was adjusted to 10⁵ per mL, and 1 mL of cell suspension was carefully added to each test tube designated to antibody and isotype control from the panel. Tubes were centrifuged for 5 min at 235 × g, the supernatant was aspirated and the cell pellet was carefully resuspended

to enable antibodies to reach each cell. Antibody concentration was used according to manufacturers' instructions. Single stained test tubes were incubated for 30 min at 4 °C. After the incubation period, 2 mL cell wash (BD Biosciences, Franklin Lakes, NJ, USA) was added and tubes were centrifuged for 5 min at 235× g to remove the excess of unbound antibodies. Finally, 500 µL of cell wash was added for flow cytometric analysis.

Table 3. Antibody panel created for the study.

Antigen	Clone	Host	Fluorophore	Reactivity	Clonality	Manufacturer/Serial Number
CD44	MEM-263	Mouse	FITC	Canine, Human, Porcine	Monoclonal	Antibodies-online, Germany/ABIN452099
Isotype IgG1	VI-AP	Mouse	FITC		Monoclonal	Antibodies-online, Germany/ABIN1741583
CD45	YKIX716.13	Rat	PE	Canine	Monoclonal	Bio-Rad, USA/MCA1042PE
Isotype IgG2b		Rat	PE		Monoclonal	Bio-Rad, USA/MCA6006PE
CD73		Rabbit	PE	Human, Mouse, Rat, Dog, Chicken	Polyclonal	Bioss antibodies, USA/bs-4834R-PE
Isotype IgG		Rabbit	PE		Polyclonal	Antibodies-online, Germany/ABIN376422
CD 29	MEM-101A	Mouse	FITC	Canine, Human, Porcine	Monoclonal	Antibodies-online, Germany/ABIN94056
Isotype IgG1	VI-AP	Mouse	FITC		Monoclonal	Antibodies-online, Germany/ABIN1741583
CD271	ME20.4-1.H4	Mouse	FITC	Human, Canine	Monoclonal	Miltenyi Biotec, Germany/130-098-103
Isotype			FITC		Monoclonal	Miltenyi Biotec, Germany/130-113-761
CD90	5E10	Mouse	APC	Human, cross-reacts with monkey, porcine, canine protein	Monoclonal	Covalab, France/mab21094
Isotype IgG1	Unknown	Mouse	APC		Monoclonal	Antibodies-online, Germany/ABIN2145334
CD105	SN6	Mouse	PE-Cy 7	Human, published species canine	Monoclonal	Thermo Fisher Scientific25-1057-42
CD14		Mouse	PE-Cy 7	Human (QC Testing), Dog (Tested in Development)	Monoclonal	BD Pharmingen
Isotype IgG2		Mouse	PE-Cy 7		Monoclonal	BD Pharmingen

Experimental settings were set up using unstained cells, and the same settings were used for all tubes in each experiment. Cell viability was checked with Propidium Iodide staining solution (BD Biosciences, Franklin Lakes, NJ, USA) at the end of the experiment.

The same gating strategy has been used for all data files. The first gate (P1) was set for the selection of a homogenous population with the exclusion of cell debris using

forward and side scatter parameters. The second gate (P2) was set using forward-scatter height and area parameters for double cell exclusion, so only singlets were selected for further analysis.

Results were analysed using FACSuite software. The results for 10,000 acquired events were expressed as median fluorescence intensity (MFI). MFI fold change was calculated by dividing the median of the appropriate antibody with the median of isotype control ($\frac{MFI \text{ Antibody}}{MFI \text{ Isotype control}}$). Obtained values (from each donor for each marker) were used to calculate the average, which was further used to present data graphically. The average MFI and standard deviation for each CD of all donors in each passage were calculated and data were graphically presented.

4.5. Gene Expression

Changes in gene expression of cAD-MSCs markers (CD90⁺, CD44⁺, CD73⁺, CD29⁺, CD105⁺ and CD45⁻) were investigated using validated RT² Profiler PCR Array Format R (Qiagen, Hilden, Germany) suitable for use with Rotor-Gene Q (Qiagen, Hilden, Germany). This array includes SYBR Green-optimized primer assays.

4.5.1. Total RNA Extraction

Total RNA was isolated from cAD-MSCs cultivated in a T75 cell culture flask. Cells were detached using a cell scraper, centrifuged at 235 × *g* for 10 min and used immediately for RNA isolation. The RNA was isolated using the RNeasy Mini Kit (Qiagen, Hilden, Germany), following the manufacturer's instructions. The integrity of isolated RNA was examined by 1% agarose gel electrophoresis; the RNA concentration and purity were determined by measuring the absorbance in a Nanophotometer P360 (Implen, Munich, Germany).

4.5.2. Real-Time PCR Array

RT² First Strand Kit (Qiagen, Hilden, Germany) was used for genomic DNA (gDNA) elimination and cDNA synthesis, which served as a template for RT² Profiler PCR Array (Qiagen, Hilden, Germany). cDNA was synthesised from 800 ng of total RNA. First, in a 10 µL reaction, gDNA was eliminated for 5 min at 42 °C and then the mixture was used in a 20 µL cDNA synthesis mixture according to the manufacturer's instructions.

Cycling conditions were set according to the manufacturer's instructions. The array contains primers specific for CD90, CD44, CD73, CD29, CD45 and CD105, and primers for gDNA, RT and PCR controls. One well is used to check gDNA control, 3 wells contain reverse-transcription controls and 3 wells contain a positive PCR control. Obtained data were analysed using RT² Profiler PCR Array Data Analysis software available online: <https://dataanalysis2.qiagen.com/pcr> (accessed on 3 February 2021). The software analyses the data using a $\Delta\Delta C_t$ method and performs statistical analysis of the data (based on Student's *t*-test); differences between gene expression levels were considered significant when $p < 0.05$. Fold change cutoff of 2 was chosen.

4.6. Statistics

The data distribution was checked with the Kolmogorov–Smirnov test. To investigate statistical significance between mean values obtained in early passages (P1–P3) and late passages (P4–P6), we used Student's *t*-test. For graphical representation, we used the Whisker box plot to reveal minimum, maximum, median and quartiles for MFI fold change values of each marker from P1 to P6.

Author Contributions: Conceptualisation, N.K.; methodology, N.K., M.P., D.V., P.K., I.L. and A.M.; software, N.K.; formal analysis, N.K., M.P.; investigation, N.K., M.P. and D.B.; resources, N.K.; data curation, N.K. and M.P.; writing—original draft preparation, N.K. and M.P.; writing—review and editing, N.K., D.B., N.T., D.V., P.K., I.L. and B.H.; visualisation, N.K., M.P. and D.B.; supervision, N.K.; project administration, N.K.; funding acquisition, N.K. All authors have read and agreed to the published version of the manuscript.

Funding: This research was funded by Croatian Science Foundation (HRZZ) and performed within Installation Research Project (UIP-2019-04-2178) “Revealing transcriptome and secretome of mesenchymal stem cells” SECRET. We thank HRZZ for supporting our research.

Institutional Review Board Statement: Veterinary Ethics Committee at the Faculty of Veterinary Medicine, University of Zagreb, and Ethics Board of Croatian Veterinary Institute approved this research; approval number 640-01/20-17/10, 640-01/20-17/55 and Z-IV-4-2022/19.

Informed Consent Statement: Owners of all canine donors included in this study provided written informed consent for the use of the biological materials of their pets in research.

Data Availability Statement: The datasets used and/or analysed within the frame of the study can be provided by the corresponding author upon reasonable request.

Acknowledgments: We thank Mihaela Stuparić Komušar for her generous help during spheroid preparation and staining.

Conflicts of Interest: The authors declare no conflict of interest.

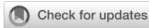
References

- Dominici, M.; Le Blanc, K.; Mueller, I.; Slaper-Cortenbach, I.; Marini, F.C.; Krause, D.S.; Deans, R.J.; Keating, A.; Prockop, D.J.; Horwitz, E.M. Minimal criteria for defining multipotent mesenchymal stromal cells. The International Society for Cellular Therapy position statement. *Cytotherapy* **2006**, *8*, 315–317. [\[CrossRef\]](#)
- Barilani, M.; Banfi, F.; Sironi, S.; Ragni, E.; Guillaumin, S.; Polveraccio, F.; Rosso, L.; Moro, M.; Astori, G.; Pozzobon, M.; et al. Low-affinity Nerve Growth Factor Receptor (CD271) Heterogeneous Expression in Adult and Fetal Mesenchymal Stromal Cells. *Sci. Rep.* **2018**, *8*, 1–11. [\[CrossRef\]](#)
- Gharibi, B.; Hughes, F.J. Effects of Medium Supplements on Proliferation, Differentiation Potential, and In Vitro Expansion of Mesenchymal Stem Cells. *Stem Cells Transl. Med.* **2012**, *1*, 771–782. [\[CrossRef\]](#)
- Tan, K.; Zhu, H.; Zhang, J.; Ouyang, W.; Tang, J.; Zhang, Y.; Qiu, L.; Liu, X.; Ding, Z.; Deng, X. CD73 expression on mesenchymal stem cells dictates the reparative properties via its anti-inflammatory activity. *Stem Cells Int.* **2019**, *2019*, 8717694. [\[CrossRef\]](#)
- Moraes, D. What the relationship between CD90 e CD44 in Mesenchymal Stem Cells? *Cytotherapy* **2018**, *20*, s47. [\[CrossRef\]](#)
- Kumar, A.; Bhanja, A.; Bhattacharyya, J.; Jagannathan, B.G. Multiple roles of CD90 in cancer. *Tumor Biol.* **2016**, *37*, 11611–11622. [\[CrossRef\]](#) [\[PubMed\]](#)
- Sauzay, C.; Voutetakis, K.; Chatziioannou, A.A.; Chevet, E.; Avril, T. CD90/Thy-1, a cancer-associated cell surface signaling molecule. *Front. Cell Dev. Biol.* **2019**, *7*, 1–11. [\[CrossRef\]](#) [\[PubMed\]](#)
- Jordan, A.R.; Racine, R.R.; Hennig, M.J.P.; Lokeshwar, V.B. The role of CD44 in disease pathophysiology and targeted treatment. *Front. Immunol.* **2015**, *6*, 1–14. [\[CrossRef\]](#)
- Xu, Y.; Wang, Y.Q.; Wang, A.T.; Yu, C.Y.; Luo, Y.; Liu, R.M.; Zhao, Y.J.; Xiao, J.H. Effect of CD44 on differentiation of human amniotic mesenchymal stem cells into chondrocytes via Smad and ERK signaling pathways. *Mol. Med. Rep.* **2020**, *21*, 2357–2366. [\[CrossRef\]](#) [\[PubMed\]](#)
- Chen, B.; Frangogiannis, N.G. Immune cells in repair of the infarcted myocardium. *Microcirculation* **2017**, *24*, 1–10. [\[CrossRef\]](#)
- Suto, E.G.; Mabuchi, Y.; Toyota, S.; Taguchi, M.; Naraoka, Y.; Itakura, N.; Matsuoka, Y.; Fujii, Y.; Miyasaka, N.; Akazawa, C. Advantage of fat-derived CD73 positive cells from multiple human tissues, prospective isolated mesenchymal stromal cells. *Sci. Rep.* **2020**, *10*, 1–9. [\[CrossRef\]](#)
- Hynes, R.O. Integrins: Versatility, modulation, and signaling in cell adhesion. *Cell* **1992**, *69*, 11–25. [\[CrossRef\]](#)
- Rodeheffer, M.S.; Birsoy, K.; Friedman, J.M. Identification of White Adipocyte Progenitor Cells In Vivo. *Cell* **2008**, *135*, 240–249. [\[CrossRef\]](#) [\[PubMed\]](#)
- Davies, O.G.; Cooper, P.R.; Shelton, R.M.; Smith, A.J.; Scheven, B.A. Isolation of adipose and bone marrow mesenchymal stem cells using CD29 and CD90 modifies their capacity for osteogenic and adipogenic differentiation. *J. Tissue Eng.* **2015**, *6*. [\[CrossRef\]](#)
- Álvarez-Viejo, M. CD271 as a marker to identify mesenchymal stem cells from diverse sources before culture. *World J. Stem Cells* **2015**, *7*, 470. [\[CrossRef\]](#) [\[PubMed\]](#)
- Guerrero-Esteo, M.; Sanchez-Elsner, T.; Letamendia, A.; Bernabeu, C. Extracellular and cytoplasmic domains of endoglin interact with the transforming growth factor-beta receptors I and II. *J. Biol. Chem.* **2002**, *277*, 29197–29209. [\[CrossRef\]](#)
- Sanz-Rodríguez, F.; Guerrero-Esteo, M.; Botella, L.M.; Banville, D.; Vary, C.P.H.; Bernabéu, C. Endoglin regulates cytoskeletal organisation through binding to ZRP-1, a member of the LIM family of proteins. *J. Biol. Chem.* **2004**, *279*, 32858–32868. [\[CrossRef\]](#) [\[PubMed\]](#)
- Bearden, R.N.; Huggins, S.S.; Cummings, K.J.; Smith, R.; Gregory, C.A.; Saunders, W.B. In-vitro characterisation of canine multipotent stromal cells isolated from synovium, bone marrow, and adipose tissue: A donor-matched comparative study. *Stem Cell Res. Ther.* **2017**, *8*, 1–22. [\[CrossRef\]](#)

19. Anderson, P.; Carrillo-Gálvez, A.B.; García-Pérez, A.; Cobo, M.; Martín, F. CD105 (Endoglin)-Negative Murine Mesenchymal Stromal Cells Define a New Multipotent Subpopulation with Distinct Differentiation and Immunomodulatory Capacities. *PLoS ONE* **2013**, *8*, e76979. [[CrossRef](#)] [[PubMed](#)]
20. Krešić, N.; Šimić, I.; Lojkić, I.; Bedeković, T. Canine Adipose Derived Mesenchymal Stem Cells Transcriptome Composition Alterations: A Step towards Standardising Therapeutic. *Stem Cells Int.* **2017**, *2017*, 4176292. [[CrossRef](#)]
21. Wagner, W.; Bork, S.; Lepperdinger, G.; Joussen, S.; Ma, N.; Strunk, D.; Koch, C. How to track cellular aging of mesenchymal stromal cells? *Aging* **2010**, *2*, 224–230. [[CrossRef](#)] [[PubMed](#)]
22. Wagner, W.; Horn, P.; Castoldi, M.; Diehlmann, A.; Bork, S.; Saffrich, R.; Benes, V.; Blake, J.; Pfister, S.; Eckstein, V.; et al. Replicative senescence of mesenchymal stem cells: A continuous and organised process. *PLoS ONE* **2008**, *3*, e2213. [[CrossRef](#)] [[PubMed](#)]
23. Haque, Z.; Rahman, M.A.; Khan, M.Z.I.; Hussan, M.T.; Alam, M.M. Alcohol-based fixatives can better preserve tissue morphology than formalin. *Int. J. Morphol.* **2020**, *38*, 1371–1375. [[CrossRef](#)]
24. Yang, Y.H.K.; Ogando, C.R.; Wang See, C.; Chang, T.Y.; Barabino, G.A. Changes in phenotype and differentiation potential of human mesenchymal stem cells aging in vitro. *Stem Cell Res. Ther.* **2018**, *9*, 1–14. [[CrossRef](#)] [[PubMed](#)]
25. Mieczkowska, A.; Schumacher, A.; Filipowicz, N.; Wardowska, A.; Zieliński, M.; Madanecki, P.; Nowicka, E.; Langa, P.; Deptuła, M.; Zieliński, J.; et al. Immunophenotyping and transcriptional profiling of in vitro cultured human adipose tissue derived stem cells. *Sci. Rep.* **2018**, *8*, 1–13. [[CrossRef](#)] [[PubMed](#)]
26. Ramos, A.; Lobba, M.; Claudia, A.; Carreira, O.; Luiz, O.; Deocesano-pereira, C.; Aparecida, C.; Cerqueira, D.; Osorio, B.; Soares, F.A.; et al. High CD90 (THY-1) expression positively correlates with cell transformation and worse prognosis in basal-like breast cancer tumors. *PLoS ONE* **2018**, *13*, e0199254.
27. Sibov, T.T.; Severino, P.; Marti, L.C.; Pavon, L.F.; Oliveira, D.M.; Tobo, P.R.; Campos, A.H.; Paes, A.T.; Amaro, E.; Gamarra, L.F.; et al. Mesenchymal stem cells from umbilical cord blood: Parameters for isolation, characterisation and adipogenic differentiation. *Cytotechnology* **2012**, *64*, 511–521. [[CrossRef](#)]
28. Moraes, D.A.; Sibov, T.T.; Pavon, L.F.; Alvim, P.Q.; Bonadio, R.S.; Da Silva, J.R.; Pic-Taylor, A.; Toledo, O.A.; Marti, L.C.; Azevedo, R.B.; et al. A reduction in CD90 (THY-1) expression results in increased differentiation of mesenchymal stromal cells. *Stem Cell Res. Ther.* **2016**, *7*, 1–14. [[CrossRef](#)] [[PubMed](#)]
29. Lee, K.S.; Cha, S.H.; Kang, H.W.; Song, J.Y.; Lee, K.W.; Ko, K.B.; Lee, H.T. Effects of serial passage on the characteristics and chondrogenic differentiation of canine umbilical cord matrix derived mesenchymal stem cells. *Asian-Australas. J. Anim. Sci.* **2013**, *26*, 588–595. [[CrossRef](#)] [[PubMed](#)]
30. Ogata, K.; Satoh, C.; Tachibana, M.; Hyodo, H.; Tamura, H.; Dan, K.; Kimura, T.; Sonoda, Y.; Tsuji, T. Identification and Hematopoietic Potential of CD45⁻ Clonal Cells with Very Immature Phenotype (CD45⁻CD34⁻CD38⁻Lin⁻) in Patients with Myelodysplastic Syndromes. *Stem Cells* **2005**, *23*, 619–630. [[CrossRef](#)]
31. Li, Q.; Qi, L.J.; Guo, Z.K.; Li, H.; Zuo, H.B.; Li, N.N. CD73⁺ adipose-derived mesenchymal stem cells possess higher potential to differentiate into cardiomyocytes in vitro. *J. Mol. Histol.* **2013**, *44*, 411–422. [[CrossRef](#)] [[PubMed](#)]
32. Lv, F.J.; Tuan, R.S.; Cheung, K.M.C.; Leung, V.Y.L. Concise review: The surface markers and identity of human mesenchymal stem cells. *Stem Cells* **2014**, *32*, 1408–1419. [[CrossRef](#)] [[PubMed](#)]
33. Cuevas-Diaz Duran, R.; González-Garza, M.T.; Cardenas-Lopez, A.; Chavez-Castilla, L.; Cruz-Vega, D.E.; Moreno-Cuevas, J.E. Age-related yield of adipose-derived stem cells bearing the low-affinity nerve growth factor receptor. *Stem Cells Int.* **2013**, *2013*, 372164. [[CrossRef](#)]
34. Takemitsu, H.; Zhao, D.; Yamamoto, I.; Harada, Y.; Michishita, M.; Arai, T. Comparison of bone marrow and adipose tissue-derived canine mesenchymal stem cells. *BMC Vet. Res.* **2012**, *8*, 150. [[CrossRef](#)] [[PubMed](#)]

8.2. Paper II: "*In vitro* aging alters the gene expression and secretome composition of canine adipose-derived mesenchymal stem cells"

The article was published in *Frontiers in Veterinary Science*, 11:1387174, in March 2024. The DOI number of the article is 10.3389/fvets.2024.1387174. (WoS JCR (2023) IF 2.6, Q1 in Veterinary Sciences; Scopus SJR (2023) 0.73, h-index 70, Q1 in Veterinary (miscellaneous)). The full paper, along with its supplementary material, is available via open access at the following link: <https://doi.org/10.3389/fvets.2024.1387174>.



OPEN ACCESS

EDITED BY
Eleonora Iacono,
University of Bologna, Italy

REVIEWED BY
Alessandra Pelagalli,
University of Naples Federico II, Italy
Amirhesam Babajani,
Iran University of Medical Sciences, Iran

*CORRESPONDENCE
Marina Prišlin
✉ prišlin@veinst.hr
Dragan Brnić
✉ brnic@veinst.hr

PRESENT ADDRESS
Dunja Vlahović,
Department of Veterinary Pathology,
Faculty of Veterinary Medicine,
University of Zagreb, Zagreb, Croatia

RECEIVED 16 February 2024
ACCEPTED 08 March 2024
PUBLISHED 28 March 2024

CITATION
Prišlin M, Butorac A, Bertoša R,
Kunić V, Ljolje I, Kostešić P, Vlahović D,
Naletilić Š, Turk N and Brnić D (2024) *In vitro*
aging alters the gene expression and
secretome composition of canine
adipose-derived mesenchymal stem cells.
Front. Vet. Sci. 11:1387174.
doi: 10.3389/fvets.2024.1387174

COPYRIGHT
© 2024 Prišlin, Butorac, Bertoša, Kunić, Ljolje,
Kostešić, Vlahović, Naletilić, Turk and Brnić.
This is an open-access article distributed
under the terms of the [Creative Commons
Attribution License \(CC BY\)](https://creativecommons.org/licenses/by/4.0/). The use,
distribution or reproduction in other forums is
permitted, provided the original author(s) and
the copyright owner(s) are credited and that
the original publication in this journal is cited,
in accordance with accepted academic
practice. No use, distribution or reproduction
is permitted which does not comply with
these terms.

In vitro aging alters the gene expression and secretome composition of canine adipose-derived mesenchymal stem cells

Marina Prišlin^{1*}, Ana Butorac², Rea Bertoša², Valentina Kunić¹, Ivana Ljolje³, Petar Kostešić⁴, Dunja Vlahović^{5†}, Šimun Naletilić⁵, Nenad Turk⁶ and Dragan Brnić^{1*}

¹Virology Department, Croatian Veterinary Institute, Zagreb, Croatia, ²Bioanalytical Laboratory II—Proteomics, Bicro Biocentre Ltd., Zagreb, Croatia, ³Veterinary Clinic for Small Animals Buba, Zagreb, Croatia, ⁴Surgery, Orthopedics and Ophthalmology Clinic, Faculty of Veterinary Medicine, University of Zagreb, Zagreb, Croatia, ⁵Department for Pathological Morphology, Croatian Veterinary Institute, Zagreb, Croatia, ⁶Department of Microbiology and Infectious Diseases with Clinic, Faculty of Veterinary Medicine, University of Zagreb, Zagreb, Croatia

Introduction: Canine adipose-derived mesenchymal stem cells (cAD-MSCs) hold therapeutic promise due to their regenerative potential, particularly within their secretome. However, concerns arise regarding the impact of *in vitro* cultivation necessitated for storing therapeutic doses, prompting this study to comprehensively explore the impact of *in vitro* aging on gene expression and secretome composition.

Methods: The study involved collecting abdominal adipose tissue samples from nine healthy female dogs, from which cAD-MSCs were extracted and cultured. Stem cells were validated through trilineage differentiation assays and flow cytometry immunophenotyping. Gene expression profiling using RT-qPCR array, and cAD-MSCs secretome LC-MS/MS analysis, were conducted at passages 3 and 6 to reveal gene expression and protein composition alterations during *in vitro* culture.

Results and Discussion: The results demonstrate that the gene expression and secretome composition of cAD-MSCs were impacted by *in vitro* aging. Among many alterations in gene expression between two passages, two significant downregulations were noted in the MSC-associated PTPRC and IL10 genes. While the majority of proteins and their functional characteristics were shared between passages, the influence of cell aging on secretome composition is highlighted by 10% of proteins being distinctively expressed in each passage, along with 21 significant up- and downregulations. The functional attributes of proteins detected in passage 3 demonstrated a greater inclination towards supporting the regenerative capacity of cAD-MSCs. Moreover, proteins in passage 6 exhibited a noteworthy correlation with the blood coagulation pathway, suggesting an elevated likelihood of coagulation events. To the best of our knowledge, this study presents the first original perspective on the changes in secretome composition that occur when cAD-MSCs age *in vitro*. Furthermore, it contributes to broadening the currently restricted knowledge base concerning the secretome of cAD-MSCs. In conclusion, our findings show that the regenerative potential of cAD-MSCs, as well as their secretome, may be compromised by *in vitro* aging. Therefore, our study suggests a preference for earlier passages when considering these cells for therapeutic applications.

KEYWORDS

canine adipose-derived mesenchymal stem cell, *in vitro*, gene expression, secretome, *in vitro* aging, long-term culture, veterinary regenerative medicine

1 Background

New approaches in veterinary regenerative medicine instill hope by providing increasing evidence of advancements in treating previously incurable diseases through stem cells (1–3). The canine adipose-derived mesenchymal stem cells (cAD-MSCs) are a focal point of current research, given the abundance, ease of collection, and higher proliferation rate of AD-MSCs in contrast to alternative mesenchymal stem cell (MSCs) resources (4–6). The cAD-MSCs have been confirmed to possess regenerative capabilities facilitated by their multipotency and, notably, their ability to modulate the immune response (7–9).

Based on most recent studies, the prospect of cellular regeneration is found in the paracrine activity of cAD-MSCs, called secretome (10–12). The secretome encompasses soluble factors, including cytokines, growth factors, morphogens, chemokines, and non-soluble factors, known as extracellular vesicles containing proteins, lipids and RNAs (12). Formerly viewed as cellular debris, it is now established that these biomolecules play a pivotal role in modulating various biological processes such as cell proliferation, survival, differentiation, immunomodulation, anti-apoptosis, and angiogenesis (11). From the current point of view, cAD-MSCs secretome provides several advantages over cAD-MSCs cell therapy, such as a lower risk of thrombosis and tumor formation and easier manufacturing, handling, and storage. Furthermore, secretome could be mass-produced under controlled conditions, tailored for therapeutic effects, and stored for immediate use in acute conditions without the need for a donor or time-consuming cell expansion (10, 12, 13).

However, to achieve and store therapeutic doses of cAD-MSCs and their secretome, *in vitro* cultivation is needed. Throughout the long-term cultivation process, MSCs undergo replicative senescence, leading to a potential reduction or absence of positive therapeutic outcomes, as extensively reviewed in human research (14, 15). Long-term cultivated MSCs undergo enlargement and adopt a hypertrophic morphology, aligning with significant changes in biological features, gene expression profile, differentiation, and immunomodulatory potential (14, 16).

In contrast to human MSCs, there has been limited investigation into the impact of *in vitro* aging on gene expression profiles and secretome composition of cAD-MSCs. Our prior research has contributed to a better understanding of gene expression changes during *in vitro* passages, albeit on a limited scale (17, 18), indicating the need for further investigation. To our knowledge, no data has been published regarding alterations in the secretome composition during

long-term culture of cAD-MSCs. Only two studies investigated cAD-MSCs' secretome; the initial characterization of soluble factors and exosomes confirmed their immunomodulatory potential (5). Moreover, additional research reaffirmed the immunosuppressive effects of cAD-MSCs secretome exosomes *in vitro* (19).

Therefore, the primary objective of this study was to enhance the understanding of the effects of *in vitro* aging on the gene expression and secretome composition of cAD-MSCs.

2 Methods

2.1 Ethics approval and consent to participate

The present research was evaluated and approved by the Ethics Board of the Croatian Veterinary Institute, approval code Z-IV-4-2022/19, May 9, 2019, and Veterinary Ethics Committee at the Faculty of Veterinary Medicine, University of Zagreb, approval code 640-01/20-17/10, February 20, 2020, 640-01/20-17/55, September 28, 2020, and 640-01/22-02/07, April 20, 2022. Canine donor's owners provided written informed consent before sampling.

2.2 Adipose tissue collection, cAD-MSCs extraction, and propagation

The research involved obtaining abdominal adipose tissue samples from nine clinically healthy female dogs (*Canis lupus familiaris*) who underwent elective ovariohysterectomy or ovariectomy surgical procedures. We decided to collect only female donors due to the abundance of adipose tissue at elective surgeries compared to male donors. The latter would need laparoscopic sampling to obtain the adequate quantity, which we considered to be against the 3R approach (20). Nevertheless, sex was not recognized as influential in cell surface marker expression, viability, proliferation, or differentiation potential (21). The acquisition of adipose tissue, cAD-MSCs extraction, and propagation adhered to the established protocol previously detailed in Krešić et al. (18). Briefly, 1–7 g of adipose tissue (Table 1), depending on the availability, was obtained from biomedical waste of ovarian mesostructure, placed into a sterile Falcon tube devoid of the medium, and stored at 4°C until transportation to the laboratory. Table 1 details the donors' age, breed, and adipose tissue mass. The extraction of cAD-MSCs was carried out within a 2-h window from sample collection. This process involved rinsing and cutting the adipose tissue with a scalpel, followed by enzymatic digestion using 0.5% collagenase type 1 (Gibco, Cat. 17100017). The obtained stromal vascular fraction was subsequently placed into T25 cell culture flasks (Nunc, Thermo Fisher Scientific) and cultured in basal media comprising 79% Dulbecco's Modified Eagle Medium with

Abbreviations: % positivity, Percent of positive cells; cAD-MSCs, canine Adipose-derived mesenchymal stem cells; CD, Cluster of differentiation; DMEM Low Glucose, Dulbecco's Modified Eagle Medium with Low Glucose; FBS, Fetal bovine serum; FDR, False discovery rate; GO, Gene ontology; ISCT, International Society for Cellular Therapy; MFI, Median fluorescence intensity; MSCs, Mesenchymal stem cell; P3, Third passage; P6, Sixth passage; RIS, RNA integrity score; SEM, Standard Error of the Mean.

TABLE 1 Donor information.

Donor	Age (months)	Breed	Adipose tissue mass (g)
6/21	12	German Spaniel	7.0
9/21	12	Labrador Retriever	7.0
13/21	7	Toy Poodle	1.0
14/21	7	Toy Poodle	1.2
1/22	10	Jack Russell Terrier	1.0
2/22	6	Lagotto Romagnolo	1.2
3/22	12	Medium Poodle	1.0
6/22	60	Portuguese Water Dog	2.5
7/22	36	Mixed	4.1

Low Glucose (DMEM Low Glucose) (Gibco, Cat. 31885049), 20% Fetal Bovine Serum (FBS) (Gibco; Cat. 1027010), and 1% Penicillin/Streptomycin (Sigma-Aldrich, Cat. P4333-100ML) at 37°C. *media* was replaced after 24 h, and when adherent cells reached 90% confluence, subculturing was performed using a solution of 0.05% Trypsin and 0.02% EDTA (Sigma-Aldrich, Cat. 59417C-500ML) until proliferation arrest was observed. All experiments conducted in this study utilized freshly isolated sterility-tested cAD-MSCs.

2.3 Stem cell identification

2.3.1 Differentiation capacity assay

In previous research (18), the multipotency of the extracted cAD-MSCs was evaluated through trilineage differentiation, encompassing adipogenic, osteogenic, and chondrogenic lineages. This assessment was conducted in the third passage (P3). In brief, cells were cultured in triplicate in a 24-well plate (Nunc, ThermoFisher Scientific) with a basal medium. Upon reaching confluence, the medium was replaced with StemMACS AdipoDiff media for adipogenic differentiation (Milteny, Cat. 130-091-677) or StemMACS OsteoDiff media for osteogenic differentiation (Milteny, Cat. 130-091-678). Control wells were maintained in basal media. Over 14 days, the media were changed every 48–72 h. Chondrogenic differentiation was induced in spheroid form within 15 mL conical polypropylene tubes using ChondroDiff Media (Milteny, Cat. 130-091-679), while a control tube was kept in basal media. The media were changed every 48–72 h during the 21-day differentiation period. All plates and tubes were incubated at 37°C with 5% CO₂ and 95% humidity, with the tube lids ajar. Oil Red O (Sigma-Aldrich, Cat. 01391-250ML) staining was employed for the identification of lipid droplets, and Sigmafast BCIP/NBT substrate (Sigma-Aldrich, Cat. B5655-25TAB) was used for the detection of alkaline phosphatase activity. For chondrogenic differentiation, following dehydration and paraffin embedding of spheroids, 1% Alcian blue 8GX, pH 2.5 (Sigma-Aldrich, Cat. A3157-25G) was utilized to assess the presence of aggrecan. After staining, slides or cells were examined using an Axio Observer D1 inverted microscope, and photographs were captured with a camera (total magnification: 50x-200x, Zeiss).

2.3.2 Flow cytometry immunophenotyping

To validate the immunophenotype of cAD-MSCs, undifferentiated cAD-MSCs at P3 were subjected to flow cytometric analysis. In our prior study (18), we systematically assessed the immunophenotypic traits of

cAD-MSCs across passages, spanning P1–P6. Statistical analysis demonstrated no significant differences in the expression of positive and negative cluster of differentiation (CD) markers between early (P1, P2, and P3) and late passages (P4, P5, and P6). Since experimental conditions adhered to the previously established protocol (18), cAD-MSC immunophenotyping was specifically conducted only at P3 for stem cell identification. These experiments were executed on the BD FACSVerse instrument (BD Biosciences). In brief, daily performance QC was maintained using CS&T beads (BD Biosciences) with lot numbers 92,323 and 13,697 before the initiation of each experiment. For the cAD-MSC immunophenotyping, a single-stain labeling approach was employed, with 3 µL of antibody per 10⁵ cells. The antibody panel used in the study is outlined in Table 2. Experimental conditions were calibrated using unstained cells, with identical conditions maintained across all test tubes during each experiment. Following the experiment, cell viability was assessed with a Propidium Iodide staining solution (BD Biosciences, Cat. 556,463). All data files were subjected to gating using the methodology previously described (18). FACSuite software was employed to analyze 10,000 collected events, with results presented regarding the median fluorescence intensity (MFI) and percent of positive cells (% positivity). Except for CD 105, where the MFI antibody was divided by the MFI of unstained cells due to a lack of adequate isotype control for canines. The MFI fold change was determined by dividing the MFI of the specific antibody by the median MFI of the corresponding isotype control. A fold change cutoff of 1.5 was applied for biological data interpretation. The statistical analysis and visualization of flow cytometry MFI and % positivity results were done using GraphPad Prism 10.1.2., represented as Mean ± Standard Error of the Mean (SEM) unless otherwise stated.

2.4 Total RNA extraction and gene expression profiling using RT-qPCR array analysis

Gene expression analysis using an RT-qPCR array was conducted following total RNA extraction at two time points during *in vitro* culture, P3 and P6. The experimental procedure followed the methodology outlined previously (17), incorporating certain modifications. The cAD-MSCs reached approximately 90% confluence in T75 cell culture flasks (Nunc, Thermo Fisher Scientific). Subsequently, the cells were detached using a cell scraper (Nunc, Thermo Fisher Scientific) and centrifuged at 235 × g for

TABLE 2 Flow cytometry antibody panel used in this study.

Antigen	Clone	Host	Fluorophore	Reactivity	Clonality	Manufacturer/Cat.
CD90	YKIX337.217	Rat	APC	Canine	Monoclonal	Thermo Fisher Scientific/17-5900-42
Isotype IgG2b, kappa	eB149/10H5	Rat	APC	N/A	Monoclonal	Thermo Fisher Scientific/17-4031-82
CD44	MEM-263	Mouse	FITC	Canine, Human, Porcine	Monoclonal	Antibodies-online/ABIN452099
Isotype IgG1	VI-AP	Mouse	FITC	N/A	Monoclonal	Antibodies-online/ABIN1741583
CD105	SN6	Mouse	PE-Cy 7	Human, published species canine	Monoclonal	Thermo Fisher Scientific/25-1057-42
CD73	N/A	Rabbit	PE	Human, Mouse, Rat, Canine, Chicken	Polyclonal	Bioss antibodies/bs-4834R-PE
Isotype IgG	N/A	Rabbit	PE	N/A	Polyclonal	Antibodies-online/ABIN376422
CD29	MEM-101A	Mouse	FITC	Canine, Human, Porcine	Monoclonal	Antibodies-online/ABIN94056
Isotype IgG1	VI-AP	Mouse	FITC	N/A	Monoclonal	Antibodies-online/ABIN1741583
CD271	ME20.4	Mouse	APC	Canine, Human, Mouse, Non-human primate, Sheep, Pig, Rabbit, Rat	Monoclonal	Thermo Fisher Scientific/17-9400-42
Isotype IgG1, kappa	P3.6.2.8.1	Mouse	APC	N/A	Monoclonal	Thermo Fisher Scientific/17-4714-42
CD45	YKIX716.13	Rat	PE	Canine	Monoclonal	Bio-Rad/MCA1042PE
Isotype IgG2b	N/A	Rat	PE	N/A	Monoclonal	Bio-Rad/MCA600P6E
CD34	1H6	Mouse	PE	Canine	Monoclonal	BD Pharmingen/559369
Isotype IgG1 kappa	N/A	Mouse	PE	N/A	Monoclonal	BD Pharmingen/550617

N/A, Not available.

10 min. Total RNA extraction was performed using the RNeasy Mini Kit (Qiagen, Cat. 74106) with 2 M dithiothreitol (Sigma-Aldrich, Cat. 43815-1G), following the manufacturer's instructions for approximately 10^7 cells. The extracted RNA was stored at -80°C until gene expression analysis.

Before commencing gene expression analysis, the RNA integrity score (RIS) and 28S:18S ratio were determined using the QIAxcel RNA QC Kit (Qiagen, Cat. 929104) on the QIAxcel Advanced capillary electrophoresis device (Qiagen) following manufacturer instructions. RIS number <7 and 28S:18S <1 were considered low-quality RNA and excluded from further analysis.

Genomic DNA elimination and complementary DNA synthesis from 800 ng of RNA was accomplished using the RT2 First Strand kit (Qiagen, Cat. 330401) as instructed by the manufacturer. Subsequently, a commercially available RT² ProfilerTM PCR Array for Dog Mesenchymal Stem Cells (PAFD-082ZR, Qiagen) with SYBR Green-optimized primer assays (Qiagen, Cat. 330603) was applied, following the manufacturer's instructions for Rotor-Gene Q (Qiagen). The array featured primers targeting 84 genes, categorized as stemness markers, MSC-specific, MSC-associated, and MSC-differentiation genes associated with osteogenesis, adipogenesis, chondrogenesis, myogenesis, and tenogenesis. Detailed information, including gene

names, symbols, and NCBI sequences, was thoroughly documented in the [Supplementary material 1](#).

Following data acquisition, normalization, and in-depth analysis were conducted using the specialized RT2 Profiler PCR Array Data Analysis software, accessible online at <https://dataanalysis2.qiagen.com/pcr> (accessed November 10, 2023). The software analyzes the data and performs statistical analysis, which is fully explained and provided in a detailed report ([Supplementary material 1](#)). The statistical significance was calculated based on a Student's t-test of the replicate $2^{\Delta(-\Delta\text{CT})}$ values for each gene in the control and treatment groups. The software automatically appointed a fold change cutoff of 2.0, equal to $\log_2\text{Fold Change} \pm 1.0$. The gene expression profiling data are publicly available on the NCBI Gene Expression Omnibus (GEO) database (Accession Number GSE255585). Data visualization was carried out using GraphPad Prism 10.1.2.

2.5 LC-MS/MS proteomic analysis of cAD-MSCs secretome

The alterations in the proteome composition of the cAD-MSCs secretome during *in vitro* culture were also assessed at two specific time

points, P3 and P6, in randomly selected six donors (6/21, 9/21, 14/21, 1/22, 6/22, and 7/22). The cells were seeded in six replicates at 10^5 cells per milliliter in 24-well plates (Nunc, Thermo Fisher Scientific). They were conditioned in basal media (with 20% FBS) at 37°C, 5% CO₂, and 95% humidity until they reached 90% confluence. Subsequently, the culture medium was aspirated, and the cells were rinsed with 100% DMEM Low Glucose before being incubated in 2 mL of 100% DMEM Low Glucose. After 48 h, the secretome was carefully collected, centrifuged at $2,100 \times g$ for 10 min, filtered through a sterile 0.45 μ m filter (Merck), and preserved at -80°C until proteomic analysis.

For sample preparation, the secretome proteins were first reduced with dithiothreitol (Sigma Aldrich, Cat. D0632-5G) at a final concentration of 10 mM at 57°C for 30 min and subsequently alkylated with iodoacetamide (Sigma, Cat. I6125-5G) at a final concentration of 25 mM for 30 min at room temperature. The extraction of secretome proteins from the culture medium was carried out using trichloroacetic acid (Merck, Cat. 1008070100) precipitation method as previously described (22). To summarize, 1,260 μ L of the medium sample was combined with sodium deoxycholate (Sigma-Aldrich, Cat. D6750-100G) at a final concentration of 0.1%. Trichloroacetic acid was added to reach a final concentration of 7.5%, causing protein precipitation on ice for 2 h. Afterward, the samples were centrifuged for 10 min at 4°C and $10,000 \times g$. The supernatant was discarded, and the pellet underwent two washes with ice-cold tetrahydrofuran (Merck, Cat. 1081011000). Finally, the pellet was reconstituted in 50 μ L of 50 mM triethylammonium bicarbonate buffer (Thermo Fisher Scientific, Cat. 90,114 1 M). Protein concentration was determined using the Bradford assay, and the concentrations of all samples were adjusted with 50 mM triethylammonium bicarbonate buffer.

The proteins were subjected to enzymatic digestion with trypsin (Promega, Cat. V5117) at a final 0.01 mg/mL concentration, carried out over 18 h at 37°C and $20 \times g$. Peptide separation was executed using the nanoLC EASY-nLC™ 1200 System (Thermo Fisher Scientific) on a 75 μ m \times 250 mm RPC column. The gradient length spanned 2 h with 0–80% acetonitrile (VWR Chemicals, Cat. 83639.320), and 0.1% formic acid (Merck, Cat. 1002641000) with a flow rate of 1 μ L/min, and the injection volume was 2 μ L. The nanoLC system was connected to the Q Exactive™ Plus Hybrid Quadrupole-Orbitrap™ Mass Spectrometer (Thermo Fisher Scientific). The mass spectrometer operated in a data-dependent mode, where MS1 spectra were recorded within the range of 350–1,800 m/z at a resolution of 70,000. The top 12 ions were selected for fragmentation (MS2) and recorded at a resolution of 17,500.

Raw data were analyzed using Scaffold Quant Q + S 5.3.0 utilizing protein sequence data of *Canis lupus familiaris* reference proteome obtained from the UniProt database Proteome ID UP000805418 (accessed on October 30, 2023, with a total of 20,991 entries). Search parameters included the allowance of a missed trypsin cleavage, carbamidomethylation as a fixed modification, and a precursor and fragment ion mass tolerance of 10 ppm. Peptide search results were subsequently analyzed with Scaffold Quant version 5.0.3, employing untargeted label-free quantification and statistical analysis based on the spectral counting method, utilizing a *t*-test to verify the results of secretome composition. The proteins were filtered to include only the ones with a minimum of two identified peptide sequences. Statistical probability was defined at the $p < 0.05$ unless otherwise stated. A fold change cutoff of 1.3 was appointed, equal to \log_2 Fold Change ± 0.3785 . Gene Ontology (GO) Panther 18.0 was utilized in the research of

cellular components, protein class, molecular function, biological process, and pathways analysis, using Fisher's exact test type and false discovery rate correction; data presented as raw *p* value and false discovery rate (FDR). The mass spectrometry proteomics data have been deposited to the ProteomeXchange Consortium via the PRIDE (23) partner repository with the dataset identifier PXD049324 and 10.6019/PXD049324. Data visualization was carried out using GraphPad Prism 10.1.2.

3 Results

3.1 Prolonged *in vitro* cultivation results in morphological changes

The cAD-MSCs cultures from all donors were successfully established. The spindle-shaped isolated cells underwent *in vitro* cultivation, where morphological changes were observed with each passage, exhibiting an increase in both size and granularity, coupled with a decrease in cell population density attributable to senescence, i.e., *in vitro* aging. Proliferation arrest, on average, occurred at P8. Microscopic images of three representative donors in P3 and P6 were presented in [Supplementary material 2](#).

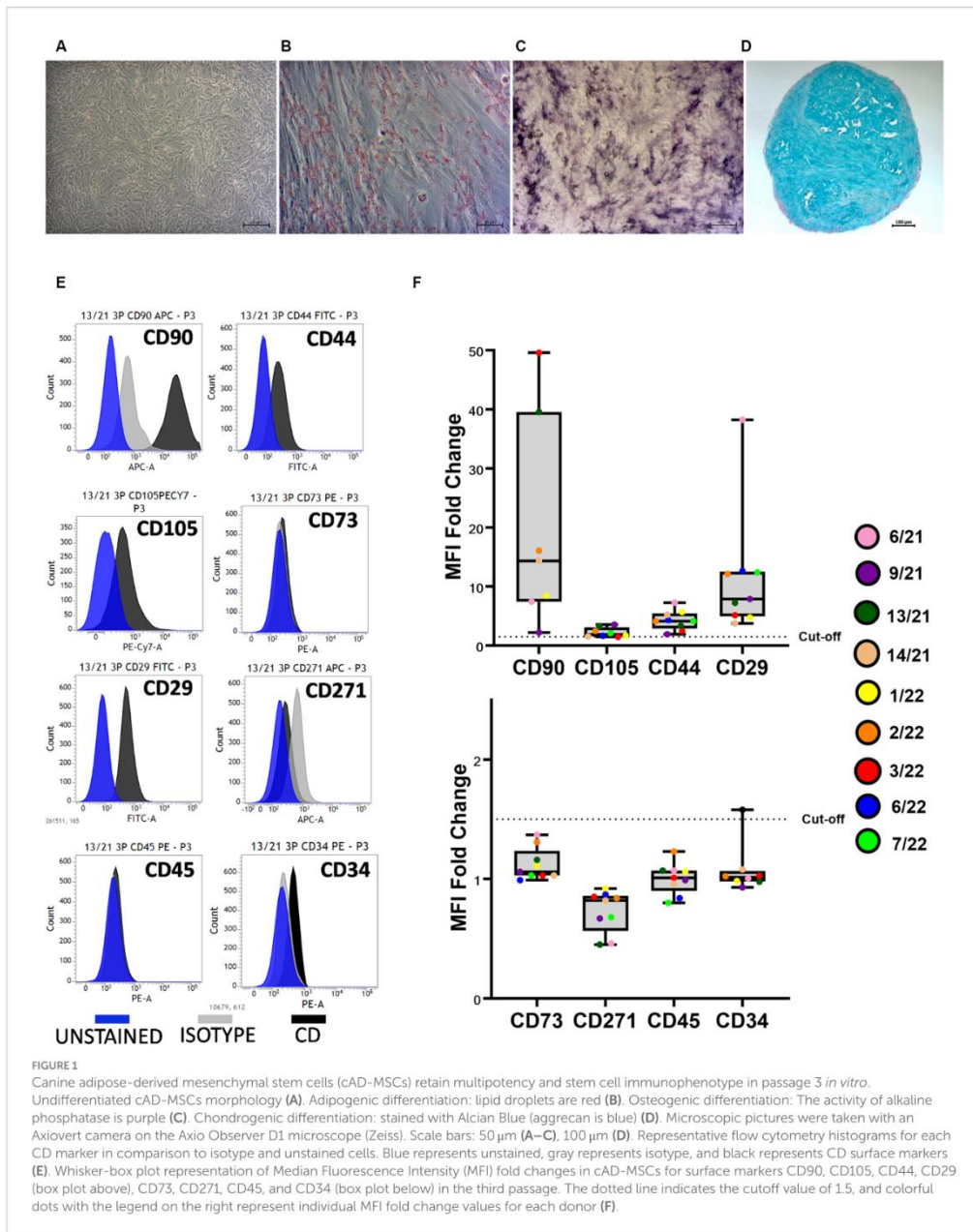
3.2 cAD-MSCs multipotency and stem cell immunophenotype are preserved *in vitro*

The trilineage differentiation capacity (adipogenic, osteogenic, and chondrogenic) of all isolated cells was preserved at P3, and the cAD-MSCs were confirmed to possess differentiation potential following the International Society for Cellular Therapy (ISCT) criteria (24). Microscopic images in [Figure 1](#) depict undifferentiated cells (A), adipogenic (B), osteogenic (C), and chondrogenic (D) differentiation from a representative 6/21 donor experiment.

Isolated cAD-MSCs at P3 underwent flow cytometry analysis, revealing the presence of markers CD90 ($87.64 \pm 5.3\%$), CD105 ($41.44 \pm 11.64\%$), CD44 ($74.32 \pm 6.33\%$), and CD29 ($97.93 \pm 0.65\%$), confirming the cells' stem cell status according to ISCT guidelines. Notably, the expression of CD73, for which a polyclonal antibody was utilized, was not observed. The analysis also showed the absence of expression for markers CD271 ($1.61 \pm 1.21\%$), CD45 (0%), and CD34 ($4.01 \pm 1.65\%$). [Figure 1E](#) represents CD surface marker expression histograms for donor 13/21 in comparison to isotype and unstained cells. Additionally, Whisker-box plots depict the MFI fold changes for all CD markers, with donor-specific data points represented by different-colored dots ([Figure 1F](#)).

3.3 Gene expression profiling of *in vitro* aged cAD-MSCs showed significant downregulation in MSC-associated genes

RNA quality analysis confirmed that the RNA in every sample was of high quality ([Table 3](#)). Gene expression analysis revealed that the overall change in expression between P3 and P6 was significantly downregulated for MSC-associated genes IL10 and PTPRC. Non-significant downregulations and upregulations were



observed in stemness, MCS-specific, MSC-associated, and MSC-differentiation genes, as indicated in Figures 2A–D. Figure 2E represents fold-regulation values for downregulated and upregulated

genes. Fold-regulation represents fold-change results in a biologically meaningful way. The complete RT2 Profiler PCR Array Data Analysis software report is attached as a Supplementary material 1.

TABLE 3 Results of RNA QC analysis; RNA integrity score (RIS), and 28S:18S ratio for individual donors.

Donor	P3		P6	
	RIS	28S:18S	RIS	28S:18S
6-21	10	2,33	9,7	1,8
9-21	9,7	1,7	9,3	1,62
13-21	10	2,56	9,9	2,03
14-21	10	1,91	9,7	1,58
1-22	10	2,43	10	2,62
2-22	9,9	2,45	9,9	2,16
3-22	9,3	2,27	9,1	2,28
6-22	9	2,2	10	2,39
7-22	10	1,87	10	2,02

3.4 Proteomic analysis of cAD-MSCs secretome showed significant up- and downregulations

During the proteomic analysis of cAD-MSCs secretome, 1,187 proteins were detected in P3 and P6, with 90% proteins in common. A complete list of detected proteins, their gene symbols, *t*-test significance, and fold change results, is provided in the [Supplementary material 3](#).

Proteins detected in P3 and P6 were compared by functional annotation to cellular components, protein class, molecular function, and biological process on GO complete analysis (Figure 3). Similar involvement in all detected functions was observed. Cellular component analysis revealed that ≈75% of protein belonged to cellular anatomical entities, 22.7% belonged to protein-containing complexes, and the rest were unassigned. More than 50% of cAD-MSCs secretome proteins comprised metabolite interconversion enzyme translational proteins, protein modifying enzymes, cytoskeletal proteins, translational proteins, and protein-binding activity modulators (Figure 3A). Their molecular functions were mainly binding and catalytic activity (Figure 3B), and they were predominantly involved in cellular and metabolic processes, biological regulation, response to stimulus, and localization (Figure 3C).

Secretome analysis of commonly produced proteins showed downregulation in 648 proteins, while 302 proteins were upregulated (Figure 4). Correlation of statistically significant ($p < 0.05$) and fold change cutoff > 1.3 proteins indicated nine biologically significant downregulated proteins—PCBP1, RPS8, HSP70, EEF1G, SRSF1, NAGA, FASN, SERPINB1, and COQ10B and 12 biologically significant upregulated proteins—DKK3a (isomer 1), PRSS23, HPRT1, LOC102152698, LOXL2, AP1B1, ME1, EIF3F, THBS3, HNRNPU, RPS19, and DKK3b (isomer 2) (Figure 4).

The 10% of explored proteins were distinctive for each passage; 63 and 52 proteins were expressed only in P3 and P6, respectively. Distinctive proteins expressed in P3 were grouped with biologically significant downregulated proteins (Group P3), while those expressed in P6 were grouped with biologically significant upregulated proteins (Group P6). Moreover, these two groups were analyzed through GO Panther Pathways analysis to see if any critical protein pathways were influenced by the *in vitro* aging of cAD-MSCs. Group P3 proteins showed significant involvement in

cytoskeletal regulation by Rho GTPase ($p = 7.45E^{-12}$, FDR = $1.2E^{-9}$), nicotinic acetylcholine receptor signaling pathway ($p = 1.2E^{-7}$, FDR = $9.8E^{-6}$), inflammation mediated by chemokine and cytokine signaling pathway ($p = 6.7E^{-7}$, FDR = $3.6E^{-5}$), Wnt signaling pathway ($p = 7.3E^{-5}$, FDR = 0.00235), and CCKR signaling map ($p = 0.000601$, FDR = 0.0161). In group P6, the expressed proteins were significantly related to the xanthine and guanine salvage pathway ($p = 0.000193$, FDR = 0.031), adenine and hypoxanthine salvage pathway ($p = 0.000377$, FDR = 0.0202), and blood coagulation pathway ($p = 0.00032$, FDR = 0.0258).

4 Discussion

In vitro culture is necessary to produce cAD-MSCs or their secretome for therapeutic applications. However, long-term culture leads to *in vitro* cell aging, thereby potentially compromising the regenerative and immunomodulatory capabilities of cAD-MSCs. Thus, this research aimed to explore the influence of *in vitro* aging on the gene expression and secretome composition of cAD-MSCs. Our findings demonstrate alterations of cAD-MSC-expressed genes and the secretome proteomic profile of cAD-MSCs induced by *in vitro* aging.

Initially, the isolated cells conformed to the criteria stipulated by the ISCT for identifying human stem cells (24) (Figure 1). Given the absence of standardized criteria for verifying canine stem cells, this investigation builds upon our prior research (17, 18) to establish the reproducibility and standardization of cAD-MSCs' immunophenotype and three-lineage multipotency. In addition to previously explored cAD-MSCs' surface markers CD90, CD44, CD29, CD105, CD73, CD45, and CD271 (18), in this study, we investigated surface marker CD34, which exhibited a % positivity of less than 5%, aligning with similar observations reported elsewhere (21, 25).

In vitro aging influenced the gene expression of cAD-MSCs, as confirmed by the present study, which detected 21 downregulated and 10 upregulated genes (Figure 2). In comparison to our earlier study (17), similar findings were observed regarding the cAD-MSCs-expressed genes, but expansion of the donor pool and advancement to later passages demonstrated significant downregulation of MSC-associated *PTPRC* and *IL10* genes (Figure 2). *PTPRC* is a gene coding for CD45 surface marker protein expressed by all hematopoietic cells including hematopoietic stem cells (26). While it is considered a negative marker for human MSCs (24), the exact criteria for cAD-MSCs are yet to be established. Immunophenotyping revealed the absence of CD45 protein on the surface of cAD-MSCs in all donors during the P3 stage. However, it revealed 4% of extracted cells were positive for hematopoietic stem cell marker CD34, and these cells can express the gene for *PTPRC*/CD45 (27). On the other hand, *IL10* is a major immune regulatory cytokine with profound anti-inflammatory functions produced by various immune and non-immune cells (28). Co-expression of *IL10* in MSCs was proven beneficial, contributing to anti-inflammatory activity in humans and canines (29–34). Our findings suggest that the observed expression of *IL10* in earlier passages, such as P3, may confer beneficial effects regarding inflammation. However, we must interpret these results with caution since the expression of *PTPRC* and *IL10* genes in the early passages may originate from various cell types within the adipose-derived stromal vascular fraction (35). Therefore, the

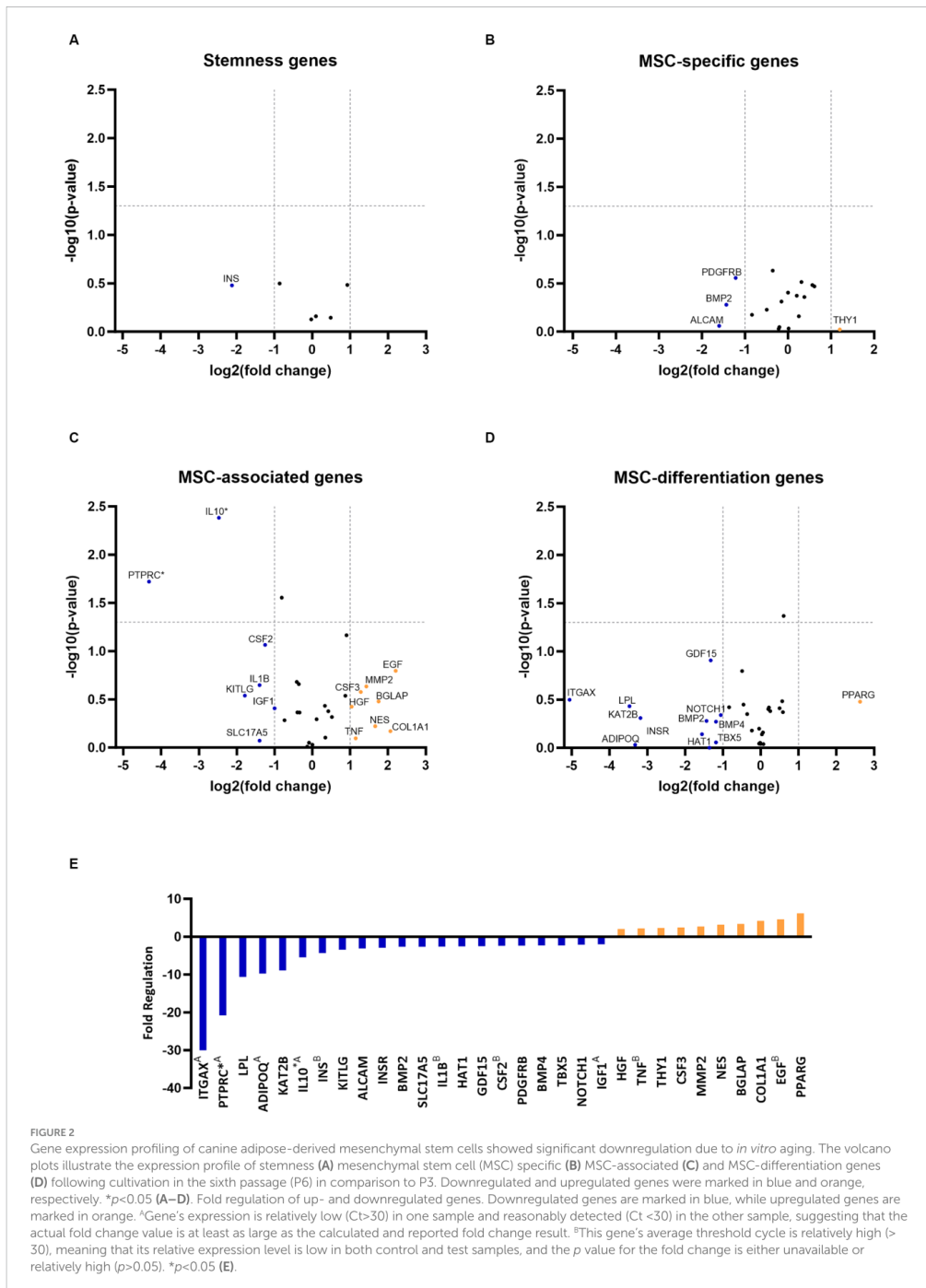


FIGURE 2

Gene expression profiling of canine adipose-derived mesenchymal stem cells showed significant downregulation due to *in vitro* aging. The volcano plots illustrate the expression profile of stemness (A) mesenchymal stem cell (MSC) specific (B) MSC-associated (C) and MSC-differentiation genes (D) following cultivation in the sixth passage (P6) in comparison to P3. Downregulated and upregulated genes were marked in blue and orange, respectively. * $p < 0.05$ (A–D). Fold regulation of up- and downregulated genes. Downregulated genes are marked in blue, while upregulated genes are marked in orange. ^AGene's expression is relatively low (Ct > 30) in one sample and reasonably detected (Ct < 30) in the other sample, suggesting that the actual fold change value is at least as large as the calculated and reported fold change result. ^BThis gene's average threshold cycle is relatively high (> 30), meaning that its relative expression level is low in both control and test samples, and the p value for the fold change is either unavailable or relatively high ($p > 0.05$). * $p < 0.05$ (E).

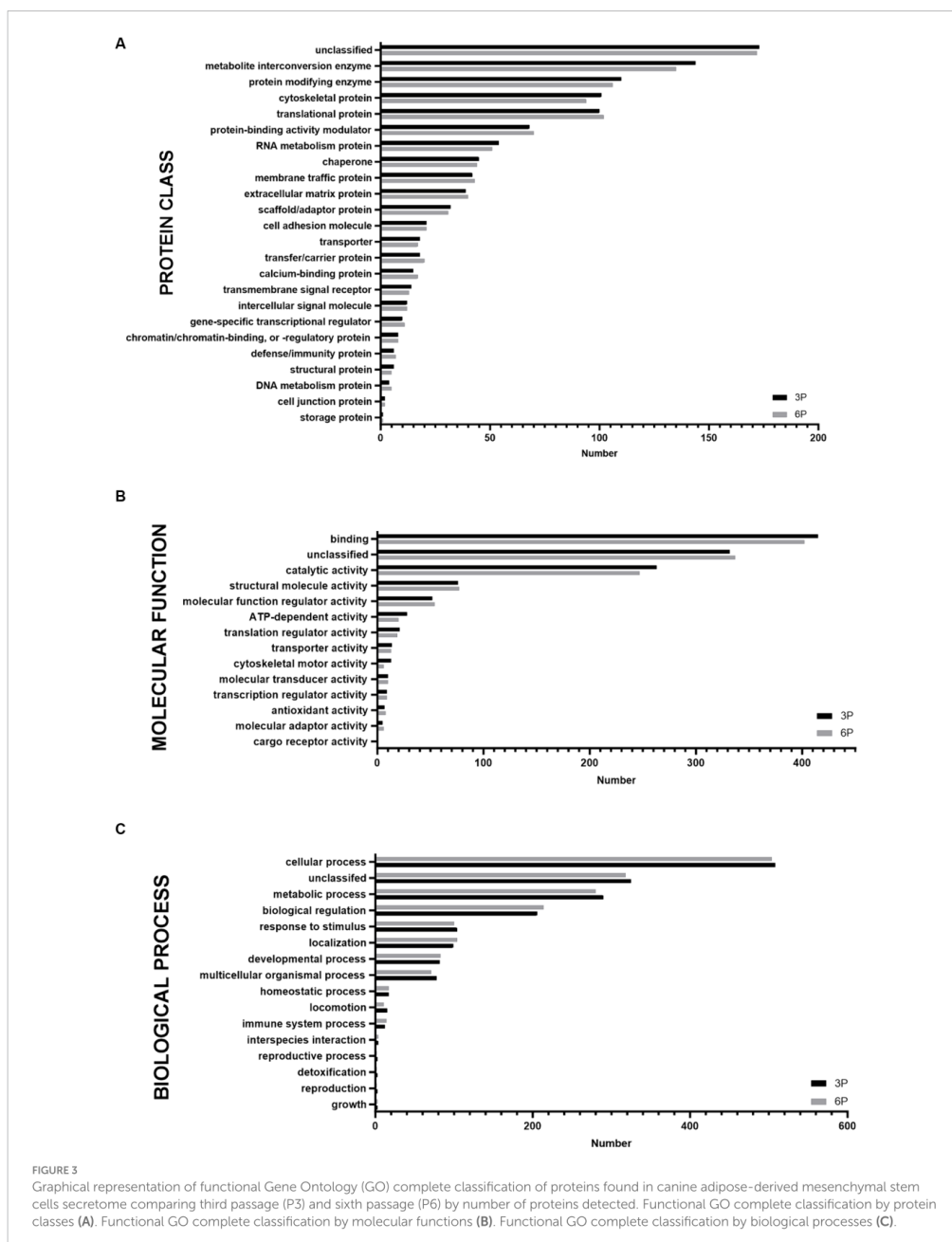
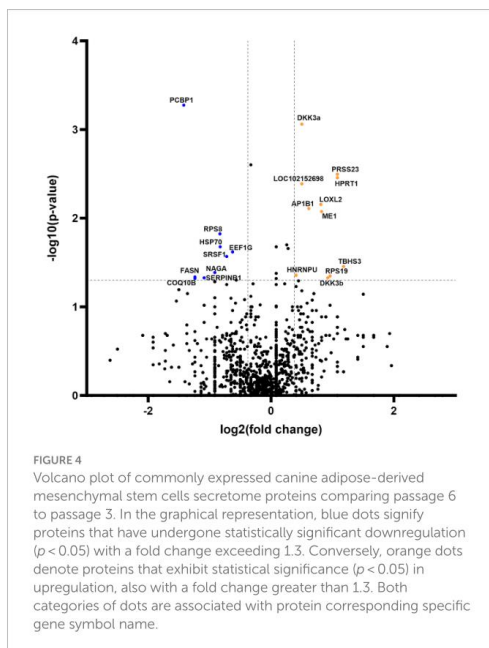


FIGURE 3 Graphical representation of functional Gene Ontology (GO) complete classification of proteins found in canine adipose-derived mesenchymal stem cells secretome comparing third passage (P3) and sixth passage (P6) by number of proteins detected. Functional GO complete classification by protein classes (A). Functional GO complete classification by molecular functions (B). Functional GO complete classification by biological processes (C).

downregulation of these two genes in later passages, such as P6, may result from the absence of these cells.

The secretome composition of cAD-MSCs was also impacted by *in vitro* aging. To our knowledge, this study represents the first

investigation into the impact of prolonged passages of cAD-MSCs on secretome composition. Furthermore, our study significantly contributes to expanding the limited database on the secretome of cAD-MSCs. Most detected proteins and their functional



characteristics were shared between early and later passages (P3 and P6) (Figure 3). Similar observations were documented in the secretome and exosomes of feline AD-MSCs (36) and canine bone marrow MSCs when compared to cAD-MSCs (5).

However, a notable functional difference was observed for the group of distinctive proteins (10% of detected proteins) in each passage (Group P3 and Group P6). Firstly, P3 exhibited substantial involvement in cytoskeletal regulation by Rho GTPase which plays pivotal roles in diverse cellular processes, encompassing gene expression, cytoskeletal dynamics, survival, cell division, cell adhesion, polarity, and vesicle trafficking (37). As cells age, these events decrease, consistent with the cellular quiescence observed in a later passage (P6) of the present study. Group P3 proteins displayed a significant association with the nicotinic acetylcholine receptor, Wnt, and CCKR signaling pathways, which play crucial roles in MSC regenerative function (38), cell proliferation/apoptosis inhibition (39), and adipocyte differentiation (40), respectively. The last, but very important finding within Group P3, concerns proteins associated with inflammation mediated by the chemokine and cytokine signaling, regulating trafficking and migration of immune cells (41). Moreover, Group P6 proteins were significantly associated with the blood coagulation pathway. Given MSCs' apparent pro-thrombotic role, it is imperative to emphasize the necessity for stringent control of culture passages before administration to prevent adverse coagulation events (42). Collectively, the results of the present study, coupled with corroborating evidence regarding human MSCs (14, 15), underscore the need for caution when extending cAD-MSCs to later passages.

In addition to groups of distinctive proteins detected in both passages, our investigation unveiled modifications in a subset of shared proteins across both passages, comprising precisely 21 entities that exhibited significant up- or downregulation (Figure 4). Notably,

the downregulated proteins in P6 (HSP70, SRSF1, SERPINB1, and COQ10B) are intricately associated with stem cells' regenerative pathways in the treatment of various diseases (43–47). Nevertheless, these findings warrant further research and confirmatory testing, which are presently constrained by the insufficient accessibility of canine-specific reagents (e.g., monoclonal antibodies).

In conclusion, our findings underscore significant alterations in the regenerative capacity of cAD-MSCs and their secretome due to *in vitro* aging. Thus, prioritizing earlier passages of these cells may be advisable to optimize their regenerative potential for therapeutic applications.

Data availability statement

The original contributions presented in the study are publicly available. This data can be found at: <https://www.ebi.ac.uk/pride/>; PXD049324. The gene expression profiling data are publicly available on the NCBI Gene Expression Omnibus (GEO) database (Accession Number GSE255585) <https://www.ncbi.nlm.nih.gov/geo/query/acc.cgi?acc=GSE255585>.

Ethics statement

The animal studies were approved by Ethics Board of the Croatian Veterinary Institute and Veterinary Ethics Committee at the Faculty of Veterinary Medicine, University of Zagreb. The studies were conducted in accordance with the local legislation and institutional requirements. Written informed consent was obtained from the owners for the participation of their animals in this study.

Author contributions

MP: Writing – review & editing, Writing – original draft, Visualization, Validation, Software, Methodology, Investigation, Formal Analysis, Data curation, Conceptualization. AB: Writing – review & editing, Writing – original draft, Software, Methodology, Investigation, Data curation. RB: Writing – review & editing, Software, Methodology, Investigation, Data curation. VK: Writing – review & editing, Visualization, Methodology, Investigation. IL: Writing – review & editing, Resources. PK: Writing – review & editing, Resources. DV: Writing – review & editing, Methodology. ŠN: Writing – review & editing, Methodology, Investigation. NT: Writing – review & editing, Supervision. DB: Writing – review & editing, Writing – original draft, Supervision, Project administration, Funding acquisition, Conceptualization.

Funding

The author(s) declare that financial support was received for the research, authorship, and/or publication of this article. This research was funded by the Croatian Science Foundation within the Installation Research Project (UIP-2019-04-2178) “Revealing transcriptome and secretome of mesenchymal stem cells” SECRET. Proteomic analysis was partially funded by the European Regional Development Fund (infrastructural project CluK, grant number KK.01.1.1.02.0016). The funding agencies did not contribute to the study's design, data collection, analysis, interpretation, or manuscript composition.

Acknowledgments

We thank Manuela Zadravec, Mihaela Stuparić Komušar, and Marko Močibob for generous help during sterility testing, spheroid preparation, and proteomic analysis, respectively. We also thank all canine donors and their owners without whom this research would not be possible.

Conflict of interest

AB and RB were employed by Bicro Biocentre Ltd.

The remaining authors declare that the research was conducted in the absence of any commercial or financial relationships that could be construed as a potential conflict of interest.

References

- Voga M, Adamic N, Vengust M, Majdic G. Stem cells in veterinary medicine—current state and treatment options. *Front Vet Sci.* (2020) 7:278. doi: 10.3389/fvets.2020.00278
- Prišlin M, Vlahović D, Kostešić P, Ljilje I, Brnić D, Turk N, et al. An Outstanding Role of Adipose Tissue in Canine Stem Cell Therapy. *Animals.* (2022) 12:1–19. doi: 10.3390/ani12091088
- El-Husseiny HM, Mady EA, Helal MAY, Tanaka R. The pivotal role of stem cells in veterinary regenerative medicine and tissue engineering. *Vet Sci.* (2022) 9:1–25. doi: 10.3390/vetsci9110648
- Russell KA, Chow NHC, Dukoff D, Gibson TWG, La Marre J, Betts DH, et al. Characterization and immunomodulatory effects of canine adipose tissue- and bone marrow-derived mesenchymal stromal cells. *PLoS One.* (2016) 11:1–18. doi: 10.1371/journal.pone.0167442
- Villatoro AJ, Alcoholado C, Martín-Astorga MC, Fernández V, Cifuentes M, Becerra J. Comparative analysis and characterization of soluble factors and exosomes from cultured adipose tissue and bone marrow mesenchymal stem cells in canine species. *Vet Immunol Immunopathol.* (2019) 208:6–15. doi: 10.1016/j.vetimm.2018.12.003
- Humenik F, Maloveska M, Hudakova N, Petrouskova P, Hornakova L, Domaniza M, et al. A comparative study of canine mesenchymal stem cells isolated from different sources. *Animals.* (2022) 12:1–13. doi: 10.3390/ani12121502
- Melief SM, Zwaginga JJ, Fibbe WE, Roelofs H. Adipose tissue-derived multipotent stromal cells have a higher immunomodulatory capacity than their bone marrow-derived counterparts. *Stem Cells Transl Med.* (2013) 2:455–63. doi: 10.5966/sctm.2012-0184
- Si Z, Wang X, Sun C, Kang Y, Xu J, Wang X, et al. Adipose-derived stem cells: Sources, potency, and implications for regenerative therapies. *Biomed Pharmacother.* (2019) 114:108765. doi: 10.1016/j.biopha.2019.108765
- Duffy MM, Ritter T, Ceredig R, Griffin MD. Mesenchymal stem cell effects on T-cell effector pathways. *Stem Cell Res Ther.* (2011) 2:34–9. doi: 10.1186/scrt75
- Chandra V, Mankuzhy P, Sharma GT. Mesenchymal stem cells in veterinary regenerative therapy: basic physiology and clinical applications. *Curr Stem Cell Res Ther.* (2022) 17:237–51. doi: 10.2174/1574888X16666210804112741
- Trzyna A, Banaś-Ząbczyk A. Adipose-derived stem cells secretome and its potential application in “stem cell-free therapy”. *Biomol Ther.* (2021) 11:878. doi: 10.3390/biom11060878
- Merlo B, Iacono E. Beyond canine adipose tissue-derived mesenchymal secretome characterization and applications. *Animals.* (2023) 13:3571. doi: 10.3390/ani13223571
- Vizoso FJ, Eiro N, Cid S, Schneider J, Perez-Fernandez R. Mesenchymal stem cell secretome: Toward cell-free therapeutic strategies in regenerative medicine. *Int J Mol Sci.* (2017) 18:1852. doi: 10.3390/ijms18091852
- Liu J, Ding Y, Liu Z, Liang X. Senescence in mesenchymal stem cells: functional alterations, molecular mechanisms, and rejuvenation strategies. *Front Cell Dev Biol.* (2020) 8:258. doi: 10.3389/fcell.2020.00258
- Yang YHK, Ogando CR, Wang See C, Chang TY, Barabino GA. Changes in phenotype and differentiation potential of human mesenchymal stem cells aging in vitro. *Stem Cell Res Ther.* (2018) 9:131–14. doi: 10.1186/s13287-018-0876-3
- Weng Z, Wang Y, Ouchi T, Liu H, Qiao X, Wu C, et al. Mesenchymal stem/stromal cell senescence: hallmarks, mechanisms, and combating strategies. *Stem Cells Transl Med.* (2022) 11:356–71. doi: 10.1093/sctm/tzab004

Publisher's note

All claims expressed in this article are solely those of the authors and do not necessarily represent those of their affiliated organizations, or those of the publisher, the editors and the reviewers. Any product that may be evaluated in this article, or claim that may be made by its manufacturer, is not guaranteed or endorsed by the publisher.

Supplementary material

The Supplementary material for this article can be found online at: <https://www.frontiersin.org/articles/10.3389/fvets.2024.1387174/full#supplementary-material>

- Krešić N, Šimić I, Lojkić I, Bedeković T. Canine adipose derived mesenchymal stem cells transcriptome composition alterations: a step towards standardizing therapeutic. *Stem Cells Int.* (2017) 2017:4176292. doi: 10.1155/2017/4176292
- Krešić N, Prišlin M, Vlahović D, Kostešić P, Ljilje I, Brnić D, et al. The expression pattern of surface markers in canine adipose-derived mesenchymal stem cells. *Int J Mol Sci.* (2021) 22:1–19. doi: 10.3390/ijms22147476
- Teshima T, Yuchi Y, Suzuki R, Matsumoto H, Koyama H. Immunomodulatory effects of canine adipose tissue mesenchymal stem cell-derived extracellular vesicles on stimulated cd4+ t cells isolated from peripheral blood mononuclear cells. *J Immunol Res.* (2021) 2021:2993043. doi: 10.1155/2021/2993043
- Fenwick N, Griffin G, Gauthier C. The welfare of animals used in science: How the “Three Rs” ethic guides improvements. *Can Vet J.* (2009) 50:523–30.
- Voga M, Kováč V, Majdic G. Comparison of Canine and Feline Adipose-Derived Mesenchymal Stem Cells/Medical Signaling Cells With Regard to Cell Surface Marker Expression, Viability, Proliferation, and Differentiation Potential. *Front Vet Sci.* (2021) 7:610240. doi: 10.3389/fvets.2020.610240
- Isola D, Marzban G, Selbmann L, Onofri S, Laimer M, Sterflinger K. Sample preparation and 2-DE procedure for protein expression profiling of black microcolonial fungi. *Fungal Biol.* (2011) 115:971–7. doi: 10.1016/j.funbio.2011.03.001
- Perez-Riverol Y, Bai J, Bandla C, García-Seisdedos D, Hewapathirana S, Kamatchinathan S, et al. The PRIDE database resources in 2022: A hub for mass spectrometry-based proteomics evidences. *Nucleic Acids Res.* (2022) 50:D543–52. doi: 10.1093/nar/gkabi1038
- Dominici M, Le Blanc K, Mueller I, Slaper-Cortenbach I, Marini FC, Krause DS, et al. Minimal criteria for defining multipotent mesenchymal stromal cells. The International Society for Cellular Therapy position statement. *Cytotherapy.* (2006) 8:315–7. doi: 10.1080/14653240600855905
- Screven R, Kenyon E, Myers MJ, Yancy HF, Skasko M, Boxer L, et al. Immunophenotype and gene expression profile of mesenchymal stem cells derived from canine adipose tissue and bone marrow. *Vet Immunol Immunopathol.* (2014) 161:21–31. doi: 10.1016/j.vetimm.2014.06.002
- Al Barashdi MA, Ali A, McMullin MF, Mills K. Protein tyrosine phosphatase receptor type C (PTPRC or CD45). *J Clin Pathol.* (2021) 74:548–52. doi: 10.1136/jclinpath-2020-206927
- Ayabe T, Hisasue M, Yamada Y, Nitta S, Kikuchi K, Neo S, et al. Characterisation of canine CD34+/CD45 diminished cells by colony-forming unit assay and transcriptome analysis. *Front Vet Sci.* (2022) 9:936623. doi: 10.3389/fvets.2022.936623
- Iyer SS, Cheng G. Role of interleukin 10 transcriptional regulation in inflammation and autoimmune disease. *Crit Rev Immunol.* (2012) 32:23–63. doi: 10.1615/critrevimmunol.v32i1.30
- Nakajima M, Nito C, Sowa K, Suda S, Nishiyama Y, Nakamura-Takahashi A, et al. Mesenchymal stem cells overexpressing interleukin-10 promote neuroprotection in experimental acute ischemic stroke. *Mol Ther Methods Clin Dev.* (2017) 6:102–11. doi: 10.1016/j.omtm.2017.06.005
- Hervás-Salcedo R, Fernández-García M, Hernando-Rodríguez M, Suárez-Cabrera C, Bueren JA, Yáñez RM. Improved efficacy of mesenchymal stromal cells stably expressing CXCR4 and IL-10 in a xenogeneic graft versus host disease mouse model. *Front Immunol.* (2023) 14:1062086. doi: 10.3389/fimmu.2023.1062086
- Choi JJ, Yoo SA, Park SJ, Kang YJ, Kim WU, Oh IH, et al. Mesenchymal stem cells overexpressing interleukin-10 attenuate collagen-induced arthritis in mice. *Clin Exp Immunol.* (2008) 153:269–76. doi: 10.1111/j.1365-2249.2008.03683.x

32. Nitahara-Kasahara Y, Kuraoka M, Oda Y, Hayashita-Kinoh H, Takeda S, Okada T. Enhanced cell survival and therapeutic benefits of IL-10-expressing multipotent mesenchymal stromal cells for muscular dystrophy. *Stem Cell Res Ther.* (2021) 12:105–15. doi: 10.1186/s13287-021-02168-1
33. Kuang PP, Liu XQ, Li CG, He BX, Xie YC, Wu ZC, et al. Mesenchymal stem cells overexpressing interleukin-10 prevent allergic airway inflammation. *Stem Cell Res Ther.* (2023) 14:369–15. doi: 10.1186/s13287-023-03602-2
34. Song WJ, Li Q, Ryu MO, Nam A, An JH, Jung YC, et al. Canine adipose tissue-derived mesenchymal stem cells pre-treated with TNF-alpha enhance immunomodulatory effects in inflammatory bowel disease in mice. *Res Vet Sci.* (2019) 125:176–84. doi: 10.1016/j.rvsc.2019.06.012
35. Hendawy H, Uemura A, Ma D, Namiki R, Samir H, Ahmed MF, et al. Tissue harvesting site effect on the canine adipose stromal vascular fraction quantity and quality. *Animals.* (2021) 11:1–14. doi: 10.3390/ani11020460
36. Villatoro AJ, Martin-Astorga MDC, Alcoholado C, Sánchez-Martin MDM, Becerra J. Proteomic analysis of the secretome and exosomes of feline adipose-derived mesenchymal stem cells. *Animals.* (2021) 11:1–15. doi: 10.3390/ANI11020295
37. Zhang Z, Liu M, Zheng Y. Role of Rho GTPases in stem cell regulation. *Biochem Soc Trans.* (2021) 49:2941–55. doi: 10.1042/BST20211071
38. Alqahtani S, Butcher MC, Ramage G, Dalby MJ, McLean W, Nile CJ. Acetylcholine receptors in mesenchymal stem cells. *Stem Cells Dev.* (2023) 32:47–59. doi: 10.1089/scd.2022.0201
39. Ma T, Fu B, Yang X, Xiao Y, Pan M. Adipose mesenchymal stem cell-derived exosomes promote cell proliferation, migration, and inhibit cell apoptosis via Wnt/ β -catenin signaling in cutaneous wound healing. *J Cell Biochem.* (2019) 120:10847–54. doi: 10.1002/jcb.28376
40. Plaza A, Merino B, Sánchez-Pernaute A, Torres-García AJ, Rubio-Herrera MA, Ruiz-Gayo M. Expression analysis of a cholecystokinin system in human and rat white adipose tissue. *Life Sci.* (2018) 206:98–105. doi: 10.1016/j.lfs.2018.05.036
41. National Center for Biotechnology Information PubChem Pathway Summary for Pathway P00031, Inflammation mediated by chemokine and cytokine signaling pathway. Source: PANTHER (2024). 2–6. Available at: <https://pubchem.ncbi.nlm.nih.gov/pathway/PANTHER:P00031> (Accessed February 5, 2024).
42. Guillamat-Prats R. Role of mesenchymal stem/stromal cells in coagulation. *Int J Mol Sci.* (2022) 23:1–10. doi: 10.3390/ijms231810393
43. Li X, Zhan J, Hou Y, Hou Y, Chen S, Luo D, et al. Coenzyme Q10 regulation of apoptosis and oxidative stress in H₂O₂ induced BMSC death by modulating the Nrf-2/NQO-1 signaling pathway and its application in a model of spinal cord injury. *Oxidative Med Cell Longev.* (2019) 2019:1–15. doi: 10.1155/2019/6493081
44. Plesa AM, Jung S, Wang HH, Omar F, Shadpour M (2023). Transcriptomic reprogramming screen identifies SRSF1 as rejuvenation factor Measuring aging using gene expression. bioRxiv. doi: 10.1101/2023.11.13.566787
45. Wang H, Hua J, Chen S, Chen Y. SERPINB1 overexpression protects myocardial damage induced by acute myocardial infarction through AMPK/mTOR pathway. *BMC Cardiovasc Disord.* (2022) 22:107–11. doi: 10.1186/s12872-022-02454-7
46. Bin CY, Lan YW, Chen LG, Huang TT, Choo KB, Cheng WTK, et al. Mesenchymal stem cell-based HSP70 promoter-driven VEGFA induction by resveratrol alleviates elastase-induced emphysema in a mouse model. *Cell Stress Chaperones.* (2015) 20:979–89. doi: 10.1007/s12192-015-0627-7
47. El Ouaamari A, Dirice E, Gedeon N, Hu J, Zhou JY, Shirakawa J, et al. SerpinB1 promotes pancreatic β Cell proliferation. *Cell Metab.* (2016) 23:194–205. doi: 10.1016/j.cmet.2015.12.001

8.3. Paper III: "Canid alphaherpesvirus 1 infection alters the gene expression and secretome profile of canine adipose-derived mesenchymal stem cells *in vitro*"

The article was published in Virology Journal 21:336, in December 2024. The DOI number of the article is 10.1186/s12985-024-02603-8 (WoS JCR (2023) IF 4.0, Q2 in Virology; Scopus SJR (2023) 1.016, h-index 99, Q1 in Infectious Diseases). The full paper, along with its supplementary material, is available via open access at the following link: <https://doi.org/10.1186/s12985-024-02603-8>.

RESEARCH

Open Access

Canid alphaherpesvirus 1 infection alters the gene expression and secretome profile of canine adipose-derived mesenchymal stem cells in vitro



Marina Prišlin Šimac^{1*}, Šimun Naletilić², Vjekoslava Kostanić¹, Valentina Kunić¹, Tomaž Mark Zorec³, Mario Poljak³, Doroteja Vlaj³, Rok Kogoj³, Nenad Turk⁴ and Dragan Brnić^{1*}

Abstract

Background Canine adipose-derived mesenchymal stem cells (cAD-MSCs) demonstrate promising tissue repair and regeneration capabilities. However, the procurement and preservation of these cells or their secreted factors for therapeutic applications pose a risk of viral contamination, and the consequences for cAD-MSCs remain unexplored. Consequently, this research sought to assess the impact of canid alphaherpesvirus 1 (CHV) on the functional attributes of cAD-MSCs, including gene expression profiles and secretome composition.

Methods To this end, abdominal adipose tissue from 12 healthy dogs was harvested to isolate cAD-MSCs. These samples were tested for CHV contamination before introducing a wild-type CHV strain via serial passages. Following CHV infection, real-time reverse transcription-polymerase chain reaction array and liquid chromatography with tandem mass spectrometry assessments enabled analyses of gene expression and secretome's proteomic profile, respectively.

Results This study showed that the initial cAD-MSC populations were devoid of CHV. cAD-MSCs showed susceptibility to infection with wild-type CHV, leading to notable modifications in gene expression and secretome profile. The observed genomic variations in gene expression indicate potential impacts on the stemness, migration, and other functional properties of cAD-MSCs, highlighting the need for further studies to evaluate their functional capacity post-infection. Moreover, gene expression and secretome analyses suggest a shift in stem cell differentiation toward an adipogenic phenotype.

Conclusion To the best of our knowledge, this is the first study of the effects of virus infection on gene expression and secretome composition in cAD-MSCs. The outcomes of our study underscore the imperative of routine viral screening prior to the therapeutic use of cAD-MSCs. Moreover, these findings provide novel insights into the pathogenic mechanisms of CHV and pave the way for future canine stem cell and virus research.

Keywords Mesenchymal stem cell, Canine stem cells, In vitro, Gene expression, Secretome, Canine herpesvirus, Virus infection, Veterinary regenerative medicine

*Correspondence:
Marina Prišlin Šimac
prislin@veinst.hr
Dragan Brnić
brnic@veinst.hr

Full list of author information is available at the end of the article



© The Author(s) 2024. **Open Access** This article is licensed under a Creative Commons Attribution 4.0 International License, which permits use, sharing, adaptation, distribution and reproduction in any medium or format, as long as you give appropriate credit to the original author(s) and the source, provide a link to the Creative Commons licence, and indicate if changes were made. The images or other third party material in this article are included in the article's Creative Commons licence, unless indicated otherwise in a credit line to the material. If material is not included in the article's Creative Commons licence and your intended use is not permitted by statutory regulation or exceeds the permitted use, you will need to obtain permission directly from the copyright holder. To view a copy of this licence, visit <http://creativecommons.org/licenses/by/4.0/>.

Background

Mesenchymal stem cells (MSCs) have the capacity to regenerate tissue in various species, including canines, presenting significant potential for treating diseases with limited therapeutic options, such as osteoarthritis, spinal cord injuries, and chronic skin wounds [1–3]. One promising stem cell source in canines is adipose tissue, abundant with canine adipose-derived mesenchymal stem cells (cAD-MSCs), which are easy to obtain and proliferate rapidly compared to other types of MSCs [4–6]. The cAD-MSCs exhibit notable regenerative properties, particularly the ability to modulate immune responses by secreting relevant molecules, i.e., the secretome [5, 7, 8]. Moreover, the application of the cAD-MSC secretome for therapy, rather than the cells themselves, offers the potential for numerous lower-risk treatments [9–12].

Acquiring and storing cAD-MSCs and secretomes in therapeutic quantities necessitates *in vitro* cultivation, thereby introducing the risk of microbial contamination. Studies have indicated that stored MSC batches may be contaminated with bacteria, fungi, or viruses [13, 14]. Bacterial and fungal contamination can be effectively mitigated with antibiotics and antimycotics [13]; however, mitigating potential viral contamination remains challenging. Available data indicate that MSCs can be permissive to infection with RNA and DNA viruses, which can lead to cell death, persistent infection, or cellular transformation and may ultimately impair their functionality [15–19]. Viral infection of MSCs has been associated with the inhibition of differentiation [20], increased secretion of proinflammatory cytokines [21], and loss of immunomodulatory function [22]. In cAD-MSCs, one study reported the susceptibility to distemper virus [23], and recent findings confirmed the possibility of viral contamination of cryobanked cAD-MSC batches by detecting canine parvovirus, influenza, parainfluenza, and canid alphaherpesvirus 1 [24].

Canid alphaherpesvirus 1 (CHV) belongs to the species *Varicellovirus canidalpha1* within the *Orthoherpesviridae* family, whose genome consists of double-stranded DNA [25]. The latent and subclinical persistence of CHV in dogs poses a significant challenge, potentially leading to infection oversight during routine clinical examination of cAD-MSC donors. Moreover, CHV is distributed globally, with seroprevalence ranging from 21.7% to 80% [26, 27], and nearly one-third of dogs are infected in Croatia [28]. This widespread prevalence makes CHV a considerable risk for contamination during sampling or culturing. Previous studies in human and equine MSCs have shown that herpesvirus infection can decrease the immunomodulatory effects of MSCs [22, 29, 30]. Since studies investigating this phenomenon in canines are currently lacking, this study aimed to assess the susceptibility and

adaptability of cAD-MSCs to CHV through serial passages. Moreover, this study sought to explore the impact of CHV infection on the gene expression and secretome composition of cAD-MSCs.

Methods

Stem cell culture establishment and characterisation

Adipose tissue collection, cAD-MSCs extraction, and propagation

This study obtained adipose tissue samples from 12 clinically healthy dogs (*Canis lupus familiaris*), 11 females and one male who underwent elective surgery. The collection of adipose tissue, extraction of cAD-MSCs and propagation were performed according to previously established protocols [8, 31]. To accomplish the objectives of this investigation, we used cells from cAD-MSC donors 6/21, 9/21, 13/21, 14/21, 1/22, 2/22, 3/22, 6/22, and 7/22, which have been described in a prior publication [8]. In addition to these samples, cells from three novel donors (7/21, 8/21, and 8/22) were used following the same procedure. Nonetheless, this research provides a distinct objective, experimental framework, and conclusions by contrasting the baseline data from uninfected cAD-MSCs with new findings following CHV infection. Table 1 contains information on the age, breed, health status, adipose tissue collection site and mass of the donors. Sterility-tested cAD-MSCs for aerobic and anaerobic bacteria, fungi and mycoplasma were used for all experiments following a previously established protocol [31]. All donor cells were cryobanked in liquid nitrogen via the standard cryobanking procedure with 10% dimethyl sulfoxide (Sigma–Aldrich, St. Louis, MO, USA, Cat. No. D2650-100ML) at passage 2 (P2) or P3 for future experiments.

Immunophenotyping and multipotency testing of cAD-MSCs

As previously described [8], the immunophenotyping and multipotency testing of the cAD-MSCs were performed at P3. FACSVerse (BD, Franklin Lakes, NJ, USA) flow cytometry was used to confirm the immunophenotype, while adipogenic, osteogenic and chondrogenic *in vitro* differentiation was performed to verify multipotency, following the criteria of the International Society for Cellular Therapy [32].

Testing of established cAD-MSCs for CHV

All donors were tested for CHV to gain insight into the possible latent infection of cAD-MSCs extracted from adipose tissue. A cryobanked batch of cells per donor at P2/P3 was first transferred at -20 °C to induce lysis of the cell membranes. After 24 h, the cell lysate was thawed at room temperature for 30 min, vortexed and subjected to nucleic acid extraction using a MagMAX CORE nucleic

Table 1 Canine adipose tissue donor information

Donor	Sex	Age (Months)	Breed	Collection site	Surgical procedure	Adipose tissue mass (grams)
6/21*	Female	12	German Spaniel	Ovarian mesostructure	Ovariohysterectomy	7.0
7/21	Female	6	Miniature Schnauzer	Ovarian mesostructure	Ovariectomy	1.4
8/21	Female	12	Mixed	Ovarian mesostructure	Ovariectomy	10.2
9/21*	Female	12	Labrador Retriever	Ovarian mesostructure	Ovariectomy	7.0
13/21*	Female	7	Toy Poodle	Ovarian mesostructure	Ovariectomy	1.0
14/21*	Female	7	Toy Poodle	Ovarian mesostructure	Laparoscopic ovariectomy	1.2
1/22*	Female	10	Jack Russell Terrier	Ovarian mesostructure	Ovariectomy	1.0
2/22*	Female	6	Lagotto Romagnolo	Ovarian mesostructure	Ovariectomy	1.2
3/22*	Female	12	Medium Poodle	Ovarian mesostructure	Ovariectomy	1.0
6/22*	Female	60	Portuguese Water Dog	Ovarian mesostructure	Ovariectomy	2.5
7/22*	Female	36	Mixed	Ovarian mesostructure	Ovariectomy	4.1
8/22	Male	12	German Shepard	Spermatic cord mesostructure	Orchiectomy	2.1

*The information from these donors was previously published [8]

acid purification kit (Thermo Fisher Scientific, Waltham, MA, USA, Cat. No. A32702) on a KingFisher Flex Purification System (Thermo Fisher Scientific) according to the manufacturer's instructions. Quantitative real-time PCR (qPCR) was applied for the detection of the CHV glycoprotein B gene according to a previously published protocol [33] using a QuantiFast Pathogen PCR+IC Kit (Qiagen, Hilden, Germany, Cat. No. 211352) on a Rotor-Gene Q (Qiagen) instrument. Beta-actin served as an endogenous control, employing the same reagents, instrument, and a previously established protocol [34]. The reaction mixture setup and thermal cycling conditions were performed as recommended by the manufacturer. The reaction mixtures' final primer and probe concentrations were adjusted to 1,000 nmol/L for CHV-For (5'-ACAGAGTTGATTGATAGAAGAGGTATG-3') and CHV-Rev (5'-CTGGTGATTAACCTTGAAGCTTTA-3') and 500 nmol/L for CHV-Pb (5'-6-FAM-TCTCTGGGGTCTTCATCCTTATCAAATGCG-BHQ1-3'). For beta-actin, primers were adjusted to 83.3 nmol/L for ACT2-1030-F (5'-AGCGCAAGTACTCCGTGTG-3') and ACT-1135-R (5'-CGGACTCATCGTACTCTGCTT-3') and 41.7 nmol/L for ACT-1081-HEX (5'-HEX-TCGCTGTCCACCTTCCAGCAGATGT-BHQ1-3').

Isolation and characterisation of autochthonous wild-type CHV

CHV recovery from clinical specimen and virus stock production

The autochthonous wild-type CHV strain 29107 was obtained from the organs (liver, spleen, and lungs) of a 6-day-old golden retriever undergoing routine CHV

diagnostics at the Croatian Veterinary Institute. The organ samples (1×1 cm each) were combined and homogenised with a cold mortar and pestle containing sterile sand and 10 mL of DMEM Low Glucose. The homogenate was freeze-thawed, centrifuged at 2,100×g for 10 min, filtered using a Millex-HP syringe filter unit 0.45 µm (Merck, Darmstadt, Germany) and stored at -80 °C. For in vitro propagation, the Madin-Darby Canine Kidney (MDCK) cell line (ATCC, Manassas, VA, USA; Cat. No. CCL-34), which is known to be susceptible to CHV [35], was used. Before inoculation, the MDCK cell line was confirmed to be CHV contamination-free. A 90% confluent MDCK (P34) monolayer in a T25 flask (Thermo Fisher Scientific) was infected with 1 mL of stock supernatant. Following two hours of adsorption at 37 °C (5% CO₂, 80% humidity), 10 mL of basal medium (79% DMEM Low Glucose (Thermo Fisher Scientific, Cat. No. 31885049), 20% fetal bovine serum (FBS) (Thermo Fisher Scientific, Cat. No. 1027010), and 1% penicillin/streptomycin (Sigma-Aldrich, Cat. No. P4333-100ML)) was added. Upon full CPE development (monitored using a Lux2 live imaging platform, Axion BioSystems, Atlanta, GA, USA) or 96 h postinfection (p.i.), the infected cell culture flask underwent a single freeze-thaw-centrifugation cycle. The final CHV stock was generated after the third viral passage on MDCK cells in T75 flasks and stored at -80 °C.

CHV virus stock titration was conducted in triplicate using a confluent MDCK monolayer (P35) seeded in a 96-well microplate (Thermo Fisher Scientific). Eight separate tenfold dilutions of stock supernatant (100 µL per well) were added to the cells. After a two-hour adsorption period, 180 µL of the basal medium was added to the

inoculum, and the plates were incubated at 37 °C with 5% CO₂ and 80% humidity for 72 h. The virus titre (TCID₅₀) was calculated using the Spearman–Kärber method.

Verification of the autochthonous wild-type CHV strain by NGS

To verify the autochthonous wild-type CHV strain 29107 and generate a whole-genome sequence, we performed next-generation sequencing (NGS). Specifically, viral DNA was extracted from 200 µL of CHV organ suspension homogenate using a DNA Blood and Tissue kit (Qiagen, Cat. No. 69506) according to the manufacturer's instructions. Sequencing libraries were prepared using the Nextera XT DNA Library Preparation Kit (Illumina Inc., San Diego, USA, Cat. No. 15032354 and No. 15032355) with Nextera DNA UD Indexes (Illumina Inc., Cat. No. 20026934) and sequenced on a NextSeq 550 sequencer (Illumina Inc., Cat. No. SY-415-1002) loaded with a NextSeq 500/550 High Output Kit v 2.5 (300 cycles) (Illumina Inc., Cat. No. 20024908) following the manufacturer's instructions. Library fragment size control and quantification were performed using a 2100 Bioanalyzer instrument with an Agilent High Sensitivity DNA Kit (Agilent Technologies, Santa Clara, CA, USA, Cat. No. 5067-4626) and a Qubit™ 4 Fluorometer with a Qubit dsDNA HS Assay Kit (Thermo Fisher Scientific, Cat. No. Q32854), respectively.

The sequence reads were assembled into contigs using the Spades software v3.15 [36]. The contigs were compared to known complete CHV genome sequences in NCBI GenBank. Sequence reads were mapped to the GenBank sequence MW353136 using Bwa mem v0.7.17 [37] and SAMtools v1.19 [38] and then used to generate a consensus assembly with Ivar v1.0 [39]. MW353136 was used as a reference because it was the most thoroughly covered by sequencing reads among the complete genome sequences of CHV (taxid:170325) in GenBank. The final novel sequence scaffold of the autochthonous wild-type CHV strain was scaffolded, curated and annotated manually. PROKKA software [40] was used to generate initial functional annotation. The autochthonous wild-type CHV strain 29107 genome sequence was deposited in GenBank under accession number PP349830.

Furthermore, phylogenetic analysis of the novel autochthonous wild-type CHV complete genome sequence was constructed from complete genome alignment of a total of 23 CHV sequences (22 reference sequences from the GenBank database) using IQTree2 software [41] and

substitution model HKY+F+I. An optimal substitution model was found using ModelFinder [42]. Multiple sequence alignment was prepared using MAFFT software [43]. The phylogenetic tree was visualised with Python scripting with the help of the module Toytree with UFBoot node support [44] values shown. Calculation of the similarity plot was aided by the Python module Numpy, and visualisation was performed using the Toyplot module. Recombinations were analysed by RDP5 [45].

In vitro cAD-MSCs infection with wild-type CHV CHV serial passages on cAD-MSCs

To demonstrate successful CHV infection in cultured cAD-MSCs, a cohort of six donors (9/21, 13/21, 14/21, 2/22, 3/22, and 7/22) was randomly chosen for five consecutive viral passage experiments. In contrast to prior experiments involving freshly utilized cAD-MSCs, cryopreserved cAD-MSCs at P2 or P3 were used for these specific infections. After thawing and expansion, cells from each donor were distributed as six replicates into 24-well plates (Thermo Fisher Scientific) at a density of 10⁵ cells/well in 1 mL of basal medium and maintained at 37 °C and 5% CO₂ (80% humidity) until they reached 90% confluence. Subsequently, the basal medium was removed, and three wells per donor were inoculated with CHV virus stock at a multiplicity of infection (MOI) of 0.5. Following a two-hour incubation period to allow virus adsorption, basal medium was added to the inoculum to a volume of 1 mL. The CHV infection experiments were conducted until the CPE reached 80% or for a maximum of 120 h if the CPE was minimal or absent. Upon meeting the criteria, the plates were frozen at –80 °C. Thawed cell lysate suspensions from each donor triplicate were individually mixed, transferred to sterile 5 mL tubes (Eppendorf, Hamburg, Germany), and subjected to a second freezing cycle. After the second thaw, the cell lysate suspensions were centrifuged at 2665×g for 10 min, and the supernatant was filtered through a 0.45 µm filter and stored in 2 mL cryovials (Cryoking, Newcastle, Australia). Subsequent passages of the CHV virus were initiated by preparing new 24-well plates as described previously, with 500 µL/well of the preceding viral passage used as inoculum for virus absorption. Five passages of the CHV virus were conducted for each cAD-MSC donor and control cell line (MDCK). The progression of CPE was documented using a microscopic camera (AxioCam ER/105/208/HD, Axio Observer D1, Zeiss, Jena, Germany) and a Lux 2 live imaging platform.

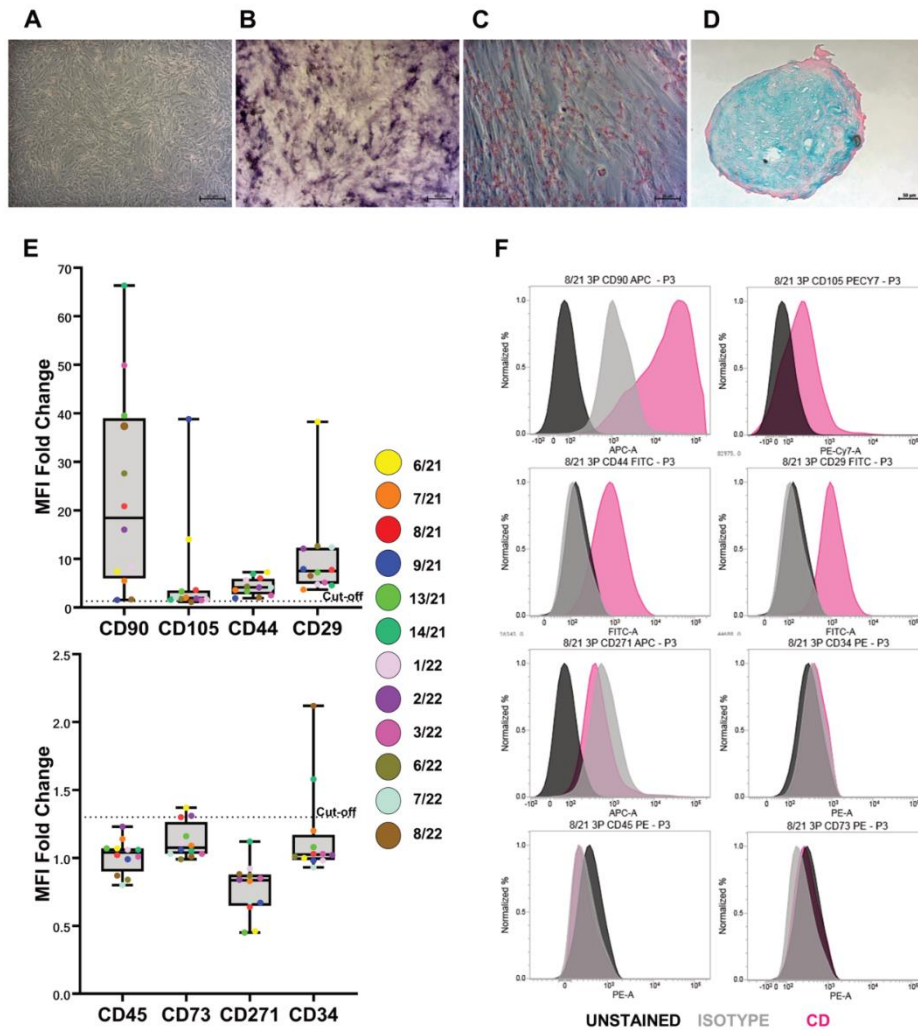


Fig. 1 Canine adipose-derived mesenchymal stem cells (cAD-MSCs) multipotency and stem cell immunophenotype at passage 3 in vitro. **A** The morphology of undifferentiated cAD-MSCs; **B** osteogenic differentiation marked by the purple staining of alkaline phosphatase activity, **C** adipogenic differentiation evident by the presence of lipid droplets, stained red, **D** chondrogenic differentiation shown by Alcian Blue staining, with aggrecan appearing blue. **A–D** Microscopic images were captured using an Axiovert camera on an Axio Observer D1 microscope (Zeiss), with scale bars of 50 μ m and 100 μ m. **E** Whisker-box plot illustrates the Median Fluorescence Intensity (MFI) fold changes for surface markers CD90, CD105, CD44, and CD29 (upper plot), as well as CD73, CD271, CD45, and CD34 (lower plot) in cAD-MSCs at passage 3. The dotted line indicates the cut-off value of 1.5, and the legend shows individual MFI fold changes for each donor by colourful dots. **F** Representative flow cytometry histograms for each CD marker, with blue representing unstained cells, grey representing isotype controls, and black representing specific CD surface markers. Results of immunophenotype and differentiation analysis from 9 out of 12 canine-adipose derived mesenchymal stem cell donors (6/21, 9/21, 13/21, 14/21, 1/22, 2/22, 3/22, 6/22, 7/22) were previously published [8]

Each passage included three wells of negative controls. Supernatants from each passage (CHV-infected and uninfected) were stored at -80°C for further qPCR experiments.

Quantification of CHV DNA with qPCR

To confirm the success of the infection, i.e., the presence of viral DNA in the supernatant of infected cAD-MSCs, we quantified the number of CHV genome copies. Total DNA was extracted from 200 μL of filtered supernatant from each viral passage after two freeze–thaw cycles using a DNA Blood and Tissue Kit (Qiagen, Cat. No. 69506) according to the manufacturer's cell extraction protocol. DNA was quantified using a Qubit 1X dsDNA High Sensitivity (HS) kit (Thermo Fisher Scientific, Cat. No. Q33230) on a Qubit 4 Fluorometer (Thermo Fisher Scientific). CHV detection was performed by qPCR as previously described.

For quantification, a triple 5-point standard curve was generated with quantitative genomic DNA from CHV strain D 004 (ATCC VR-552DQ, lot: 70054940). The following values of the standard curve were obtained: $R^2=0.99945$, slope = -3.57263 , Y-intercept = 35.24627 , and reaction efficiency = 91% . The limit of detection (LOD, $\geq 95\%$ detection in 20 replicates) was 3.31 genomic copies (gc)/reaction. Theoretically, this assay provides an LOD of 6.44×10^2 gc/mL of cell lysate supernatant. The limit of quantification (LOQ, coefficient of variability $\leq 35\%$ in 20 replicates) was set at 136.94 gc/reaction, theoretically providing a CHV LOQ of 2.66×10^4 gc/mL for the cell lysate supernatant. The results are presented as the mean \pm SEM unless otherwise stated.

Gene expression profiling of CHV-infected cAD-MSCs

Gene expression analysis via RT–qPCR array was conducted on P3 of CHV-infected and uninfected cAD-MSCs from twelve donors. Two T75 flasks (Thermo Fisher Scientific) were seeded with $\approx 10^6$ cAD-MSCs per flask in basal medium and incubated until they reached 90% confluence (24–48 h). One flask was inoculated with CHV stock at an MOI of 0.5, allowing for a two-hour adsorption period, while the second flask served as a negative control. Twenty-four hours p.i., gene expression

profiling was conducted following an established procedure [8]. In brief, RNA extraction was performed with an RNeasy Mini kit (Qiagen, Cat. No. 74106) following the manufacturer's instructions. The quality of the extracted RNA was verified using an RNA QC kit (Qiagen, Cat. No. 50–727–743). Finally, gene expression profiling was conducted using the RT2 ProfilerTM PCR Array for Dog Mesenchymal Stem Cells (PAFD-082ZR, Qiagen). The RNA QC and raw gene expression data from nine uninfected cAD-MSC donors (6/21, 9/21, 13/21, 14/21, 1/22, 2/22, 3/22, 6/22, and 7/22), which were previously published [8], were analysed together with new data from three additional uninfected cAD-MSC donors (7/21, 8/21, and 8/22). This way, a comparative analysis was performed with new results from all 12 CHV-infected cAD-MSC donors.

After data acquisition, the specialised RT2 Profiler PCR Array Data Analysis Software, accessible online at <https://dataanalysis2.qiagen.com/pcr> (accessed 19 March 2024), enabled normalisation and comprehensive analysis. The gene expression analysis results, researched gene names, symbols, and NCBI sequences are listed in Additional file 1. Statistical significance was determined via Student's t-test applied to replicated $2^{-\Delta\Delta\text{CT}}$ values within both the control and treatment groups with $p < 0.05$. The software automatically established a fold change cut-off value of 2.0, corresponding to a log2fold change ± 1.0 . Gene expression profile data were publicly deposited in the NCBI Gene Expression Omnibus database under accession number GSE267402. The data were visualised with GraphPad Prism 10.2.2.

Proteomic analysis of the CHV-infected cAD-MSCs secretome

The alterations in the proteomic composition of the secretome of cAD-MSCs were also analysed in P3 under two conditions, uninfected and CHV-infected cAD-MSCs, in six randomly selected donors (6/21, 9/21, 14/21, 1/22, 6/22, and 7/22). The cells were seeded in six replicates at 10^5 cells/mL density in 24-well plates (Thermo Fisher Scientific) and conditioned in the basal medium at 37°C , $5\% \text{CO}_2$ and 80% humidity until they reached 90% confluence. The culture medium was then

(See figure on next page.)

Fig. 2 Development of cytopathogenic effects (CPE) following Canid alphaherpesvirus 1 (CHV) infection *in vitro*. **A** Progression of CPE after CHV virus stock infection in the Madin-Darby canine kidney cell line (MDCK) over time (marked in days, hours, minutes, and seconds). **B** Progression of CPE after CHV virus stock infection in canine adipose-derived mesenchymal stem cells (cAD-MSCs) over time (marked in days, hours, minutes, and seconds). **C** cAD-MSC negative control (left) and CPE development in six cAD-MSC donors 48 h after infection with the CHV stock (right). **D** CHV genome copies per mL of cell lysate supernatant for each virus passage in cAD-MSCs (boxplots) and MDCK cells (line graph). Microscopy images were acquired with the Lux 2 live imaging platform (Axion Biosystems) (**A**, **B**) or with the microscopic camera Axiocam ER/105/208/HD on Axio Observer D1 (Zeiss, magnification 50–100x, scale bar 200 μm) (**C**)

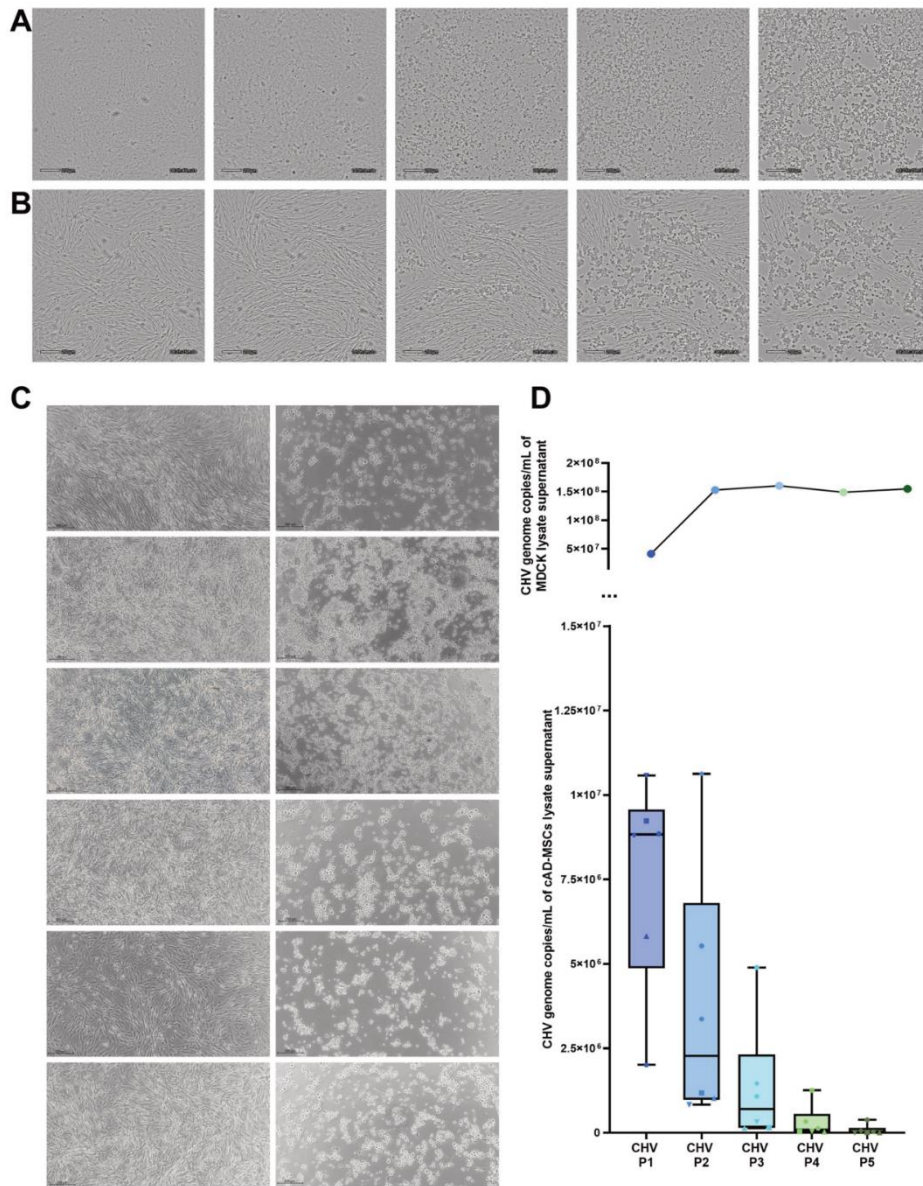


Fig. 2 (See legend on previous page.)

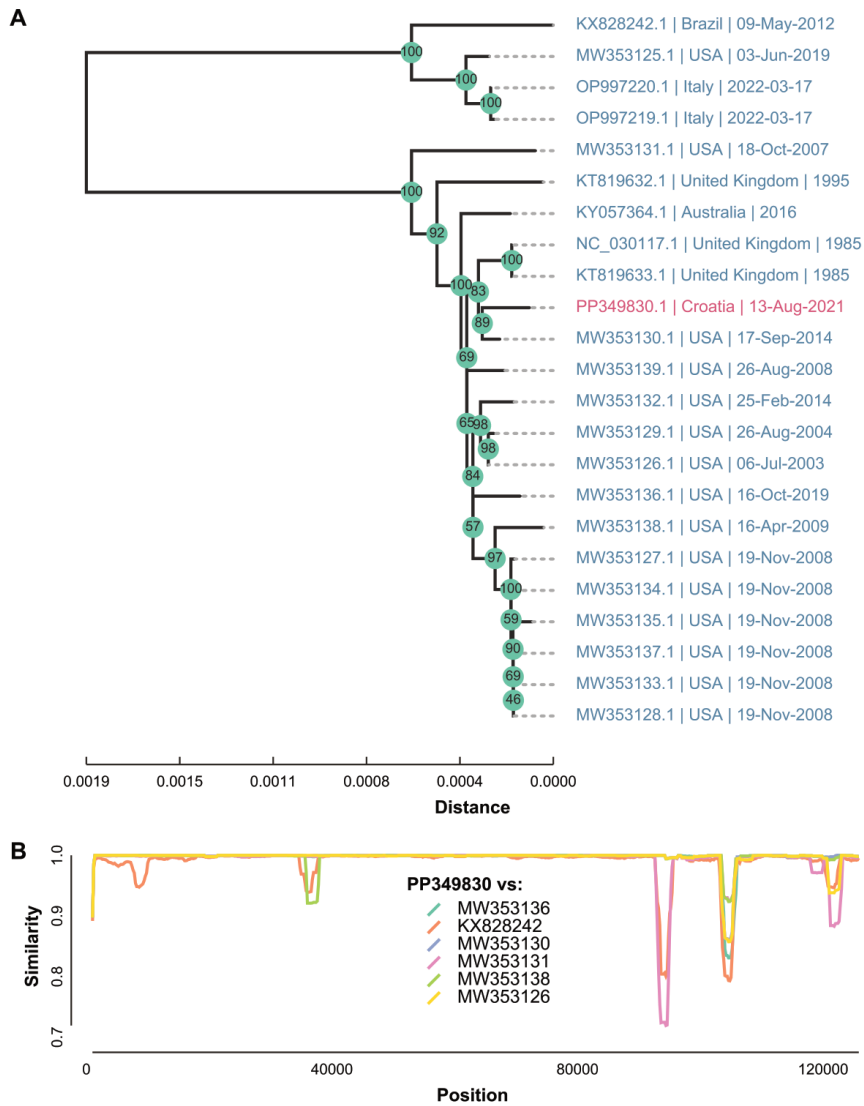


Fig. 3 Phylogenetic analysis of the novel wild-type CHV complete genome sequence. **A** Phylogenetic placement of the wild-type autochthonous CHV (PP349830) among the 22 complete CHV sequences from the GenBank database. The wild-type CHV is highlighted in pink. Tips are labeled with GenBank accession numbers, collection locations, and dates. **B** Local similarity plot of PP349830 vs representative context sequences (KX828242, MW353130, MW353131, MW353136 and MW353138) along the length of the genome sequence. Context sequences shown were chosen to most representatively sample CHV genome diversity as represented by the phylogenetic tree (A). Local hamming similarities versus target sequences were computed in sliding windows (length=1000 nt, step=100)

aspirated, and three wells of uninfected cells were rinsed with 2 × 2 mL DMEM Low Glucose before being incubated in 2 mL of the same medium. On the other hand, three wells of CHV-infected cAD-MSCs were inoculated with a MOI 0.5 of CHV viral stock, the virus was allowed to absorb for 2 h, and then the CHV-infected cells were rinsed with 2 × 2 mL of DMEM Low Glucose and incubated in 2 mL of the same medium. Forty-eight hours later, the secretome of the cAD-MSCs was collected as previously described [8].

Following a previously published protocol [8], the samples were prepared for liquid chromatography with tandem mass spectrometry (LC-MS/MS) analysis. In brief, the secretome proteins were reduced and extracted from the culture medium. The protein concentrations were adjusted via the Bradford assay, and enzymatic digestion followed, with peptide separation conducted using the nanoLC EASY-nLC 1200 system (Thermo Fisher Scientific). The mass spectra were recorded using a Q Exactive Plus Hybrid Quadrupole-Orbitrap tandem mass spectrometer (Thermo Fisher Scientific).

Raw data analysis utilised Scaffold Quant Q + S 5.3.0, employing protein sequence data from the *Canis lupus familiaris* reference proteome (UniProt Proteome ID UP000805418, accessed on 30 October 2023, with a total of 20,991 entries). Scaffold Quant version 5.0.3 was utilised for subsequent analysis, employing untargeted label-free quantification and statistical analysis based on spectral counting. Statistical significance, verified via t-tests, was defined as $p < 0.05$, with proteins filtered to include only those with at least two identified peptide sequences. A cut-off value of 1.3 was applied, corresponding to a log₂fold change ± 0.3785 . The mass spectrometry proteomics data were deposited with the ProteomeXchange consortium via the PRIDE [46] partner repository with the dataset identifiers PXD052289 and <https://doi.org/10.6019/PXD052289>. In this study, we incorporated previously published raw proteomic data from six uninfected cAD-MSC donors (6/21, 9/21, 14/21, 1/22, 6/22, and 7/22) [8] to facilitate a comparative analysis with new secretome proteome data from six cAD-MSCs following CHV infection.

Bioinformatics analysis of the detected proteins was performed with Gene Ontology (GO) Panther 18.0 to

analyse cellular components, protein classes, molecular functions, and biological processes. GO enrichment analysis was used to determine affected protein pathways using Fisher's exact test and false discovery rate (FDR) correction, with data presented as raw p values < 0.05 and FDR < 0.05 . Additionally, a protein-protein interaction network analysis was conducted using STRING (v12.0) [47], employing a high confidence interaction score of 0.700, an FDR < 0.05 , and a strength score > 0.75 . To elucidate protein pathways and interactions lost due to CHV infection, the proteins secreted distinctively in uninfected samples were grouped with the biologically significant downregulated proteins (uninfected group). In contrast, distinct proteins secreted in CHV-infected samples were grouped with biologically significantly upregulated proteins (CHV-infected group) to elucidate the protein pathways activated after CHV infection. The data visualisation was performed with GraphPad Prism 10.2.2.

Results

Extracted cAD-MSCs showed stem cell properties and tested negative for CHV

The identity of the stem cells has already been published for nine cAD-MSC donors [8], except for donors 7/21, 8/21 and 8/22. All donors included in this study were positive for the mesenchymal markers CD90, CD105, CD44 and CD29 and negative for the hematopoietic markers CD34 and CD45 (Fig. 1). Furthermore, they differentiated into three mesodermal lineages: adipogenic, as confirmed by the presence of Oil Red O-positive fat droplets; osteogenic, as confirmed by purple staining indicating alkaline phosphatase activity; and chondrogenic, as confirmed by spheroids showing aggrecan (a proteoglycan in articular cartilage) when stained with Alcian blue (Fig. 1).

qPCR analysis revealed that all 12 cAD-MSC donors were negative for CHV.

The autochthonous wild-type CHV strain was successfully isolated and verified by whole-genome sequencing

The autochthonous CHV strain was successfully recovered from the affected organs and further propagated on the MDCK cell line. The first signs of CPE were observed

(See figure on next page.)

Fig. 4 Gene expression profile of canine adipose-derived mesenchymal stem cells following canine herpesvirus infection in vitro.

Significantly downregulated and upregulated genes are labelled blue and orange, respectively. Volcano plots illustrate the expression profiles of genes related to stemness (A), mesenchymal stem cell (MSC)-specific genes (B), MSC-associated genes (C) and MSC differentiation genes (D) after CHV infection. The bar chart shows the fold-regulation of the significantly downregulated and upregulated genes (E). *Gene expression was lower in the uninfected sample and more readily detectable in the CHV-infected sample, indicating that the fold change was at least as high as the calculated value

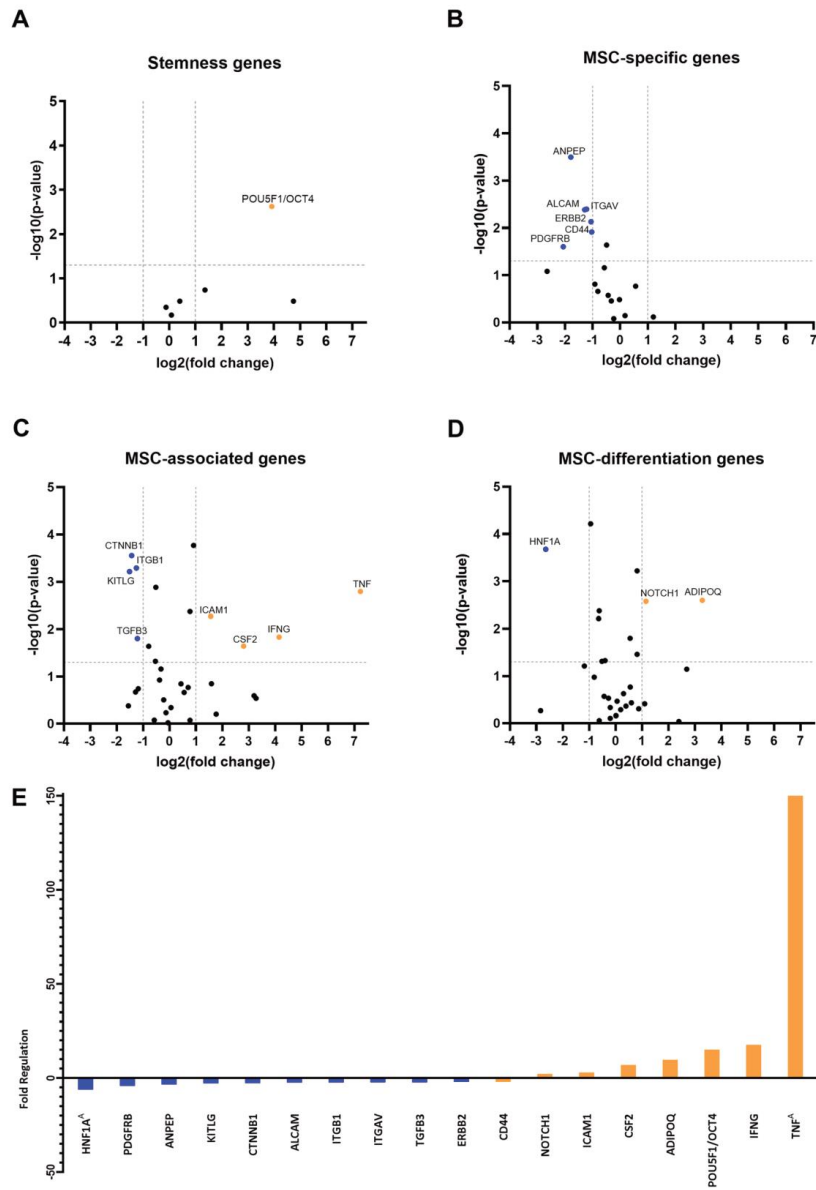


Fig. 4 (See legend on previous page.)

at ≈ 30 h p.i., characterised by cell rounding. The number of cells affected by viral activity increased progressively over time. Further progression of CHV infection induced clustering of rounded cells, leaving blank spaces between clusters. The characteristic CPE was fully developed at 96–120 h p.i. (Fig. 2A; Additional file 2). The established virus consistently exhibited CPEs at comparable intervals during the two subsequent passages on MDCK cells used to generate the CHV virus stock. The created CHV virus stock was titrated in triplicate, yielding an average titre of $10^{5.04}$ TCID₅₀/mL.

The isolated autochthonous wild-type CHV strain 29,107 was verified by deep sequencing, and the complete genome was characterised. The consensus CHV genome sequence was generated by mapping reads to the GenBank sequence MW353136 and deposited to GenBank under the accession number PP349830. The CHV genome was 124,854 bases long and was covered by 234,338 sequencing reads (150 bp) with a mean base depth of 250 \times and a mean base quality of 34.1 (PHRED). Phylogenetic analysis showed that the novel wild-type CHV was most closely related to the GenBank sequence MW353130 (Fig. 3A). MW353130 was most similar to PP349830 along the entire genome length, except in a region spanning positions 102,000 and 106,000, where it was most similar to MW353131 and MW353138 (Fig. 3B). This region encodes one set of copies of the virion proteins US10 and US1 and the regulatory protein V67. The abrupt drop in local similarity to the globally closest sequence suggests possible evolutionary forces, such as recombination, acting on virion proteins under selective pressure. RDP5 analysis detected weak recombination signals in this region of the CHV genome alignment. However, distinguishing recombination from other evolutionary processes is challenging given the similarity levels (global $\sim 99\%$, local 92–93% to MW353131, and 86–87% to MW353130).

The CHV genome sequence contained all 75 alphaherpesvirus genes present in MW353130. The CHV genome

contained 41 mutations (18 noncoding mutations, 11 synonymous mutations and 12 nonsynonymous mutations) with respect to MW353130, including seven insertions (four single nucleotides, one dinucleotide and two trinucleotide insertions), eight deletions (four single nucleotides, two dinucleotides, one trinucleotide and one heptanucleotide deletion) and 26 single nucleotide mutations. Coding mutations in CHV were localised to the CHV genes RS1 (n=6), RS36 (n=3), US1 (n=2), and US10 (n=2) and UL50, UL42, UL37, UL34, UL25, UL8, RL2, US7, US8 and US9 (n=1 each). Mutations harboured by the wild type CHV are listed in Additional file 3.

The cAD-MSCs are susceptible to CHV

We demonstrated that CHV can infect cAD-MSCs from all 12 cAD-MSC donors, while six are represented in Fig. 2C. Similar to MDCK cells, all cAD-MSCs displayed focal cell rounding; however, the time to develop CPE was 24–48 h p.i. These rounded cells clustered together, creating empty spaces between them. At 72–96 h p.i., the typical CPE was observed throughout the culture (Fig. 2B; Additional file 4).

However, serial passages of CHV have shown that the time for cAD-MSCs to develop CPE has been prolonged. In CHV P3, CPE was observed in only 2/6 donors, and no observable CPE developed in any of the donor cAD-MSCs in later passages, CHV P4 and CHV P5. The qPCR results corroborated the in vitro observations. The CHV genome copy number decreased with each consecutive passage (Fig. 2D). However, it remained detectable at all five passages, detecting 7,550,146 \pm 1,278,419 gc/mL, 3,757,414 \pm 1,562,144 gc/mL, 1,338,312 \pm 744,417 gc/mL, 301,236 \pm 196, 130 gc/mL, and 79,131 \pm 60,755 gc/mL in CHV P1, CHV P2, CHV P3, CHV P4, and CHV P5, respectively. Conversely, in the MDCK cell line, the CHV genome copy number increased from P1 to P2 and remained stable across all subsequent passages.

(See figure on next page.)

Fig. 5 Proteomic analysis of the secretome from canine adipose-derived mesenchymal stem cells. **A–C** Complete functional protein classification of secretomes comparing uninfected and CHV-infected canine adipose-derived mesenchymal stem cells by protein class (**A**), by molecular function (**B**), and according to biological processes (**C**). Bars indicate the number of categorized secreted proteins. **D** Volcano plot showing commonly secreted proteins in the secretome of canine adipose-derived mesenchymal stem cells, comparing uninfected with CHV-infected cells. A comprehensive list of all detected proteins, including their accession numbers, gene names, molecular weights, t-test p values, and fold change data, is provided in Additional File 6. In the graphical representation and Additional file 6, the blue color represents significantly downregulated proteins ($p < 0.05$) with a fold change exceeding 1.3. Conversely, the orange color signifies proteins demonstrating statistical significance ($p < 0.05$) in upregulation, with a fold change greater than 1.3. **E** String protein interaction network representing significant protein interactions occurring due to CHV infection. The coloured nodes represent interactions with a high confidence score (0.700) and strength > 0.75 . Red represents interactions of proteins involved in the aminoacyl-tRNA synthetase multienzyme complex; pink represents interactions involving the proteasome complex; yellow represents interactions involving pyruvate metabolism and carbon metabolism; green represents interactions involving glycolysis; and blue represents interactions involving the enolase, C-terminal TIM barrel domain and glycolysis

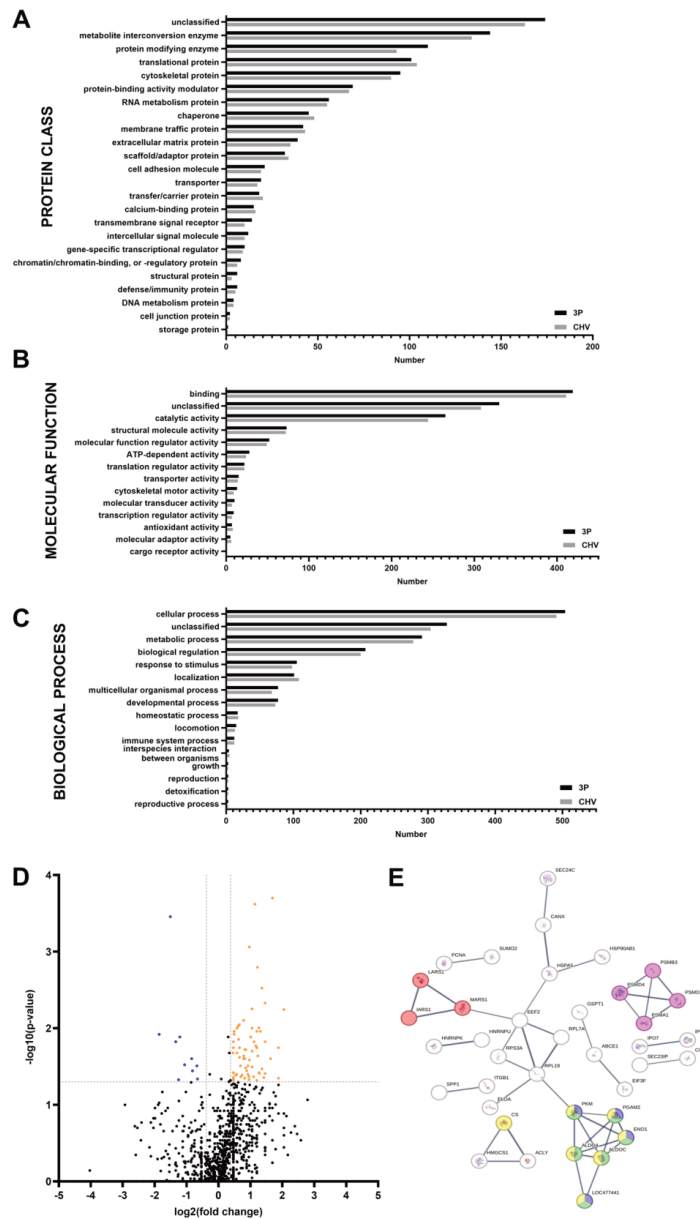


Fig. 5 (See legend on previous page.)

Table 2 Protein pathway analysis of the uninfected and CHV-infected canine adipose MSC secretomes via Gene Ontology Panther

	Gene Ontology Panther protein pathways analysis	Raw p value*	False discovery rate (FDR)*	Gene names of proteins involved in the pathway
Uninfected group	Nicotinic acetylcholine receptor signalling pathway	2.09E-04	3.37E-02	MYH1, MYH2, MYH4
	Cytoskeletal regulation by Rho GTPase	2.09E-04	1.69E-02	MYH1, MYH2, MYH4
	Wnt signalling pathway	7.28E-04	3.90E-02	CDH13, CDH2, MYH1, MYH2, MYH4
CHV-infected group	Pyruvate metabolism	6.42E-05	3.45E-03	ACLY, CS, PKM
	Cell cycle	4.89E-04	1.97E-02	PSMD4, EIF3F, PSMD14
	Glycolysis	6.92E-06	5.57E-04	ALDOA, ALDOC, ENO1, PGAM2, LOC477441

*Analysis criteria were raw p values < 0.05 and FDR < 0.05

Table 3 Protein pathway analysis of the secretome of uninfected and CHV-infected canine adipose MSCs via STRING

	STRING protein interaction analysis	Strength score*	False discovery rate*	Gene names of proteins involved in interaction	
Uninfected group	Extracellular matrix organisation, and Extracellular matrix	1.24	5.58E-08	ECM2, POSTN, ADAMTS1, FBLN5, MFAP2, BGN, MMP12, MMP9, PCOLCE2, COL6A1, PRELP, ITGBL1	
	Extracellular matrix organisation, and Extracellular matrix	1.22	3.25E-07	ECM2, POSTN, ADAMTS1, FBLN5, MFAP2, BGN, MMP12, MMP9, PCOLCE2, COL6A1, PRELP	
	Mixed, incl. Collagen formation, and Degradation of the extracellular matrix	1.19	1.79E-05	POSTN, ADAMTS1, FBLN5, MFAP2, BGN, MMP12, MMP9, PCOLCE2, COL6A1	
	Collagen formation, and Molecules associated with elastic fibres	1.27	2.32E-05	POSTN, ADAMTS1, FBLN5, MFAP2, BGN, MMP12, PCOLCE2, COL6A1	
	Collagen biosynthesis and modifying enzymes, and Proline metabolic process	1.3	8.20E-04	POSTN, ADAMTS1, BGN, MMP12, PCOLCE2, COL6A1	
	Collagen biosynthesis and modifying enzymes, and Fibrillar collagen, C-terminal	1.39	2.40E-03	POSTN, BGN, MMP12, PCOLCE2, COL6A1	
	Mixed, incl. Glycosaminoglycan degradation, and Glycosphingolipid metabolism	1.28	6.50E-03	CLN5, TPP1, NAGLU, MAN2B1, GLB1	
	Mixed, incl. Exopeptidase activity, and Maturity onset diabetes of the young	1.07	8.50E-03	LOC102156614 (CTS1), PAM, LGMN, CTSK, DPP7, CPE	
	Collagen biosynthesis and modifying enzymes, and Fibrillar collagen, C-terminal	1.36	1.92E-02	POSTN, BGN, MMP12, COL6A1	
	Mixed, incl. Banded collagen fibril, and small leucine-rich proteoglycan, class I, decorin/ asporin/byglycan	1.61	3.57E-02	POSTN, BGN, COL6A1	
	Mixed, incl. Exopeptidase activity, and Papain family cysteine protease	1.22	4.88E-02	LOC102156614 (CTS1), LGMN, CTSK, DPP7	
	Mixed, incl. Glycosaminoglycan degradation, and Glycosphingolipid metabolism	1.22	4.88E-02	CLN5, TPP1, NAGLU, GLB1	
	CHV-infected group	Glycolysis	1.49	3.90E-04	ENO1, ALDOA, ALDOC, LOC477441, PGAM2, PKM
		Enolase, C-terminal TIM barrel domain, and Glycolysis	1.73	2.30E-03	ENO1, LOC477441, PGAM2, PKM
aminoacyl-tRNA synthetase multienzyme complex		2.08	3.80E-03	MARS1, IARS1, LARS1	
Pyruvate metabolic process, and Carbon metabolism		0.97	6.50E-03	ENO1, ALDOA, ALDOC, LOC477441, CS, PGAM2, PKM	
Proteasome complex		1.24	3.49E-02	PSMD14, PSMD4, PSMB3, PSMA1	

*The analysis criteria were a high confidence interaction score of 0.700, FDR < 0.05, and strength score > 0.75

CHV infection significantly alters the gene expression of cAD-MSCs

The RNA QC results indicated high RNA quality across all uninfected and CHV-infected samples (Additional file 5). Gene expression analysis revealed significant alterations in 20.9% (18/85) of the total genes included in the array between uninfected and CHV-infected cAD-MSCs. Specifically, expression changes were observed for 16.7% (1/6) of the total stemness genes, 33.3% (6/18) of the total MSC-specific genes, 25.8% (8/31) of the total MSC-associated genes, and 9.7% (3/31) of the total MSC differentiation genes (Figs. 4A–D). Fold regulation values for all downregulated and upregulated genes are shown in Fig. 4E. The full report of the RT2 Profiler PCR Array Data Analysis Software is attached as Additional file 1.

CHV infection significantly alters protein secretion in the cAD-MSC secretome

The proteomic analysis of the cAD-MSC secretome identified 1,181 proteins. A comprehensive list of all detected proteins, including their accession numbers, gene names, molecular weights, t-test p values, and fold change data, is provided in Additional File 6. The 86.8% (1,025/1,181) of proteins were common between uninfected and CHV-infected samples. The commonly detected proteins were further compared by GO enrichment analysis, i.e., cellular components, protein classes, molecular functions, and biological processes (Fig. 5A–C). Similar involvement in all annotated functions was observed. Analysis of cellular components revealed that $\approx 60\%$ (788/1181 and 754/1181 in uninfected and CHV-infected samples, respectively) of proteins belonged to cytoskeletal proteins, $\approx 19\%$ (239 in uninfected and 235 in CHV-infected samples) belonged to protein-containing complexes, and the rest (154 in uninfected and 192 in CHV-infected) were not assignable to cellular component GO terms. More than 50% of the cAD-MSC secretome proteins were metabolite conversion enzymes, translational proteins, protein-modifying enzymes, and cytoskeletal proteins (Fig. 5A). Their molecular functions were mainly binding and catalytic activity (Fig. 5B), and they were predominantly involved in cellular and metabolic processes, biological regulation, response to stimuli and localisation (Fig. 5C). Among the commonly secreted proteins, 10 were significantly downregulated, whereas 66 were significantly upregulated (Fig. 5D; Additional file 6).

Within the subset of proteins exhibiting distinctive secretion patterns (comprising 13.2% of the total proteins), 105 proteins were specific to uninfected samples, whereas 51 proteins were specific to CHV-infected samples. Subsequent bioinformatic analysis was subsequently conducted to gain insight into protein pathway involvement. The results of the GO enrichment analysis are presented in Table 2, while the outcomes of the STRING analysis are detailed in Table 3 and Fig. 5F.

Discussion

In vitro manipulations are unavoidable for acquiring and conserving therapeutic quantities of cAD-MSCs and their secretome. Nevertheless, these procedures involve an inherent risk of microbial contamination and the potential spread of pathogens, including viruses, originating from infected donor cells. Therefore, we aimed to investigate the interaction between globally distributed CHV and cAD-MSCs and to assess whether CHV infection affects the gene expression and secretome composition of cAD-MSCs. To the best of our knowledge, this study represents the first investigation of the effects of viral infection on the gene expression and secretome profile of cAD-MSCs. To achieve the aim, an autochthonous CHV strain was established. This strain should reflect the natural virus-host interplay more accurately than culture-adapted and extensively propagated CHV strains in vitro. The novel complete genome sequence of the autochthonous CHV strain from Croatia contributes to the knowledge of the complete genome diversity of CHV. Prior to this contribution, the GenBank database contained 22 complete CHV genome sequences, with only five sequences from Europe, three from the United Kingdom and two from Italy.

In vitro susceptibility to CHV, as indicated by the characteristic CPE of *Orthoherpesviridae* viruses [48], was likewise observed in cAD-MSCs and MDCK cells (Fig. 2A, B; Additional files 2 and 4). However, successive passages of CHV on cAD-MSCs exhibited a gradual reduction and disappearance of CPE, which was corroborated by diminishing yet persistent CHV genome copy numbers (Fig. 2C) in the supernatants of cell lysates, indicating abortive infection. The abortive infection has recently been documented in herpes simplex virus in vitro research [49], which proves that herpesviruses can infect nonneuronal cells, remain quiescent and be reactivated, challenging the current paradigm of herpesvirus latency. Our results seem to resemble the above

scenario, but further experimental validation is needed to assign abortive infection status to this specific virus-host interaction.

The effects of CHV infection on cAD-MSCs were further explored at the gene expression level, and the results revealed that CHV infection significantly affected the expression of researched genes (Fig. 4). The upregulated genes were associated with proliferation [50], differentiation [51], and the immunosuppressive response [52–54]. Similar alterations in gene expression attributed to virus infections have been documented in previous studies on human stem cells [21, 55]. The most significantly upregulated gene in infected cAD-MSCs, *TNF* (Fig. 4C), encodes a protein responsible for various cellular processes, including proliferation, differentiation, and, interestingly, immune suppression in MSCs [54, 56]. It remains unclear whether canine MSCs can produce TNF; however, in human MSCs, there is clear evidence of their inability to produce TNF [57]. Nevertheless, cAD-MSCs are adipocyte progenitors, and adipocytes and their progenitors are well known for secreting TNF [58]. In this study, high *TNF* production combined with alterations in other genes primarily suggested increased adipocyte differentiation in CHV-infected cells. Moreover, the upregulation of *ADIPOQ* and *NOTCH1* [59, 60] coupled with the downregulation of several genes related to stemness and regenerative capacity [61–64] further support the initiation of differentiation processes, predominantly adipogenesis, in CHV-infected cAD-MSCs. These findings indicate that CHV infection may drive cAD-MSC differentiation, affecting their regenerative potential and altering their typical stem cell properties.

The proteomic composition of the cAD-MSC secretomes further corroborated the initiation of adipogenesis in CHV-infected cells observed at the RNA level. GO enrichment analysis of the uninfected group revealed that proteins significantly involved in the WNT signalling pathway were absent in CHV-infected cells (Table 2). This finding suggests that CHV infection leads to the loss of the WNT signalling pathway, and its deactivation in MSCs is considered crucial for inducing adipogenesis [65, 66]. Furthermore, both GO enrichment and STRING analyses (Tables 2 and 3) revealed the presence of essential protein pathways involved in cell self-renewal, structure, survival, homing, and migration [67, 68] in the uninfected group, which were lost after CHV infection. These losses at the proteomic level align with the microscopically observed loss of cellular structure, survival, and migration following CPE development (Fig. 2; Additional files 2 and 4).

Additionally, the observed microscopic reduction in cell survival was further supported by findings from the CHV-infected group cAD-MSC secretomes. GO enrichment and STRING analyses revealed upregulated glycolysis and elevated levels of proteins associated with the enolase and pyruvate metabolism pathways (Tables 2 and 3). This virus's takeover of host cell resources and metabolic machinery prioritises viral particle production over normal cellular functions, ultimately leading to cell damage and death. Similar alterations were previously documented in studies on viral-host interactions in other *Orthoherpesviridae* infections, such as human cytomegalovirus [69] and herpes simplex virus [70, 71] infections.

Although novel knowledge is unravelled in this study, future studies should deepen the understanding of cAD-MSC-CHV interactions by examining transcriptome and secretome alterations throughout serial passages and identifying any coinciding variants in the viral genome. Furthermore, as the AD-MSC secretome has recently been shown to have an antiviral effect [72] in felines, our research provides a direction for overcoming the currently limited knowledge on utilising stem cells to treat viral diseases in canines.

In conclusion, our study demonstrated the susceptibility of cAD-MSCs to CHV infection. The observed genomic variations in gene expression indicate potential impacts on the stemness, migration, and other functional properties of cAD-MSCs, highlighting the need for further studies to evaluate their functional capacity post-infection. Moreover, gene expression and secretome analyses suggest a shift in stem cell differentiation toward an adipogenic phenotype. These cumulative changes can negatively impact the regenerative properties of cAD-MSCs. These findings highlight the critical importance of screening cAD-MSC batches intended for therapeutic applications to ensure the absence of CHV prior to administration.

Abbreviations

cAD-MSCs	Canine adipose-derived mesenchymal stem cells
CD	Cluster of differentiation
CHV	Canid alphaherpesvirus 1
CPE	Cytopathogenic effect
DMEM Low Glucose	Dulbecco's modified eagle medium with low glucose
FBS	Fetal bovine serum
FDR	False discovery rate
GO	Gene ontology
LOD	Limit of detection
LOQ	Limit of quantification
MDCK	Madin-Darby canine kidney cell culture
MSC	Mesenchymal stem cell
NGS	Next-generation sequencing
P(number)	Passage (number)

p.i.	Postinfection
qPCR	Quantitative polymerase chain reaction
RT-qPCR	Reverse transcription-quantitative polymerase chain reaction
TCID50	50% tissue culture infectious dose.

Supplementary Information

The online version contains supplementary material available at <https://doi.org/10.1186/s12985-024-02603-8>.

Additional file 1 This additional report was generated through the analysis of gene expression data employing the RT² Profiler PCR Array Data Analysis Software. In addition to the analysis results, the investigated gene names, symbols, and corresponding NCBI sequences were comprehensively described. (PDF 321 KB)

Additional file 2 This movie additionally illustrates the progression of cytopathogenic effects in the Madin-Darby canine kidney cell line after infection with canid alphaherpesvirus 1. A scale bar of 200 μm is provided, along with a time bar delineated in days, hours, minutes, and seconds. (MP4 18067 KB)

Additional file 3 The table lists all mutations found in the wild-type CHV (GenBank accession number PP349830) relative to the closest relative, MW353130. Mutation positions, effects, gene genes affected, and protein-level consequences are also listed. (XLSX 13 KB)

Additional file 4 This movie additionally illustrates the progression of cytopathogenic effects in canine adipose-derived mesenchymal stem cells after infection with canid alphaherpesvirus 1. A scale bar of 200 μm is provided, along with a time bar delineated in days, hours, minutes, and seconds. (MP4 20489 KB)

Additional file 5 This additional table displays the RNA quality control (QC) analysis results, including the RNA integrity score and 28:18S ratio for all assessed total RNA samples. (XLSX 10 KB)

Additional file 6 This table provides each identified protein's accession number, gene name, and molecular weight. Furthermore, t-tests were used to determine the significance and fold changes in secretome protein secretion between CHV-infected and uninfected samples. The list is organised in ascending order based on the t-test p values. The blue color represents significantly downregulated proteins (p < 0.05) with a fold change exceeding 1.3. Conversely, the orange color signifies proteins demonstrating statistical significance (p < 0.05) in upregulation, with a fold change greater than 1.3. A "missing value" indicates that the protein is secreted exclusively in uninfected samples, while a "reference missing" indicates that the protein is secreted solely in CHV-infected samples. (XLSX 108 KB)

Acknowledgements

We thank Ivana Ljolje, Petar Kostešić, and all canine donors and their owners for providing the canine adipose tissue. Furthermore, we thank Manuela Zadavec, Mihaela Stuparić Komušar, Dunja Vlahović, and Marko Močibob for their generous help during sterility testing, chondrodifferentiation preparation, chondrodifferentiation interpretation, and proteomic analysis, respectively.

Author contributions

MPŠ, DB, and NT developed the study concept. MPŠ, TMZ, DV, RK, and DB developed the methodology. MPŠ, ŠN, MPo, RK, and DB provided resources. MPŠ, ŠN, VKu, TMZ, DV, and DB performed the investigation. MPŠ, VKo, and TMZ collected the data and performed the formal analysis. TMZ performed the software analysis. MPŠ, VKo, TMZ and DB validated the results. MPŠ visualised the results. DB acquired funding; MP and RK acquired funding for NGS. DB provided project administration. DB, MP, RK, and NT supervised the study. MPŠ wrote the original draft, while TMZ and DB wrote sections of the manuscript. All authors reviewed the manuscript drafts and approved the final version of the manuscript.

Funding

This research was funded by the Croatian Science Foundation within the Installation Research Project (UIP-2019-04-2178) "Revealing transcriptome and secretome of mesenchymal stem cells" (SECRET). The next-generation sequencing analysis was funded by the Slovenian Research and Innovation Agency (grants P3-0083 and J3-3062). Proteomic analysis was partially funded by the European Regional Development Fund (infrastructural project CluK, grant number KK.01.1.1.02.0016). The funding agencies did not contribute to the study's conceptualisation, design, data collection, analysis, decision to publish, or manuscript preparation.

Availability of data and materials

The datasets generated and analysed during the current study are available in the NCBI GenBank [<https://www.ncbi.nlm.nih.gov/nuccore/PP349830>], Gene Expression Omnibus repository [<https://www.ncbi.nlm.nih.gov/geo/query/acc.cgi?acc=GSE267402>] and ProteomeXchange repository [<https://www.ebi.ac.uk/pride/archive/projects/PXD052289>]. This manuscript and additional files include other data generated or analysed during this study.

Declarations

Ethics approval and consent to participate

The animal research was evaluated and approved by the Ethics Board of the Croatian Veterinary Institute (approval code Z-IV-4-2022/19) and the Veterinary Ethics Committee at the Faculty of Veterinary Medicine, University of Zagreb, Croatia (approval codes 640-01/20-17/10, 640-01/20-17/55, and 640-01/22-02/07). Canine donor owners provided written informed consent before sampling.

Consent for publication

Not applicable.

Competing interests

The authors declare that they have no competing interests.

Author details

¹Virology Department, Croatian Veterinary Institute, Zagreb, Croatia. ²Department for Pathological Morphology, Croatian Veterinary Institute, Zagreb, Croatia. ³Institute of Microbiology and Immunology, Faculty of Medicine, University of Ljubljana, Ljubljana, Slovenia. ⁴Department of Microbiology and Infectious Diseases With Clinic, Faculty of Veterinary Medicine, University of Zagreb, Zagreb, Croatia.

Received: 27 June 2024 Accepted: 9 December 2024

Published online: 27 December 2024

References

- Voga M, Adamic N, Vengust M, Majdic G. Stem cells in veterinary medicine—current state and treatment options. *Front Vet Sci*. 2020;7:278. <https://doi.org/10.3389/fvets.2020.00278>.
- Prišlin M, Vlahović D, Kostešić P, Ljolje I, Brnić D, Turk N, et al. An outstanding role of adipose tissue in canine stem cell therapy. *Animals*. 2022;12:1088. <https://doi.org/10.3390/ani12091088>.
- El-Husseiny HM, Mady EA, Helal MAY, Tanaka R. The pivotal role of stem cells in veterinary regenerative medicine and tissue engineering. *Vet Sci*. 2022;9:648. <https://doi.org/10.3390/vetsci9110648>.
- Russell KA, Chow NHC, Dukoff D, Gibson TWG, La Marre J, Betts DH, et al. Characterisation and immunomodulatory effects of canine adipose tissue- and bone marrow-derived mesenchymal stromal cells. *PLoS ONE*. 2016;11:e0167442. <https://doi.org/10.1371/journal.pone.0167442>.
- Villatoro AJ, Alcohollado C, Martín-Astorga MC, Fernández V, Cifuentes M, Becerra J. Comparative analysis and characterisation of soluble factors and exosomes from cultured adipose tissue and bone marrow mesenchymal stem cells in canine species. *Vet Immunol Immunopathol*. 2019;208:6–15. <https://doi.org/10.1016/j.vetimm.2018.12.003>.
- Humenik F, Maloveska M, Hudakova N, Petrouskova P, Hornakova L, Domaniza M, et al. A comparative study of canine mesenchymal stem

- cells isolated from different sources. *Animals*. 2022;12:1502. <https://doi.org/10.3390/ani12121502>.
7. Teshima T, Yuchi Y, Suzuki R, Matsumoto H, Koyama H. Immunomodulatory effects of canine adipose tissue mesenchymal stem cell-derived extracellular vesicles on stimulated cd4+T cells isolated from peripheral blood mononuclear cells. *J Immunol Res*. 2021;2021:2993043. <https://doi.org/10.1155/2021/2993043>.
 8. Prišlin M, Butorac A, Bertoša R, Kunić V, Ljolje I, Kostešić P, et al. In vitro aging alters the gene expression and secretome composition of canine adipose-derived mesenchymal stem cells. *Front Vet Sci*. 2024;11:1387174. <https://doi.org/10.3389/fvets.2024.1387174>.
 9. Chandra V, Mankuzhy P, Sharma GT. Mesenchymal stem cells in veterinary regenerative therapy: basic physiology and clinical applications. *Curr Stem Cell Res Ther*. 2022;17:237–51. <https://doi.org/10.2174/1574888X1666210804112741>.
 10. Trzyna A, Banaś-Ząbczyk A. Adipose-derived stem cells secretome and its potential application in "stem cell-free therapy". *Biomolecules*. 2021;11:878. <https://doi.org/10.3390/biom11060878>.
 11. Merlo B, Iacono E. Beyond canine adipose tissue-derived mesenchymal secretome characterization and applications. *Animals*. 2023;13(22):3571. <https://doi.org/10.3390/ani13223571>.
 12. Vizoso FJ, Eiro N, Cid S, Schneider J, Perez-Fernandez R. Mesenchymal stem cell secretome: Toward cell-free therapeutic strategies in regenerative medicine. *Int J Mol Sci*. 2017;18:1852. <https://doi.org/10.3390/ijms18091852>.
 13. Szablowska-Gadomska I, Humi M, Plączkowska J. Microbiological aspects of pharmaceutical manufacturing of adipose-derived stem cell-based medicinal products. *Cells*. 2023;12(5):680. <https://doi.org/10.3390/cells12050680>.
 14. Martín PG, González MB, Martínez AR, Lara VG, Naveros BC. Isolation and characterisation of the environmental bacterial and fungi contamination in a pharmaceutical unit of mesenchymal stem cell for clinical use. *Biologicals*. 2012;40:330–7. <https://doi.org/10.1016/j.biologicals.2012.06.002>.
 15. Khatri M, O'Brien TD, Goyal SM, Sharma JM. Isolation and characterisation of chicken lung mesenchymal stromal cells and their susceptibility to avian influenza virus. *Dev Comp Immunol*. 2010;34:474–9. <https://doi.org/10.1016/j.dci.2009.12.008>.
 16. Khatri M, Saif YM. Influenza virus infects bone marrow mesenchymal stromal cells in vitro: implications for bone marrow transplantation. *Cell Transpl*. 2013;22:461–8. <https://doi.org/10.3727/096368912X656063>.
 17. Nazari-Shafti TZ, Freisinger E, Roy U, Bulot CT, Sensi C, Dupin CL, et al. Mesenchymal stem cell derived hematopoietic cells are permissive to HIV-1 infection. *Retrovirology*. 2011;8:3. <https://doi.org/10.1186/1742-4690-8-3>.
 18. Ma R, Xing Q, Shao L, Wang D, Hao Q, Li X, et al. Hepatitis B virus infection and replication in human bone marrow mesenchymal stem cells. *Virology*. 2011;8:486. <https://doi.org/10.1186/1743-422X-8-486>.
 19. Sundin M, Örvell C, Rasmusson I, Sundberg B, Ringdén O, Le Blanc K. Mesenchymal stem cells are susceptible to human herpesviruses, but viral DNA cannot be detected in the healthy seropositive individual. *Bone Marrow Transpl*. 2006;37:1051–9. <https://doi.org/10.1038/sj.bmt.1705368>.
 20. Roy E, Shi W, Duan B, Reida SP. Chikungunya virus infection impairs the function of osteogenic cells. *mSphere*. 2020;5:e00347-20. <https://doi.org/10.1128/mSphere.00347-20>.
 21. Behzadi Fard M, Kaviani S, Atashi A. Parvovirus B19 infection in human bone marrow mesenchymal stem cells affects gene expression of IL-6 and TNF- α and also affects hematopoietic stem cells differentiation. *Indian J Hematol Blood Transfus*. 2019;35:765–72. <https://doi.org/10.1007/s12288-019-01097-7>.
 22. Meisel R, Heseler K, Nau J, Schmidt SK, Leineweber M, Pudelko S, et al. Cytomegalovirus infection impairs immunosuppressive and antimicrobial effector functions of human multipotent mesenchymal stromal cells. *Mediators Inflamm*. 2014;2014:898630. <https://doi.org/10.1155/2014/898630>.
 23. Altamirano-Samaniego F, Enciso-Benavides J, Rojas N, Iglesias-Pedraz JM, Enciso N, Fossatti M, et al. First report of canine morbillivirus infection of adipose tissue-derived stem cells from dogs with distemper. *Vet World*. 2022;15:1835–42. <https://doi.org/10.14202/vetworld.2022.1835-1842>.
 24. Pekker E, Priskin K, Szabó-Kriston É, Csányi B, Buzás-Bereczki O, Adorján L, et al. Development of a large-scale pathogen screening test for the biosafety evaluation of canine mesenchymal stem cells. *Biol Proced Online*. 2023;25:33. <https://doi.org/10.1186/s12575-023-00226-x>.
 25. ICTV. Varicellovirus taxonomy [Internet]. 2024 [cited 2024 25 March]. Available from: <https://ictv.global/report/chapter/orthohespesviridae/orthohespesviridae/varicellovirus>
 26. Dahlborn M, Johnsson M, Myllys V, Taponen J, Andersson M. Seroprevalence of canine herpesvirus-1 and *Brucella canis* in Finnish breeding kennels with and without reproductive problems. *Reprod Domest Anim*. 2009;44:128–31. <https://doi.org/10.1111/j.1439-0531.2007.01008.x>.
 27. Krogenæs A, Rootwelt V, Larsen S, Sjøberg EK, Akselsen B, Skår TM, et al. A serological study of canine herpes virus-1 infection in the Norwegian adult dog population. *Theriogenology*. 2012;78:153–8. <https://doi.org/10.1016/j.theriogenology.2012.01.031>.
 28. Gracin K. Dijagnostika herpesvirusne infekcije u pasa u Republici Hrvatskoj i njezin utjecaj na poremećaje reprodukcije. Ph.D. Thesis. University of Zagreb, Veterinary Faculty; 2020.
 29. de la Garza-Rodea AS, Verweij MC, Boersma H, van der Velde-van DI, de Vries AAF, Hoeben RC, et al. Exploitation of herpesvirus immune evasion strategies to modify the immunogenicity of human mesenchymal stem cell transplants. *PLoS ONE*. 2011;6:e14493. <https://doi.org/10.1371/journal.pone.0014493>.
 30. Claessen C, Favoreel H, Ma G, Osterrieder N, De Schauwer C, Piepers S, et al. Equid herpesvirus 1 (EHV1) infection of equine mesenchymal stem cells induces a pUL56-dependent downregulation of select cell surface markers. *Vet Microbiol*. 2015;176:32–9. <https://doi.org/10.1016/j.vetmic.2014.12.013>.
 31. Krešić N, Prišlin M, Vlahović D, Kostešić P, Ljolje I, Brnić D, et al. The expression pattern of surface markers in canine adipose-derived mesenchymal stem cells. *Int J Mol Sci*. 2021;22:7476. <https://doi.org/10.3390/ijms22147476>.
 32. Dominici M, Le Blanc K, Mueller I, Slaper-Cortenbach I, Marini FC, Krause DS, et al. Minimal criteria for defining multipotent mesenchymal stromal cells. The International Society for Cellular Therapy position statement. *Cytotherapy*. 2006;8:315–7. <https://doi.org/10.1080/14653240600855905>.
 33. Decaro N, Amorisco F, Desario C, Lorusso E, Camero M, Bellacicco AL, et al. Development and validation of a real-time PCR assay for specific and sensitive detection of canid herpesvirus 1. *J Virol Methods*. 2010;169:176–80. <https://doi.org/10.1016/j.jviromet.2010.07.021>.
 34. Wernike K, Hoffmann B, Kalthoff D, König P, Beer M. Development and validation of a triplex real-time PCR assay for the rapid detection and differentiation of wild-type and glycoprotein E-deleted vaccine strains of Bovine herpesvirus type 1. *J Virol Methods*. 2011;174:77–84. <https://doi.org/10.1016/j.jviromet.2011.03.028>.
 35. Eisa M, Loucif H, Grevenynghe J, Pearson A. Entry of the Varicellovirus Canid herpesvirus 1 into Madin-Darby canine kidney epithelial cells is pH-independent and occurs via a macropinosytosis-like mechanism but without increase in fluid uptake. *Cell Microbiol*. 2021;23:e13398. <https://doi.org/10.1111/cmi.13398>.
 36. Bankevich A, Nurk S, Antipov D, Gurevich AA, Dvorkin M, Kulikov AS, et al. SPAdes: a new genome assembly algorithm and its applications to single-cell sequencing. *J Comput Biol*. 2012;19:455–77. <https://doi.org/10.1089/cmb.2012.0021>.
 37. Li H. Aligning sequence reads, clone sequences and assembly contigs with BWA-MEM. *arXiv [Internet]*. 2013;1303:3997. Available from: <http://arxiv.org/abs/1303.3997>
 38. Danecek P, Bonfield JK, Liddle J, Marshall J, Ohan V, Pollard MO, et al. Twelve years of SAMtools and BCFtools. *Gigascience*. 2021;10:giab008. <https://doi.org/10.1093/gigascience/giab008/6137722>.
 39. Grubaugh ND, Gangavarapu K, Quick J, Matteson NL, De Jesus JG, Main BJ, et al. An amplicon-based sequencing framework for accurately measuring intrahost virus diversity using PrimalSeq and iVar. *Genome Biol*. 2019;20:8. <https://doi.org/10.1186/s13059-018-1618-7>.
 40. Seemann T. Prokka: rapid prokaryotic genome annotation. *Bioinformatics*. 2014;30:2068–9. <https://doi.org/10.1093/bioinformatics/btu153>.

41. Nguyen L-T, Schmidt HA, von Haeseler A, Minh BQ. IQ-TREE: a fast and effective stochastic algorithm for estimating maximum-likelihood phylogenies. *Mol Biol Evol*. 2015;32:268–74. <https://doi.org/10.1093/molbev/msu300>.
42. Kalyaanamoorthy S, Minh BQ, Wong TKF, von Haeseler A, Jermiin LS. ModelFinder: fast model selection for accurate phylogenetic estimates. *Nat Methods*. 2017;14:587–9. <https://doi.org/10.1038/nmeth.4285>.
43. Rozewicki J, Li S, Amada KM, Standley DM, Katoh K. MAFFT-DASH: integrated protein sequence and structural alignment. *Nucleic Acids Res*. 2019;47:W5–10. <https://doi.org/10.1093/nar/gkz342/5486273>.
44. Hoang DT, Chernomor O, von Haeseler A, Minh BQ, Vinh LS. UFBoot2: improving the ultrafast bootstrap approximation. *Mol Biol Evol*. 2018;35:518–22. <https://doi.org/10.1093/molbev/msx281>.
45. Martin DP, Varsani A, Roumagnac P, Botha G, Maslamoney S, Schwab T, et al. RDP5: a computer program for analysing recombination in, and removing signals of recombination from, nucleotide sequence datasets. *Virus Evol*. 2021. <https://doi.org/10.1093/ve/veaa087/6020281>.
46. Perez-Riverol Y, Bai J, Bandla C, Garcia-Seisdedos D, Hewapathirana S, Kamatchinathan S, et al. The PRIDE database resources in 2022: a hub for mass spectrometry-based proteomics evidences. *Nucleic Acids Res*. 2022;50:D543–52. <https://doi.org/10.1093/nar/gkab1038>.
47. Szklarczyk D, Kirsch R, Koutrouli M, Nastou K, Mehryary F, Hachilif R, et al. The STRING database in 2023: protein-protein association networks and functional enrichment analyses for any sequenced genome of interest. *Nucleic Acids Res (Oxford University Press)*. 2023;51:D638–46. <https://doi.org/10.1093/nar/gkac1000>.
48. Suchman E, Blair C. Cytopathic effects of viruses. In: ASM Conference Undergraduate Education 2007. *Am Soc Microbiol [Internet]*. 2007. p. 1–13. Available from: <https://asm.org/Protocols/Cytopathic-Effects-of-Viruses-Protocols>
49. Cohen EM, Avital N, Shamay M, Kobiler O. Abortive herpes simplex virus infection of nonneuronal cells results in quiescent viral genomes that can reactivate. *Proc Natl Acad Sci USA*. 2020;117:635–40. <https://doi.org/10.1073/pnas.1910537117>.
50. Han SH, Jang G, Bae BK, Han SM, Koh YR, Ahn JO, et al. Effect of ectopic OCT4 expression on canine adipose tissue-derived mesenchymal stem cell proliferation. *Cell Biol Int*. 2014;38:1163–73. <https://doi.org/10.1002/cbin.10295>.
51. Park SR, Cho A, Kim JW, Lee HY, Hong IS. A novel endogenous damage signal, CSF-2, activates multiple beneficial functions of adipose tissue-derived mesenchymal stem cells. *Mol Ther*. 2019;27:1087–100. <https://doi.org/10.1016/j.jymthe.2019.03.010>.
52. Deng J, Li D, Huang X, Li W, Zhao F, Gu C, et al. Interferon- γ enhances the immunosuppressive ability of canine bone marrow-derived mesenchymal stem cells by activating the TLR3-dependent IDO/kynurenine pathway. *Mol Biol Rep*. 2022;49:8337–47. <https://doi.org/10.1007/s11033-022-07648-y>.
53. Rubtsov Y, Goryunov K, Romanov A, Suzdaltseva Y, Sharonov G, Tkachuk V. Molecular mechanisms of immunomodulation properties of mesenchymal stromal cells: a new insight into the role of ICAM-1. *Stem Cells Int*. 2017;2017:6516854. <https://doi.org/10.1155/2017/6516854>.
54. Yang HM, Song WJ, Li Q, Kim SY, Kim HJ, Ryu MO, et al. Canine mesenchymal stem cells treated with TNF- α and IFN- γ enhance anti-inflammatory effects through the COX-2/PGE 2 pathway. *Res Vet Sci*. 2018;119:19–26. <https://doi.org/10.1016/j.rvsc.2018.05.011>.
55. Li Q, Yu P, Wang W, Zhang P, Yang H, Li S, et al. Gene expression profiles of various cytokines in mesenchymal stem cells derived from umbilical cord tissue and bone marrow following infection with human cytomegalovirus. *Cell Mol Biol Lett*. 2014;19:140–57. <https://doi.org/10.2478/s11658-014-0187-3>.
56. Yan L, Zheng D, Xu R-H. Critical role of tumor necrosis factor signaling in mesenchymal stem cell-based therapy for autoimmune and inflammatory diseases. *Front Immunol*. 2018;9:1658. <https://doi.org/10.3389/fimmu.2018.01658/full>.
57. van den Berk LCJ, Jansen BJH, Siebers-Vermeulen KGC, Roelofs H, Figdor CG, Adema GJ, et al. Mesenchymal stem cells respond to TNF but do not produce TNF. *J Leukoc Biol*. 2010;87:283–9. <https://doi.org/10.1189/jlb.0709467>.
58. Cawthorn WP, Sethi JK. TNF- α and adipocyte biology. *FEBS Lett*. 2008;582:117–31. <https://doi.org/10.1016/j.febslet.2007.11.051>.
59. Nedvídková J, Smitka K, Kopský V, Hainer V. Adiponectin, an adipocyte-derived protein. *Physiol Res*. 2005;54:133–40.
60. Shan T, Liu J, Wu W, Xu Z, Wang Y. Roles of notch signaling in adipocyte progenitor cells and mature adipocytes. *J Cell Physiol*. 2017;232:1258–61. <https://doi.org/10.1002/jcp.25697>.
61. Tanabe S, Kawabata T, Aoyagi K, Yokozaki H, Sasaki H. Gene expression and pathway analysis of CTNNB1 in cancer and stem cells. *World J Stem Cells*. 2016;8:384–95. <https://doi.org/10.4252/wjsc.v8.i11.384>.
62. Enciso N, Ostronoff LLK, Mejias G, León LG, Fermin ML, Merino E, et al. Stem cell factor supports migration in canine mesenchymal stem cells. *Vet Res Commun*. 2018;42:29–38. <https://doi.org/10.1007/s11259-017-9705-x>.
63. Cao Z, Xie Y, Yu L, Li Y, Wang Y. Hepatocyte growth factor (HGF) and stem cell factor (SCF) maintained the stemness of human bone marrow mesenchymal stem cells (hBMSCs) during long-term expansion by preserving mitochondrial function via the PI3K/AKT, ERK1/2, and STAT3 signaling pathways. *Stem Cell Res Ther*. 2020;11:329. <https://doi.org/10.1186/s13287-020-01830-4>.
64. Wang S, Mo M, Wang J, Sadia S, Shi B, Fu X, et al. Platelet-derived growth factor receptor beta identifies mesenchymal stem cells with enhanced engraftment to tissue injury and pro-angiogenic property. *Cell Mol Life Sci*. 2018;75:547–61. <https://doi.org/10.1007/s00018-017-2641-7>.
65. Visweswaran M, Pohl S, Arfuso F, Newsholme P, Dilley R, Pervaiz S, et al. Multi-lineage differentiation of mesenchymal stem cells—toward Wnt, or not Wnt. *Int J Biochem Cell Biol*. 2015;68:139–47. <https://doi.org/10.1016/j.biocel.2015.09.008>.
66. Ling L, Nurcombe V, Cool SM. Wnt signaling controls the fate of mesenchymal stem cells. *Gene*. 2009;433:1–7. <https://doi.org/10.1016/j.gene.2008.12.008>.
67. Zhang Z, Liu M, Zheng Y. Role of Rho GTPases in stem cell regulation. *Biochem Soc Trans*. 2021;49:2941–55. <https://doi.org/10.1042/BST20211071>.
68. Alqahtani S, Butcher MC, Ramage G, Dalby MJ, McLean W, Nile CJ. Acetylcholine receptors in mesenchymal stem cells. *Stem Cells Dev*. 2023;32:47–59. <https://doi.org/10.1089/scd.2022.0201>.
69. Moreno I, Rodríguez-Sánchez I, Schafer X, Munger J. Human cytomegalovirus induces neuronal enolase to support virally mediated metabolic remodeling. *Proc Natl Acad Sci USA*. 2022;119:e2205789119. <https://doi.org/10.1073/pnas.2216830120>.
70. Kun-Varga A, Gubán B, Miklós V, Parvaneh S, Guba M, Szűcs D, et al. Herpes simplex virus infection alters the immunological properties of adipose-tissue-derived mesenchymal-stem cells. *Int J Mol Sci*. 2023;24:11989. <https://doi.org/10.3390/ijms241511989>.
71. Zhuo C, Zheng D, He Z, Jin J, Ren Z, Jin F, et al. HSV-1 enhances the energy metabolism of human umbilical cord mesenchymal stem cells to promote virus infection. *Future Virol*. 2017;12:349–60. <https://doi.org/10.2217/fvl-2017-0038>.
72. Teshima T, Yasumura Y, Suzuki R, Matsumoto H. Antiviral effects of adipose tissue-derived mesenchymal stem cells secrete against feline calicivirus and feline herpesvirus type 1. *Viruses*. 2022;14:1687. <https://doi.org/10.3390/v14081687>.

Publisher's Note

Springer Nature remains neutral with regard to jurisdictional claims in published maps and institutional affiliations.

9. BIOGRAPHY OF THE AUTHOR WITH BIBLIOGRAPHY OF PUBLISHED WORK

Marina Prišlin Šimac was born on 1 May 1994 in Zagreb. After graduating from the Vladimir Prelog High School of Natural Sciences in 2013, she enrolled in the Faculty of Veterinary Medicine at the University of Zagreb. She graduated in 2020 and began working as an assistant on the Croatian Science Foundation project "Revealing Mesenchymal Stem Cells Transcriptome and Secretome" at the Croatian Veterinary Institute. In 2021, she enrolled in the postgraduate doctoral programme of Veterinary Sciences. In 2023, she received a scholarship from the University in São Paulo, Brazil, for participating in the São Paulo School of Advanced Science on Stem Cell Biology. In addition, she has completed several training programmes, including flow cytometry, whole genome sequencing, proteomics and bioinformatic analysis. Marina has published 14 scientific papers, 10 of which have been cited in Web of Science and Scopus, and actively participated in 20 international and national conferences, with an h-index of 4.

Scientific articles in WoS journals

- PRIŠLIN ŠIMAC, M., Š. NALETILIĆ, V. KOSTANIĆ, V. KUNIĆ, T. M. ZOREC, M. POLJAK, D. VLAJ, R. KOGOJ, N. TURK, D. BRNIĆ (2024):** Canid alphaherpesvirus 1 infection alters the gene expression and secretome profile of canine adipose-derived mesenchymal stem cells in vitro. *Virol. J.*, 21, 335:1-18. doi: 10.1186/s12985-024-02603-8
- KOSTANIĆ, V., V. KUNIĆ, M. PRIŠLIN ŠIMAC, M. LOLIĆ, T. SUKALIĆ, D. BRNIĆ (2024):** Comparative Insights into Acute Gastroenteritis in Cattle Caused by Bovine Rotavirus A and Bovine Coronavirus. *Vet. Sci.*, 11, 671:1-15. doi: 10.3390/vetsci11120671
- PRIŠLIN, M., A. BUTORAC, R. BERTOŠA, V. KUNIĆ, I. LJOLJE, P. KOSTEŠIĆ, D. VLAHOVIĆ, Š. NALETILIĆ, N. TURK, D. BRNIĆ (2024):** In vitro aging alters the gene expression and secretome composition of canine adipose-derived mesenchymal stem cells. *Front. Vet. Sci.* 11, 1387174:1-12. doi: 10.3389/fvets.2024.1387174
- KUNIĆ, V., T. MIKULETIĆ, R. KOGOJ, T. KORITNIK, A. STEYER, S. ŠOPREK, G. TEŠOVIĆ, V. KONJIK, I. ROKSANDIĆ KRIŽAN, M. PRIŠLIN, L. JEMERŠIĆ, D. BRNIĆ (2023):** Interspecies transmission of porcine-originated G4P[6] rotavirus A

between pigs and humans: a synchronized spatiotemporal approach. *Front. Microbiol.* 14, 1194764:1-14. doi: 10.3389/fmicb.2023.1194764

PRIŠLIN, M., D. VLAHOVIĆ, P. KOSTEŠIĆ, I. LJOLJE, D. BRNIĆ, N. TURK, I. LOJKIĆ, V. KUNIĆ, T. KARADJOLE, N. KREŠIĆ (2022): An Outstanding Role of Adipose Tissue in Canine Stem Cell Therapy. *Animals.* 12 (9), 1088:1-19. doi: 10.3390/ani12091088

KREŠIĆ, N., M. PRIŠLIN, D. VLAHOVIĆ, P. KOSTEŠIĆ, I. LJOLJE, D. BRNIĆ, N. TURK, A. MUSULIN, B. HABRUN (2021): The Expression Pattern of Surface Markers in Canine Adipose-Derived Mesenchymal Stem Cells. *Int. J. Mol. Sci.* 22 (14), 7476:1-19. doi: 10.3390/ijms22147476

Scientific articles in Scopus journals

PRIŠLIN, M., Š. NALETILIĆ, M. HOHŠTETER, V. KUNIĆ, N. KREŠIĆ, N. TURK, I. LOJKIĆ, L. JEMERŠIĆ, D. BRNIĆ (2024): Patologija pseće herpesviroze *Vet. Stn.* 55 (1), 99-110. doi: <https://doi.org/10.46419/vs.55.1.7>

LOJKIĆ, I., A. JUNGIĆ, M. PRIŠLIN, D. NOVOSEL, Š. NALETILIĆ, J. PRPIĆ, I. KILVAIN, T. ANDREANSZKY, M. LOLIĆ, M. ŠKRIVANKO, L. JEMERŠIĆ, V. SAVIĆ (2024): Avian influenza in wild canids: an animal and public health threat. *Vet. Stn.* 55 (6), 631-640. doi: <https://doi.org/10.46419/vs.55.6.6>

KUNIĆ, V., Ž. GOTTSTEIN, M. PRIŠLIN, V. SAVIĆ, D. BRNIĆ (2024): Health repercussions of Avian Rotaviruses on Poultry and Fancy Pigeons. *Vet. Stn.* 55 (6), 677-689. doi: <https://doi.org/10.46419/vs.55.6.3>

Scientific articles in other journals

PRIŠLIN, M., L. PINCAN, O. ŠIFTAR, A. SHEK VUGROVEČKI, L. RADIN, L. VRANKOVIĆ, J. ALADROVIĆ (2017): Životne, prehrambene navike i stavovi studenata druge godine studija veterinarske medicine. *Veterinar.* 55 (2), 21-30.

Conference papers (in Proceedings)

PRIŠLIN, M., N. KREŠIĆ, D. VLAHOVIĆ, I. LJOLJE, P. KOSTEŠIĆ, N. TURK, V. KUNIĆ, I. LOJKIĆ, D. BRNIĆ (2023): Primjena mezenhimskih matičnih stanica masnog tkiva u liječenju bolesti pasa. Zbornik radova znanstveno-stručnog skupa s međunarodnim sudjelovanjem Veterinarski dani 2023. 26-29 October 2023, Osijek, Croatia, pp. 49-53.

- PRIŠLIN M., D. VLAHOVIĆ, I. LJOLJE, P. KOSTEŠIĆ, N. TURK, Š. NALETILIĆ, D. BRNIĆ, N. KREŠIĆ (2023):** Influence of In Vitro Cultivation on Differentiation Gene Expressions in Canine Adipose-Derived Mesenchymal Stem Cells. *Advances in Biomedical and Veterinary Engineering*. 20-22 October 2022, Zagreb, Croatia, pp. 1-19. doi: https://doi.org/10.1007/978-3-031-42243-0_1
- KREŠIĆ, N., M. PRIŠLIN, D. BRNIĆ, D. VLAHOVIĆ, P. KOSTEŠIĆ, I. LJOLJE (2021):** Učinak kultivacije in vitro na svojstva matičnih stanica iz masnog tkiva pasa. *Zbornik radova međunarodnog znanstveno stručnog skupa Veterinarski dani 2021*. 26-29 October 2021, Vodice, Croatia, pp. 119-123.
- ZIDAR, B., J. ALADROVIĆ, L. PINCAN, O. ŠIFTAR, M. PRIŠLIN, LJ. BEDRICA (2016):** Utjecaj anestetika na temperaturu, krvni tlak i frekvenciju srca mačaka povrgnutih kastraciji. *Zbornik radova međunarodnog znanstveno stručnog skupa 6. Hrvatski veterinarski kongres*. 26-29 October 2016, Opatija, Croatia, pp. 437-446.

Conference abstracts (Book of Abstracts)

- PRIŠLIN ŠIMAC, M., V. KUNIĆ, V. KOSTANIĆ, R. BECK, D. JURKOVIĆ ŽILIĆ, S. DUVNJAK, I. REIL, I. LOJKIĆ, D. BRNIĆ (2024):** Procjena kontaminacije patogenima u pripravcima mezenhimskih matičnih stanica porijeklom iz masnog tkiva pasa. *Zbornik radova međunarodnog znanstveno stručnog skupa 7. Hrvatski veterinarski kongres*. 24-27 October 2024, Dubrovnik, Croatia, pp. 123-124.
- BRNIĆ, D., V. KOSTANIĆ, V. KUNIĆ, M. PRIŠLIN ŠIMAC, M. RUBIN (2024):** Epizootska hemoragijska bolest: emergentna prijetnja u Europskoj uniji. *Zbornik radova međunarodnog znanstveno stručnog skupa 7. Hrvatski veterinarski kongres*. 24-27 October 2024, Dubrovnik, Croatia, p. 152.
- KOSTANIĆ, V., V. KUNIĆ, M. PRIŠLIN ŠIMAC, M. LOLIĆ, T. SUKALIĆ, D. BRNIĆ (2024):** Klinički i epidemiološki uvid u akutni gastroenteritis uzrokovan rotavirusom A i koronavirusom kod goveda *Zbornik radova međunarodnog znanstveno stručnog skupa 7. Hrvatski veterinarski kongres*. 24-27 October 2024, Dubrovnik, Croatia, p. 145.
- KUNIĆ, V., T. MIKULETIĆ, T. KORITNIK, A. STEYER, D. KONJEVIĆ, M. BUJANIĆ, M. PRIŠLIN ŠIMAC, D. BRNIĆ (2024):** Porcine-Originated rotavirus a shows significant genetic heterogeneity and interspecies transmission potential. *9th European Rotavirus Biology Meeting Abstract Book*. 2-4 October 2024, Valencia, Spain: University of Valencia, p. 49.

- PRIŠLIN ŠIMAC, M., Š. NALETILIĆ, V. KOSTANIĆ, V. KUNIĆ, T. M. ZOREC, M. POLJAK, D. VLAJ, R. KOGOJ, N. TURK, D. BRNIĆ (2024):** In vitro interaction between canid alphaherpesvirus 1 and canine adipose-derived mesenchymal stem cells: impact on cell gene expression and secretome profile. Power of Viruses 2024: Book of abstracts. 25-28 September 2024 Zadar, Croatia, p. 48.
- PRIŠLIN, M., A. BUTORAC, R. BERTOŠA, V. KUNIĆ, I. LJOLJE, P. KOSTEŠIĆ, D. VLAHOVIĆ, Š. NALETILIĆ, N. TURK, D. BRNIĆ (2024):** In vitro ageing changes the gene expression and secretome proteomic profile of canine adipose-derived mesenchymal stem cells. ISSCR Annual Meeting 2024 Poster Abstract Guide. 10-13 July 2024, Hamburg, Germany, p. 659.
- KUNIĆ, V., T. MIKULETIČ, R. KOGOJ, T. KORITNIK, A. STEYER, S. ŠOPREK, G. TEŠOVIĆ, V. KONJIK, I. ROKSANDIĆ KRIŽAN, M. PRIŠLIN, L. JEMERŠIĆ, D. BRNIĆ (2023):** Interspecies transmission of G4P[6] rotavirus A between pigs and humans revealed by synchronized spatiotemporal approach in Croatia. Abstract book MEEGID XVI. 14-17 November 2023, Dresden, Germany, p. 145.
- PRIŠLIN, M., T. M. ZOREC, D. VLAHOVIĆ, Š. NALETILIĆ, I. LJOLJE, P. KOSTEŠIĆ, V. KUNIĆ, N. TURK, D. BRNIĆ (2023):** In vitro interaction of canine adipose-derived mesenchymal stem cells with canid alphaherpesvirus: influence on cell differentiation genes and variations of viral genome ISSCR's International Symposium, "From Concepts to Clinic: Advances in Stem Cell Research." Abstract book. 22-24 September 2023, Sao Paulo, Brazil, pp. 76-77.
- KREŠIĆ N., M. PRIŠLIN, I. LJOLJE, Š. NALETILIĆ, P. KOSTEŠIĆ, D. VLAHOVIĆ, Ž. MIHALJEVIĆ, D. BRNIĆ, N. TURK, B. HABRUN (2022):** Canine Adipose Derived Mesenchymal Stem Cells Support Canid Alphaherpesvirus 1 Infection In Vitro. ESVV2022 Abstract Book. 20-23 September 2022, Ghent, Belgium, p. 157.
- KREŠIĆ, N., M. PRIŠLIN, D. VLAHOVIĆ, P. KOSTEŠIĆ, D. BRNIĆ, I. LJOLJE (2021):** Variations of stemness genes expression of canine mesenchymal stem cells during in vitro cultivation. 9th International Congress Veterinary Science and Profession Abstract Book. 9 October 2021, Zagreb, Croatia, p. 88.
- VLAHOVIĆ, D., M. PRIŠLIN, P. KOSTEŠIĆ, D. BRNIĆ, I. LJOLJE, I. ŠOŠTARIĆ-ZUCKERMANN, B. ARTUKOVIĆ, A. GUDAN KURILJ, M. HOHŠTETER, L. MEDVEN ZAGRADIŠNIK, I. MIHOKOVIĆ BUHIN, N. KREŠIĆ (2021):** Histological evaluation of chondro-differentiated cAD-MSC spheroids. 9th International Congress

- Veterinary Science and Profession Abstract Book. 9 October 2021, Zagreb, Croatia, p. 118.
- ŠIFTAR, O., L. PINCAN, **M. PRIŠLIN**, L. VRANKOVIĆ, I. DELAŠ, M. BUJANIĆ, D. KONJEVIĆ, Z. STOJEVIĆ, J. ALADROVIĆ (2019): Composition of fatty acids in liver, kidney and subcutaneous adipose tissue in edible dormouse (*Glis glis*). 8th International Congress Veterinary Science and Profession Abstract Book. 10-12 October 2019, Zagreb, Croatia, p. 118.
- ŠIFTAR, O., L. PINCAN, M. ŠURBEK, A. ZUPČIĆ, **M. PRIŠLIN**, L. VRANKOVIĆ, I. DELAŠ, M. BUJANIĆ, D. KONJEVIĆ, Z. STOJEVIĆ, J. ALADROVIĆ (2018): Masnokiselinski sastav potkožnog i abdominalnog masnog tkiva sivog puha (*Glis glis*) Book of Abstracts of 6th International Congress of Nutritionists. 26-28 October 2018, Zagreb, Croatia, 2018. p. 171.
- PRIŠLIN, M.**, B. BEER LJUBIĆ, D. BROZIĆ, D. ANTOLIĆ, J. ALADROVIĆ, JASNA (2017): Effect of organic selenium supplementation on level of alkaline phosphatase and zinc in chicken tissues at the end of the fattening period and after fasting. Tudományos Diákköri Konferencia 2017 Abstract Book. 22 November 2017, Budapest, Hungary, p. 132.
- PINCAN, L., **M. PRIŠLIN**, O. ŠIFTAR, L. VRANKOVIĆ, J. ALADROVIĆ (2017): Eating habits and attitudes of veterinary medicine students who live at home or away from home. Book of Abstracts of 5th International Congress of Nutritionists. 17-19 October 2017, Zagreb, Croatia, p. 172.
- PRIŠLIN, M.**, B. BEER LJUBIĆ, N. MALTAR- STRMEČKI, R. LAŠKAJ, L. VRANKOVIĆ, M. LOJKIĆ, V. NERVO, J. ALADROVIĆ (2017): Effect of age and follicle size on lipid profile and antioxidant potential of bovine follicular fluid. 7th International Congress Veterinary Science and Profession Abstract Book. 5-7 October 2017, Zagreb, Croatia, p. 67.